

Cyclic di-GMP controls a bacterial cell cycle phosphorylation network

Inauguraldissertation

zur

Erlangung der Würde eines Doktors der Philosophie

vorgelegt der

Philosophisch-Naturwissenschaftlichen Fakultät

der Universität Basel

von

Christoph von Arx

aus Olten, Schweiz

Basel, 2018

Originaldokument gespeichert auf dem Dokumentenserver der Universität Basel

edoc.unibas.ch

Genehmigt von der Philosophisch-Naturwissenschaftlichen Fakultät auf
Antrag von:

Prof. Dr. Urs Jenal

Prof. Dr. Marek Basler

Basel, den 14.11.2017

Prof. Dr. Martin Spiess

Dekan

ABSTRACT

Proliferation by cell division is essential for all living organisms and needs to be tightly controlled. While much is known about metazoan development, cell cycle control in bacteria is less well understood. The bacterial cell cycle is divided into three stages, the period from birth until the initiation of chromosome replication (G1); chromosome replication (S); and the time between the completion of replication and the end of cell division (G2). The lengths of G1 and the G1-to-S phase transition largely determine bacterial proliferation rates as the S and G2 periods remain essentially constant over a wide range of growth rates. Although recent work has improved our understanding of cell growth and cell cycle progression, a molecular frame of the regulatory network driving G1/S transition is still largely missing. *Caulobacter crescentus* strictly separates its cell cycle stages in an eukaryote-like manner, initiating chromosome replication only once per division cycle. Moreover, *Caulobacter* divides asymmetrically to generate a replication-competent stalked cell (ST) and a morphologically distinct replication-inert swarmer cell (SW). The latter remains in G1 for a defined period of time before differentiating into a ST cell, a process that is coupled to the initiation of chromosome replication. These unique features make *C. crescentus* a prime model organism to study bacterial cell cycle control.

Recent findings suggest that *C. crescentus* cell cycle progression is controlled by oscillating levels of the second messenger c-di-GMP. While c-di-GMP levels are low in SW cells, a sharp c-di-GMP increase directs the SW-to-ST cell transition and mediates S-phase entry when levels of the second messenger peak in stalked cells. In particular, c-di-GMP switches the cell cycle kinase CckA from kinase to phosphatase mode, thereby inactivating the response regulator CtrA, which in its phosphorylated form acts as a replication initiation inhibitor. Here we add another layer of c-di-GMP mediated cell cycle control. We show that c-di-GMP orchestrates the G1/S specific gene expression program by activating the ShkA-TacA phosphorylation pathway. The phosphorylated form of TacA, TacA~P, acts as a transcription factor for several genes involved in the morphogenetic program and in preparing cells for S phase entry. A combination of genetic and biochemical experiments revealed that c-di-GMP controls the ShkA-TacA pathway by directly binding to the ShkA sensor histidine kinase to strongly stimulate its kinase activity. Upon c-di-GMP mediated autophosphorylation, ShkA transfers phosphate to its C-terminal receiver domain from where it is passed on via the phosphotransfer protein ShpA to the transcription factor TacA. We demonstrate that c-di-GMP binds to a pseudo-receiver domain, which is positioned between the kinase core and the

receiver domain and inhibits ShkA kinase activity. Alleviated ShkA auto-inhibition leads to the activation of the ShkA-TacA pathway. We show that c-di-GMP-mediated activation of ShkA and the subsequent c-di-GMP mediated proteolysis of ShkA together define a window of ShkA activity during the cell cycle. The activity of this pathway is further sharpened to a narrow G1/S specific period by TacA degradation, which precedes the degradation of ShkA. Thus, *C. crescentus* orchestrates G1/S specific gene expression in high temporal resolution through a combination of c-di-GMP mediated activation and degradation of ShkA-TacA phosphorylation components. Because ShkA binds c-di-GMP with higher affinity than CckA, the ShkA-mediated G1/S transcriptional network precedes the CckA switch leading to chromosome replication initiation as c-di-GMP levels are building up during the cell cycle. Together, these results propose a model, where an upshift of c-di-GMP drives consecutive steps of the G1/S cell cycle progression in *C. crescentus* by sequentially activating hierarchized phosphorylation pathways.

CONTENTS

1	INTRODUCTION	1
1.1	Regulation of cell cycle progression	1
1.2	Systems to transfer information across the membrane	2
1.3	Proteolysis	9
1.4	Second messengers in bacteria	10
1.5	Alphaproteobacteria	13
1.6	Caulobacter crescentus	14
1.7	Caulobacter crescentus cell division	16
2	AIM OF THE THESIS	22
3	PROJECT ABSTRACT	23
4	PROJECT INTRODUCTION	24
5	RESULTS	28
5.1	C-di-GMP controls the ShkA-TacA phosphorelay	29
5.2	C-di-GMP stimulates ShkA kinase activity	33
5.3	C-di-GMP binding alleviates ShkA auto-inhibition	36
5.4	C-di-GMP binds to the ShkA REC1 pseudo-receiver domain	40
5.5	C-di-GMP-mediated activation and proteolysis defines the ShkA-TacA activity window during the cell cycle	45
5.6	The ShkA-TacA pathway limits gene expression to G1/S	48
6	DISCUSSION & OUTLOOK	53
7	MATERIAL & METHODS	59
7.1	Strains used in this study	59
7.2	Plasmids	61

7.3	Growth conditions	69
7.4	Phos-Tag immunoblotting	70
7.5	Immunoblotting	70
7.6	Capture Compound Mass Spectrometry (CCMS)	70
7.7	Protein expression and purification	71
7.8	Kinase in vitro assays	71
7.9	Isothermal titration calorimetry (ITC) measurements	71
7.10	β -galactosidase measurements	72
7.11	Microscopy	72
7.12	Selection/screen for c-di-GMP independent mutations in shkA	72
8	REFERENCES	74
9	ACKNOWLEDGMENTS	87
10	CURRICULUM VITAE	88

1 INTRODUCTION

Bacteria are omnipresent in our environment and can survive and grow almost everywhere, even in extreme environments¹. To live in different niches, bacteria have evolved a high variety of specialized enzymes, that can even be used in biotechnological applications². Some industries rely heavily on bacteria, which are important for the treatment of wastewater³ or can be used to produce antibiotics. Bacteria can also be utilized for the production of amino acid on a million-ton scale, for example to produce the flavor enhancer Glutamic acid⁴. Traditionally, bacteria are an important component in the production of foods like yoghurt, cheese, sourdough, sauerkraut, or kimchi.

Colonizing almost every ecosystem, bacteria are heavily involved in forming the biosphere of our planet. In the holobiont, the ecological system formed between plants and their microbiome, plants and bacteria influence each other and are interdependent⁵. On the other hand, bacteria can have a negative effect on plant growth, for example by leading to losses in food harvest⁶. Likewise, bacteria reside in and on the bodies of animals and humans. Bacteria can live in symbiosis with the animal or human hosts, affecting the metabolism and immune system positively⁷. Conversely, pathobionts invading the host's microbiota can lead to infections.

Because bacteria influence humans and their environment in so many ways, deepening our understanding of bacterial growth and behavior is essential for our well-being. Among others, this knowledge will help us to find treatments for infections, improve crop harvest, optimize industrial processes, and possibly solve the energy needs of our industrialized societies.

1.1 REGULATION OF CELL CYCLE PROGRESSION

Proliferation by cell division is essential for all living organisms and needs to be tightly controlled to provide appropriate numbers of specialized cells and to avoid pathological side effects like cancer. In metazoan tissue, stem cells need to proliferate and specialize. Coordinating cell division and cell differentiation is thereby central⁸. In eukaryotic cells, a highly complex network of cyclin-dependent kinases and protein degradation drives the process of the unidirectional cell cycle transition. Different cyclins oscillate to time the different stages in eukaryotic cell division. This process begins with the synthesis of specific cyclins at the beginning of the next cell cycle phase. These cyclins then activate cyclin-

dependent kinases (Cdks) by binding to them. The so formed cyclin-Cdks complexes regulate specific events to progress the cell cycle like chromatin remodeling or centrosome duplication. Degradation then removes the current cyclin and thereby deactivates the Cdks. This allows the next cyclin to take over⁹.

Conceptually, the aquatic bacterium *Caulobacter crescentus* controls cell cycle progression similarly to eukaryotes. In *C. crescentus*, three regulatory mechanisms drive the unidirectional cell cycle progression: A complex network of two-component systems advances cell division, and proteolysis specifically removes proteins that are not needed anymore. The third regulatory mechanism consists of the oscillating bacterial second messenger c-di-GMP to orchestrate the timing of cell cycle progression¹⁰. The following chapters will introduce each of these mechanisms in detail.

1.2 SYSTEMS TO TRANSFER INFORMATION ACROSS THE MEMBRANE

1.2.1 One-component systems

The most widely used mechanism for prokaryotes to sense their environment is by utilizing one-component signaling systems. These systems consist of proteins with two specialized domains: An external input domain that senses a specific environmental signal, and an internal output domain that leads to a cellular response (Figure 1.1). One-component systems can sit in the membrane and sense environmental stimuli. The corresponding output is often carried out by a HTH domain that can bind to a ligand or DNA. For example, ToxR is a transmembrane transcription factor regulating virulence in *Vibrio cholerae*. ToxR consists of a cytosolic DNA binding domain and a periplasmic domain that senses pH and bile salts¹¹. In a similar way, CadC in *Escherichia coli* also senses pH and induces the transcription of stress response genes¹². One-component systems are encoded in the genomes of almost all bacteria and archaea¹³. This is exemplified by the archaeon *Sulfolobus acidocaldarius* that regulates swimming with the one-component system ArnR¹⁴.

Proteins with a similar architecture can also remain in the cytosol where they bind environmental cues that can penetrate the cell envelope or are imported. One example for a cytosolic one-component regulator is the tetrameric *E. coli* protein LacI. LacI binds to the promoter of the *lac* operon and inhibits transcription by forming a DNA loop¹⁵. In its DNA bound form, the LacI tetramer is stabilized by interactions between the regulatory domains. Binding of the LacI substrate allolactose or IPTG induces a hinge-like motion within the protein,

releasing this interaction. This leads to a conformational change in the DNA-binding domain, releasing LacI from the DNA¹⁶.

One-component systems that reside in the membrane are limited in binding to DNA, while cytoplasmic one-component systems are restricted in sensing the outside. This limitation likely led to the evolution of two-component systems. In those systems, the input and the output domain are separated, and phosphorylation links the two proteins together. This separation allows the input domain to sit in the membrane, interacting with signals from the outside, while the output domain remains in the cytoplasm and can directly interact with DNA¹⁷.

1.2.2 Two-component systems and phosphorelays

Similar to one-component systems, two-component systems allow bacteria to respond to their environment. These systems fulfill many roles in cellular signaling circuits. The most basic set-up consists of two proteins, the histidine kinase (HK) and the response regulator (RR). A sensor HK usually has an input domain and always two kinase domains, the catalytically active CA domain and the DHp domain with a conserved His residue that can be phosphorylated. The RR contains a highly conserved receiver domain with an Asp residue onto which the phosphate is transferred. This leads to a conformational change and an output (see below and Figure 1.1). Sensor histidine kinases can react to a wide variety of inputs, from light, temperature or gas to specific low molecular weight molecules like amino acids or nucleotides¹⁸. Upon sensing a signal, the HK autophosphorylates on the conserved His residue. Subsequently, the phosphate is then transferred to an Asp residue on the RR, which in turn activates an effector domain to carry out a task¹⁹. The basic two-component system can be adapted to a more complex phosphorelay (Figure 1.1). In this case the phosphorylation scheme is His→Asp→His→Asp over multiple proteins. Phosphorelays often involve hybrid kinases in which the histidine kinase and the first receiver domain are fused together, and phosphotransfer proteins that shuttle the signal to the response regulator²⁰. These more complex systems can be used to branch a signal to multiple response regulators (one-to-many), for example in the *E. coli* chemotaxis pathway, or to integrate signals from multiple kinases on one response regulator (many-to-one)²¹. One example for a one-to-many pathway can be found in the central *C. crescentus* CckA-ChpT-CtrA pathway (see below). Here the phosphotransfer protein ChpT donates phosphoryl groups to the response regulators CtrA and CpdR, which act as transcription factor and as protease adaptor, respectively²².

The function of a response regulator is ultimately determined by the biochemical activity of its output domain. These are diverse but consist mostly (63 %) of DNA binding domains²³. These

domains include the OmpR-like winged-helix domain, the NarL four-helix helix-turn-helix domain, the NtrC-like helix-turn-helix domain and the LytR-like DNA binding domain with an unusual β -fold²³. Alternatively, these domains can mediate protein-protein interactions²⁴ or have an enzymatic output. For instance they can produce second messengers like bis-(3' 5')-cyclic diguanylic acid (c-di-GMP) with a dedicated GGDEF domain²⁵. Members of this protein family lacking an output domain are called single domain response regulators and can have multiple cellular functions. A prominent example is the *E. coli* chemotaxis protein CheY that mediates motility control via its interaction with the flagellar motor switch²⁶ (Chapter Chemotaxis, Page 7) or DivK from *C. crescentus*, which in its phosphorylated form allosterically controls the activity of a histidine kinase, thereby interconnecting two phosphorylation pathways²⁷ (see below).

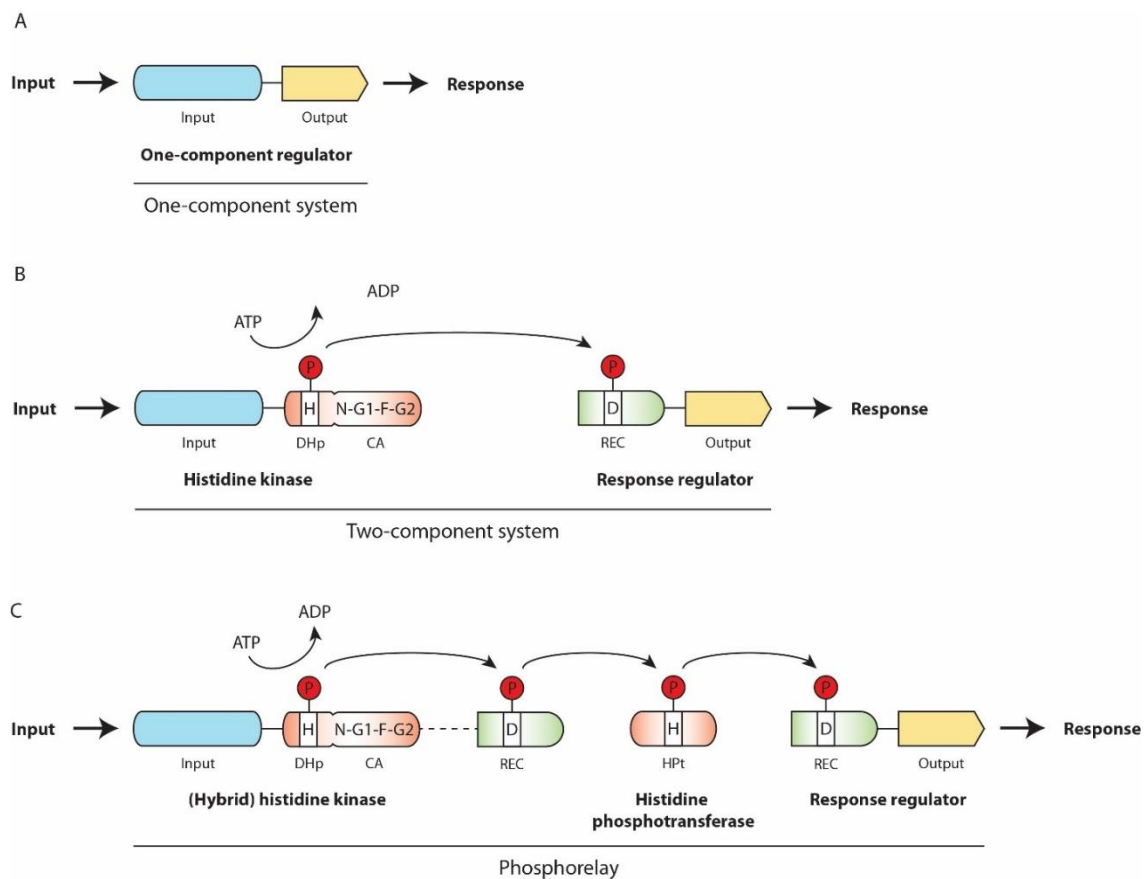


Figure 1.1: Schematic diagrams of a one-component system, a two-component system and a phosphorelay. (A) The most basic signaling system comprises of a single protein with an input domain and an output domain. (B) In general, two-component systems consist of a histidine kinase and a response regulator. The CA domain of the histidine kinase binds ATP with the highly conserved N, G1, F, and G2 box. The phosphate is transferred to the His residue of the DHp domain. The phosphate is then transferred to the Asp residue on the receiver domain of the response regulator. (C) The more complex phosphorelay extends on the two-component system in a highly modular fashion. With an additional receiver domain that is often fused to the histidine kinase, and a histidine phosphotransferase, the phosphorylation scheme is His-Asp-His-Asp over multiple proteins. Adapted from^{13,23}.

Many sensor histidine kinases are bifunctional enzymes that can also act as phosphatases^{28,29}. This allows the pathway to suppress nonspecific phosphorylation of its own response regulator. Additionally, by switching a sensor histidine kinase from its kinase to its phosphatase mode, the cellular function controlled by this pathway can be quickly and efficiently shut off³⁰.

Two-component systems are widely distributed in bacteria and are also found in all other domains of life. Their modular architecture makes histidine kinases and response regulators versatile signaling pathways, connecting a large variety of upstream signals with different downstream processes. However, even though input and output mechanisms are different, structure and function of the central domains involved in phosphorylation are well conserved²³. Histidine kinases form homodimers and two domains define the cytoplasmic kinase core. The CA domain is catalytically active and binds ATP. Structurally it consists of a five-stranded β -sheet and three α -helices packed against it that form an α/β -sandwich³¹. This domain contains specific motifs, the N, G1, F, and G2 box, that form a highly conserved ATP binding cavity³². The phosphate is then transferred to the conserved His residue that resides in the DHp domain (Figure 1.1). This central kinase domain is responsible for dimerization, phosphotransfer and phosphatase activity. The DHp consists of two α -helices that form a four-helix bundle with the other protomer^{33,34}. A conformational change between the CA and the DHp domain, mediated by the input domain, regulates autophosphorylation by moving the CA domain towards the DHp domain³⁵. The conformation of the loop at the base of the helical DHp dimerization domain determines whether the histidine kinase autophosphorylates in *trans* or in *cis*³⁶. The catalytic mechanism of autophosphorylation is independent of *cis*- or *trans*-directionality, however it might be important for response regulator specificity³⁷. The process of autophosphorylation and phosphotransfer is separated, as phosphotransfer requires the movement of the CA domain to free the access to the phosphorylated His residue for the receiver domain. However, these two reactions still occur simultaneously in neighboring protomers of a dimer. Each protomer then switches to take over the function of the other protomer with a conformational change, a process that might be triggered by the interacting receiver domain³⁸. To control the activation of the pathway, two-component systems often display phosphatase activity. The phosphate travels back from the response regulator and is removed by the DHp domain of the histidine kinase. However, this is not just a reversal of kinase activity, as the His residue of the DHp domain is not phosphorylated in this

process³⁹. Nonetheless, it was shown that conserved key residues in the DHP domain are necessary for phosphatase activity⁴⁰.

The abundance of two-component systems in many bacteria requires high specificity to avoid crosstalk between different signaling pathways. A small subset of coevolving residues in the interface of histidine kinases and response regulators is enough to determine specificity⁴¹. These amino acids can be artificially exchanged to change specificity of a histidine kinase to another response regulator⁴². Response regulators themselves contain highly conserved receiver domains, formed by a central five-stranded parallel β -sheet and five α -helices surrounding it⁴³. Receiver domains are not passive, they catalyze their own phosphorylation and dephosphorylation reactions. For this reaction five essential residues are necessary: A divalent metal ion required for phosphorylation is bound by three Asp residues, while Lys and Thr/Ser residues are crucial for signal transduction⁴⁴. Phosphorylation leads to a conformational change of the distal α 4- β 5- α 5 surface, which in turn mediates interaction with the neighboring output domain protomer or with other proteins⁴⁵.

Examples of receiver domains without the key residues for phosphorylation can be found in multiple species^{46,47}. Pseudo-receiver domains can act as sensory domains. CikA, a protein of *Synechococcus elongates* circadian system contains a pseudo receiver domain that binds a small organic quinone molecule. Upon binding of its ligand, the protein becomes quickly degraded. This allows the cell to measure light indirectly over the cells redox state⁴⁸. Similarly, it was shown recently that a subclass of CheY-like single domain response regulators interact with the flagellar motor not in response to phosphorylation, but in response to binding c-di-GMP (Nesper *et al.* 2017, in revision).

In the more complex phosphorelays, as represented for example by the CckA-ChpT-CtrA pathway in *C. crescentus*, a histidine phosphotransferase shuttles the phosphate from the (hybrid) histidine kinase to the response regulator (Figure 1.1). Two different types of phosphotransferases can be found in bacteria: dimeric transferases like ChpT and monomeric transferases like ShpA from the *C. Crescentus* ShkA-TacA pathway. ChpT structurally represents a histidine kinase, the CA domain however is not functional. The site of phosphorylation resembles a dimeric four-helix bundle similar to a DHP domain⁴⁹. The monomeric ShpA also forms a four-helix bundle, but different to ChpT it has no degenerate CA domains⁵⁰.

1.2.2.1 Chemotaxis

The best understood example of bacterial signal transduction is chemotaxis. Many free-swimming bacteria and archaea move towards attractants, or away from repellents, by sensing molecule concentrations. *E. coli* perform a biased random walk by measuring changes of gradients while swimming in one direction. Worsening conditions or no gradient change leads to earlier tumbling and directional change. This means bacteria can sense current ligand concentrations and remember past ligand concentrations at the same time⁵¹. Transmembrane chemoreceptors, called methyl-accepting chemotaxis proteins (MCPs), mediate this behavior. MCPs form a complex together with the histidine autokinase CheA and its regulator CheW. Phosphorylation activity of CheA is dependent on ligand binding and receptor sensitivity, which in turn is regulated by methylation of specific modification sites. Methylation of these sites decreases receptor sensitivity to its ligand, likely by inducing conformational changes⁵².

Without ligand, CheA is active and phosphorylates the response regulator CheY, which interacts with the flagellar motor to induce tumbling. After ligand binding of the MCP, the kinase is turned off, leading to dephosphorylation of CheY by the phosphatase CheZ and subsequently longer swimming phases. In this state, the methyltransferase CheR decreases sensitivity of the MCP to its ligand by methylating specific sites in the dimer. The subsequent loss of ligand binding means that a steady or decreasing ligand concentration activates CheA. As a consequence, CheA phosphorylates and thereby activates the methylesterase CheB. The removal of methyl-residues increases MCP sensitivity once again. In addition, CheA activity also induces tumbling, allowing the bacterium to change direction. This feedback loop leads to a memory of a few seconds⁵³ (Figure 1.2).

Although MCPs in *E. coli* are the most studied and best understood, this unique prokaryotic chemotaxis system is highly conserved in bacteria genomes⁵⁴. In *C. crescentus*, chemoreceptors are expressed only in the swarmer cells and localized to the flagellar pole where they are partially ordered in a complex array, similar to other bacteria⁵⁵. *E. coli* MCPs expressed in *C. crescentus* are localized to the same pole, further emphasizing the highly conserved nature of these receptors⁵⁶. Initial binding of a ligand leads to a small conformational change within the receptor dimer. This conformational change is then transmitted through the entire array, greatly amplifying the initial signal⁵⁷.

Next to many repellents and attractants like sugars and other nutrients, bacterial chemotaxis can also react to AI-2, a general signal of quorum sensing⁵⁸.

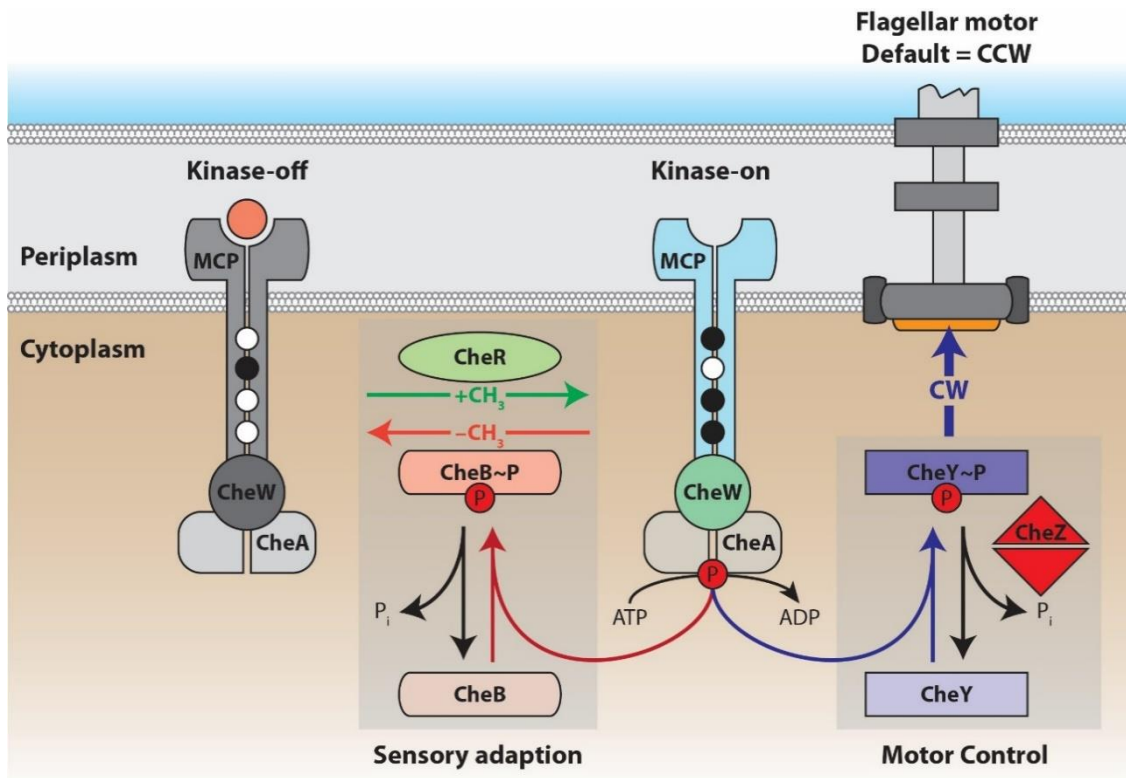


Figure 1.2: Chemotaxis pathway: Methyl-accepting chemotaxis proteins (MCPs) form a complex with the histidine autokinase CheA and its regulator CheW. CheA is only active when no ligand is bound to the MCP and its phosphorylation activity controls two separate modules: (1) Motor control and (2) sensory adaption. (1) Motor control is achieved by the phosphorylation of the response regulator CheY. CheY switches the flagellar motor from a CCW rotation to CW rotation, leading to tumbling. When no ligand is bound and CheA is inactive, the phosphatase CheZ inactivates CheY, leading to a longer swimming phase. (2) Sensory adaption allows the bacterium to respond to ligand gradients. Without a ligand bound, CheA phosphorylates the methylesterase CheB, thereby activating it. Removal of methyl-residues from the MCP increases its sensibility until it can bind a ligand. This deactivates CheA and allows CheR to methylate the MCP to decrease sensibility of the ligand. Together, these two modules allow the adaption to molecule gradients. If a ligand concentration remains steady or decreases, MCP sensibility will decrease and induce tumbling, while at the same time increasing MCP sensibility again. Adapted from⁵⁷.

1.2.2.2 Chemoreceptors with other functions

Apart from the mediation of chemotaxis, chemoreceptors can also have other functions, many of them unknown. Chemoreceptors are structurally diverse and frequently found in bacteria⁵⁹. In *Pseudomonas aeruginosa*, the Wsp signal transduction complex is homologous to chemoreceptor systems mediating chemotaxis. However, in this case activation of the chemoreceptor WspA leads to an increase of biofilm formation⁶⁰. The homologue of CheY in this system, WspR, has a GGDEF-domain that produces c-di-GMP. WspA is very similar to other MCPs, but it is not localized to the cell pole due to few amino acid changes⁶¹. Another example in the same bacterium is the Chp system. Upon receiving its signal, it modulates cAMP levels and twitching motility⁶².

1.3 PROTEOLYSIS

For all domains of life, it is a necessity to remove proteins in a controlled fashion. Protein homeostasis must be upheld by the degradation of damaged proteins or protein fragments from mistranslation or cleavage. Just as important is protein degradation to control cellular processes like cell-cycle progression or differentiation, and degradation as a stress response. Responsible for the active removal of proteins are oligomeric AAA+ proteases⁶³. Numerous AAA+ protease complexes exist in bacteria with the basic architecture of an AAA+ ring that denatures proteins, and a compartmental protease degrading the proteins⁶⁴. In the paradigmatic AAA+ protease ClpXP complex, the chaperone ClpX targets specific proteins to deliver them to the protease ClpP. ClpXP can thereby even degrade aggregated proteins that form under stress conditions⁶⁵. In *C. crescentus*, ClpXP is essential. This is due to the toxin SocB that accumulates and leads to cell death without degradation by ClpXP. If SocB is lacking, ClpX can be deleted, however affected cells show deficits in growth and morphology⁶⁶.

ClpX recognizes proteins by short and unstructured peptide sequences. One example is the SsrA-tag in *E. coli* that is recognized by both ClpXP and ClpAP. The SsrA tag is added to proteins when translation is stalling and allows the cell to quickly remove these potentially harmful protein fragments⁶⁷. Another example is the phage protein MuA, which is also recognized by ClpXP⁶⁸. In total, ClpXP binds to at least five different degradation motifs, three N-terminal and two C-terminal. The C-terminal motifs share either homology with the hydrophobic SsrA recognition motif (**LAA-COOH**) or the MuA recognition motif (**RRKKAI-COOH**)⁶⁹. Two proteins that are targeted by ClpXP with an SsrA homology motif are the *C. crescentus* proteins CtrA (**NAA-COOH**) and TacA (**EAG-COOH**). This specificity can be negated with a double mutation of the C-terminus to the negatively charged amino acid aspartic acid, for example in TacA with **EAG-COOH** to **EDD-COOH**⁷⁰.

The SsrA tag requires another protein, SsrB, to be efficiently targeted to its protease. SsrB thereby acts as an adaptor of SsrA⁷¹. Adapter proteins expand and diversify the substrate recognition capabilities of proteases and allow specific cell responses to altering conditions⁷². In the Gram-positive bacterium *Bacillus subtilis*, CtsR is a repressor of *clp* gene expression and therefore proteolysis. CtsR is active at a basal level under normal conditions. When exposed to stress, the protein McsA was found to activate the adapter protein McsB. McsB targets CtsR to the protease ClpCP where it is degraded. Subsequently, this allows the upregulation of stress response genes⁷³. Adaptor proteins can also modulate protease specificity directly. The

adaptor ClpS binds to the protease ClpAP and inhibits degradation of SsrA-tagged proteins. At the same time, ClpS enhances degradation of protein aggregates⁷⁴.

Protein degradation is often part of cell cycle regulation and then needs to be exactly timed and regulated. This additional level of control can also be achieved with adaptor proteins, allowing the degradation of a specific target at a specific time⁷⁵. The adaptors themselves are also degraded by ClpXP, however they are shielded from degradation by binding their specific substrate⁷⁶.

1.4 SECOND MESSENGERS IN BACTERIA

1.4.1 The role of c-di-GMP

C-di-GMP was first described as a regulator of cellulose synthesis in *Acetobacter xylinum*⁷⁷, and is now recognized as a major second messenger that coordinates major decisions in bacterial life style and in cell cycle progression⁷⁸. In general, cells low on c-di-GMP are motile, while a c-di-GMP increase switches the cell to a sessile lifestyle in multicellular biofilms (Figure 1.3). In addition, c-di-GMP is thought to be involved in regulating virulence. While motile low-c-di-GMP bacteria are responsible for acute infections, high-c-di-GMP cells are involved in chronic infections⁷⁹.

The second messenger c-di-GMP itself consists of two guanine bases that are linked to a cycle by ribose and phosphate⁸⁰. It was suggested that c-di-GMP binds to its target likely as a dimer⁸¹. However, under physiological conditions c-di-GMP is most likely available as a monomer⁸². Within the bacterial cell, c-di-GMP levels and the complex, corresponding responses are regulated by the antagonistic action of diguanylate cyclases that produce c-di-GMP, and phosphodiesterases that degrade c-di-GMP^{77,83,84} (Figure 1.3). These proteins are widespread and abundant in bacterial genomes⁸⁵.

The asymmetric cell cycle of *C. crescentus* is strongly dependent on c-di-GMP with the swarmer cell having low levels and the predivisional and stalked cell having higher levels of c-di-GMP⁸⁶. A mutant strain lacking all diguanylate cyclases (cdG^0) loses cell polarity and cell differentiation, expresses no stalks, pili, holdfast, or flagellum, resulting in a phenotype of elongated and apolar cells⁸⁷.

While c-di-GMP is abundant in the phylum *Proteobacteria*, c-di-GMP is absent in other phyla like *Bacteroidetes* or *Fusobacteria*⁸⁸. However, these bacteria could potentially be controlled by other second messengers like c-di-AMP. Interestingly, in some bacteria of the phyla

Firmicutes and *Actinobacteria*, both signaling systems, c-di-AMP and c-di-GMP, might be present⁸⁹.

1.4.2 Diguanylate cyclases and phosphodiesterases

Diguanylate cyclases contain a GGDEF domain which is necessary for c-di-GMP production⁹⁰. GGDEF domains are highly conserved over bacterial kingdoms and the domain itself is sufficient for c-di-GMP production, however regulatory domains are necessary for high activity⁹¹. GGDEF domains act in a similar way as adenylate cyclases, however with a different nucleotide-binding mode. For c-di-GMP synthesis, two GGDEF domains are necessary, requiring dimerization of the diguanylate cyclases⁹². For c-di-GMP formation, it is likely that two GTP molecules have to be arranged in an antiparallel orientation by the GGDEF domains⁹³. Different mechanisms have evolved to achieve this interaction between GGDEF domains that provide a regulatory basis for c-di-GMP synthesis⁹⁴. Additional control of c-di-GMP production is provided by allosteric inhibition of some GGDEF domains by c-di-GMP itself⁹⁵.

As direct antagonists to diguanylate cyclases, phosphodiesterases hydrolyze c-di-GMP. One major class of phosphodiesterases contains an EAL domain. This domain hydrolyzes c-di-GMP into linear dimeric GMP (pGpG) in an Mg²⁺ or Mn²⁺ dependent manner. In contrast, Ca²⁺ can inhibit phosphodiesterase activity⁹⁶. The activity of some phosphodiesterases is dependent on allosteric activation by GTP. In this case, inactive GGDEF domains can regulate EAL domains by binding the required GTP⁹⁷. Activity of EAL domains can be regulated by conformational changes induced by an input domain that catalytically optimizes the active site. This is the case in the light-sensing protein BlrP1 in *Klebsiella pneumoniae*⁹⁸. The product of phosphodiesterases with EAL domains pGpG needs to be further hydrolyzed. In *P. aeruginosa*, the oligoribonuclease Orn can degrade pGpG to two GMPs and thereby remove pGpG from the cell⁹⁹.

Another widely distributed type of phosphodiesterases utilizes HD-GYP domains to directly convert c-di-GMP to two GMPs¹⁰⁰. However, a first hydrolysis step produces pGpG. HD-GYP domains can also accept pGpG as a primary substrate and further hydrolyze it to two GMPs^{101,102}.

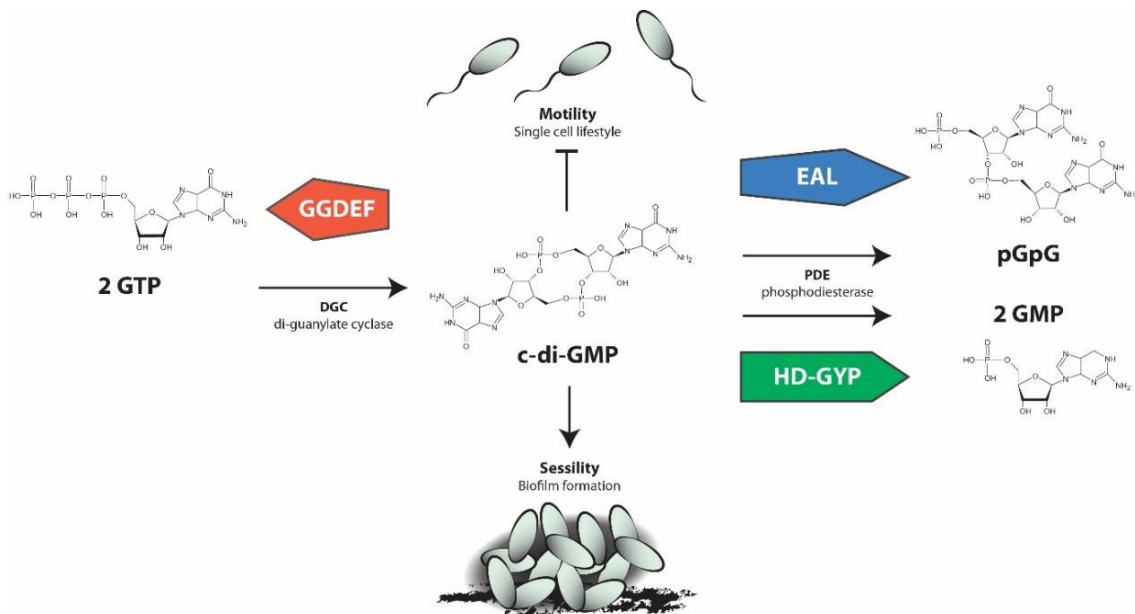


Figure 1.3: Diguanylate cyclases containing a GGDEF domain produce c-di-GMP from two GTP molecules. Removal of c-di-GMP is carried out by phosphodiesterase with either an EAL domain, producing linear dimeric GMP (pGpG), or an HD-GYP domain that hydrolyzes c-di-GMP to two GMP in a two-step process. High cellular c-di-GMP levels are generally associated with a decreased motility, biofilm formation and modulated virulence.

1.4.3 C-di-GMP receptors

A broad variety of c-di-GMP receptors can be found in bacteria. A strong and common c-di-GMP receptor is resembled by PilZ domain proteins that can be found in various bacterial species⁸⁴. PilZ domains can be dimeric or monomeric and express a wide-range of mechanistic principles and binding stoichiometries. However, in general they lead to a allosteric rearrangement with a hinge-like movement, after c-di-GMP binds to the PilZ signature consensus RxxxR¹⁰³.

GGDEF domains can also bind c-di-GMP and act as receptors⁹⁵. An example of a c-di-GMP receptor with a degenerated GGDEF motif, which is catalytically inactive, is the *C. crescentus* adaptor-protein PopA¹⁰⁴. In a similar way, degenerate phosphodiesterases can act as a c-di-GMP receptors with an inactive EAL domain. This is the case for FimX, a *P. aeruginosa* protein¹⁰⁵.

It is important to note, that many c-di-GMP receptors do not show a common motif or a conserved domain. An example without a general c-di-GMP-binding domain can be found in *P. aeruginosa*, where the transcriptional regulator FleQ is de-repressed upon binding to c-di-GMP¹⁰⁶. In *C. crescentus*, the histidine kinase CckA binds c-di-GMP on its CA domain. This leads to an interaction with the DHp domain that allows the kinase to switch from a kinase to a phosphatase state²⁹.

Not only proteins can bind c-di-GMP. A special class of c-di-GMP binders is represented by RNA molecules. C-di-GMP binding bacterial riboswitches are highly specific and can undergo a global structural rearrangement upon ligand binding¹⁰⁷. Riboswitches can have multiple functions and c-di-GMP binding can regulate transcriptional regulation or translation¹⁰⁸. One example is the *Vibrio cholerae* class I riboswitch Vc1 that, in response to c-di-GMP, positively regulates downstream gene expression of a colonization factor¹⁰⁹.

1.4.4 Alternative second messengers in bacteria

Apart from c-di-GMP, many more linear and cyclic nucleotides are known to act as second messengers in bacteria. These signals include cAMP¹¹⁰, cGMP¹¹¹, (p)ppGpp¹¹², c-di-AMP¹¹³ and even hybrid cyclic AMP-GMP molecules¹¹⁴ that are involved in pathogenicity of bacteria¹¹⁵.

The second messenger cAMP was first described as an alarmone in *E. coli*, that responds to glucose levels¹¹⁶. In low-glucose conditions, cAMP is produced by an adenylate cyclase and regulates biofilm formation positively¹¹⁷. However, cAMP is recognized as an essential signal involved in bacterial virulence in several pathogens by now¹¹⁸.

The linear nucleotide (p)ppGpp is another alarmone that is synthesized under stress conditions or during starvation. Thereby, (p)ppGpp can have a multitude of effects on bacteria including development and virulence¹¹⁹. In *C. crescentus*, the enzyme SpoT synthesizes (p)ppGpp under starving conditions. Increasing levels of the (p)ppGpp alarmone influence levels of the proteins DnaA and CtrA directly, inhibiting G1-to-S phase transition and keeping the cell in the swarming state¹²⁰.

Several Gram-positive bacteria were shown to use the second messenger c-di-AMP. There, c-di-AMP can control essential processes like cell wall homeostasis or ensures DNA integrity⁸⁹. In *Bacillus subtilis* and related pathogens, c-di-AMP is essential and controls potassium homeostasis¹²¹.

As many of those molecules were only discovered recently and considering the abundance of GGDEF domains in bacterial genomes¹²², it is likely that even more roles of second messenger signaling in bacteria will emerge in the future.

1.5 ALPHAPROTEOBACTERIA

Alphaproteobacteria is an omnipresent class of gram-negative bacteria with diverse ecological niches, from free-living environmental species to host-associated pathogens¹²³. For example, the intracellular pathogen *Rickettsia prowazekii* that is responsible for epidemic typhus in

humans¹²⁴, is also thought to be a close ancestor to mitochondria¹²⁵. *Alphaproteobacteria* can have positive or negative effects on plants. The plant family Leguminosae can form a specific symbiose with many different Rhizobiales, for example *Rhizobium*, to fix atmospheric nitrogen¹²⁶. However, plants can be affected by the pathogen *Agrobacterium tumefaciens* that can ontogenically transform plant cells¹²⁷. Some *Alphaproteobacteria* can grow under extreme conditions, like *Polymorphobacter multimanifer* that lives within stones in Antarctica¹²⁸.

Even though there is a high diversity in *Alphaproteobacteria*, the cell cycles of bacteria in this class still rely on similar mechanisms with conserved central pathways¹²⁹. The oligotrophic bacterium *C. crescentus* is a bacterial model organism with an obligate asymmetric cell division that gives rise to two distinct cell types, a motile replication-inert swarmer cell and a sessile replication-competent cell^{130,131}.

1.6 CAULOBACTER CRESCENTUS

The ubiquitous *Caulobacter* genus was initially defined by the ability to form stalks¹³². Stalks are cell envelope extensions that are always polar in *Caulobacter*, however can also be subpolar or bipolar in another *Alphaproteobacterium* genus, *Asticcacaulis*¹³³. The stalk of *Hyphomonas neptunium*, also belonging to the same genus, is directly involved in cell division. This bacterium uses a budding mechanism, in which the daughter cell grows at the end of the stalk. In this asymmetric process, the emerging cell does not have a stalk¹³⁴. In *C. crescentus*, stalks are the hallmark of the replication-competent cell type. The cytoplasmic composition of the stalk lacks most proteins of the cell body, however it includes proteins for nutritional uptake¹³⁵. In addition, the long and thin form of the stalk is ideal for the uptake of diffusing nutrients¹³⁶. The end of the stalk consists of a strong adhesive holdfast, allowing the bacterium to attach to surfaces^{137,138}.

After cell division, genome replication is inhibited in the motile swarmer cell (G1 phase). During the irreversible transition into a sessile stalked cell (S phase), the cell starts the replication cycle. Swarming daughter cells are then shed off from the opposite pole of the stalk¹³⁹ (Figure 1.4). If the new-born swarmer cell is in contact with a surface, a holdfast is immediately formed¹⁴⁰. The characteristic curved (crescent) shape of *C. crescentus* helps the predivisional cell to contact the surface, enhancing colony formation¹⁴¹.

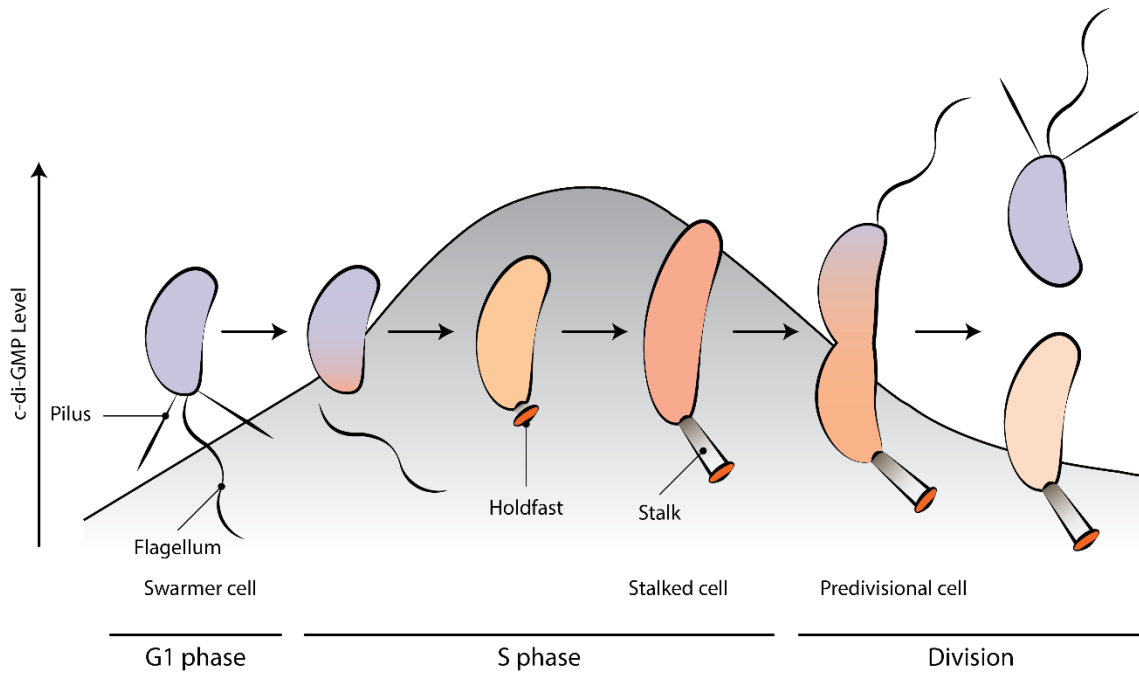


Figure 1.4: The *C. crescentus* cell cycle: Motile swarmer cells differentiate to sessile stalked cells by losing the flagellum and pili, replacing them with a holdfast and later the stalk. The stalked cell begins replication of the genome, initializing an asymmetric cell division. The stalked cell remains replication-competent, while the daughter cell differentiates into a replication-inert swarmer cell. The orange color indicates rising c-di-GMP levels during G1-to-S phase transition, while the swarmer cell does not have c-di-GMP (blue). The peak of c-di-GMP levels is qualitatively shown as a grey curve.

1.7 CAULOBACTER CRESCENTUS CELL DIVISION

To undergo the complex process of cell differentiation and division, *C. crescentus* uses an intricate set of mechanisms that is tightly controlled. Protein expression, levels of c-di-GMP and protein degradation together irreversibly allow the cell to transit through G1-to-S-phase. The following chapters describe the *C. crescentus* cell division in detail.

1.7.1 The initiation of chromosome replication

A central step of cell division is the controlled replication of the chromosome. In bacteria, a single origin of replication (*oriC*) acts as starting site for chromosome replication. This genetic region likely encodes species-specific instructions for the binding and regulation of proteins that form the initiation complex. Core of the initiation complex is the initiator protein DnaA. The *dnaA* gene is present in almost all bacteria with the exception of few obligate endosymbiotic species¹⁴².

As an AAA+ type protein, DnaA binds ATP with high affinity and after reaching peak level, forms multimeric complexes on the *oriC* region. Mediated by this complex and other proteins, duplex DNA can unwind and the DNA helicase is allowed to initiate the construction of replication forks¹⁴³. In fast growing bacteria like *E. coli*, another round of replication can be initiated before duplication has finished, dramatically speeding up cell division time. *C. crescentus* on the other hand is limited to one replication cycle at the time¹⁴⁴.

DnaA is controlled on many levels, including expression, ATP hydrolysis and ultimately protein degradation¹⁴⁵. However, *C. crescentus* adds an additional layer of control. While DnaA oscillates in the stalked cell to constantly replicate the chromosome, DnaA is inhibited in the swarmer cell by the response regulator CtrA. There, CtrA in its phosphorylated state binds to the *oriC* and thereby silences the origin of replication, ensuring the asymmetric life cycle of *C. crescentus*. For replication to start, CtrA has to be dephosphorylated and subsequently removed from the cell¹⁴⁶.

1.7.2 The master cell fate regulators of *Caulobacter crescentus* control the CckA-ChpT-CtrA pathway and c-di-GMP levels during the G1-to-S phase transition

Central in *C. crescentus* cell division is the activity and the localization of the kinases DivJ and PleC, which control the master cell fate regulator DivK in a complex phosphorylation network¹⁴⁷. These factors together control the activity of the CckA-ChpT-CtrA pathway and modulate c-di-GMP levels within the cell, which in turn together influence protein degradation¹⁴⁸.

The central transcription factor CtrA is essential for *C. crescentus* cell division and development¹⁴⁹. In addition to controlling almost hundred cell cycle-regulated genes directly¹⁵⁰, including TacA¹⁵¹, CtrA also specifically represses DNA replication in the swarmer cell by binding to the chromosome replication origin of *C. crescentus*. Therefore, to enter S-phase, CtrA first has to be dephosphorylated and then removed from the swarmer cell during G1-to-S phase transition¹⁵².

CtrA itself is regulated and phosphorylated by the essential histidine kinase CckA and the histidine phosphotransferase ChpT. ChpT branches the CckA-ChpT-CtrA pathway to additionally control the proteolysis adapter protein CpdR negatively^{153,154}. CpdR first needs to be dephosphorylated to act as a polar localization factor and as an adaptor for ClpXP to degrade CtrA with the adaptor proteins RcdA and PopA^{155,156}. This happens when CckA switches from a kinase to a phosphatase during G1-to-S phase transition, dephosphorylating ChpT and subsequently CtrA and CpdR¹⁵⁷. This kinase to phosphatase switch is promoted by DivK which needs to be phosphorylated during swarmer to stalked cell transition.

In the swarmer cell, PleC sits at the flagellated pole and acts as a phosphatase on DivK, thereby keeping it inactive and cytoplasmic. Early in the G1-to-S phase transition, DivJ kinase levels begin to rise. DivJ phosphorylates DivK and DivK~P is then localized to the pole¹⁵⁸. This induces a positive feedback loop in which DivK~P switches PleC from a phosphatase to a kinase, which phosphorylates more DivK. Enforcing this feedback loop, DivK~P also enhances DivJ kinase activity further. PleC and DivJ together phosphorylate the diguanylate cyclase PleD, which leads to an increase of cellular c-di-GMP levels²⁷.

To control the CckA-ChpT-CtrA pathway, DivK~P localizes to the pole and inhibits the noncanonical kinase DivL, a protein that keeps the CckA-ChpT-CtrA pathway active in the swarmer cell. DivL then localizes CckA to the pole¹⁵⁹. However, some CckA is still present in the cytoplasm. There, c-di-GMP acts as an additional switch on delocalized CckA molecules to tightly move the entire cellular pool into phosphatase mode¹⁰. All these processes together release the cell into S phase.

During the G1-to-S phase transition, DivJ is localized to the flagellated pole by SpmX and PopZ where the flagellum is shed, and the stalk and holdfast are produced^{151,160}. PleC is then localized to the opposite pole by the freshly expressed localization factor PodJ_L in the predivisional cell^{161,162}. There it likely sequesters DivK~P, allowing DivL to become active again and establishes the two cell fates after division¹⁶³ (Figure 1.7).

1.7.3 Timed protein degradation is essential for the *Caulobacter crescentus* cell cycle

In *C. crescentus*, a cascade of adapters guide proteins to ClpXP during the cell cycle. These adapters bind to each other in a hierarchical manner, and allow controlled degradation at specific time-points during G1-to-S phase transition¹⁵⁶. The first adaptor for ClpXP is the CckA-ChpT controlled protein CpdR. After the CckA kinase to phosphatase switch, this protein targets the phosphodiesterase PdeA for ClpXP degradation, allowing for an increase of c-di-GMP levels in the cell. This corresponds with the activation of the diguanylate cyclase PleD¹⁶⁴. In addition to binding to PdeA, the ClpXP-CpdR complex can also bind the next adaptor RcdA. RcdA targets the stalk regulator TacA and other proteins for degradation^{70,156}. RcdA substrates compete with the last adaptor PopA. This means PopA can also act as an antiadaptor, inhibiting RcdA mediated degradation. To be active and degrade CtrA, PopA needs to bind c-di-GMP. CtrA degradation is therefore dependent on high c-di-GMP levels^{104,156}, meaning that protein degradation is closely linked to c-di-GMP control. This is also the case for the polar flagellum regulator TipF. TipF localizes to the pole upon binding to c-di-GMP where it recruits other factors involved in flagellar synthesis. When c-di-GMP levels are decreasing in the swarmer compartment of the predivisional cell, TipF is released from the pole and degraded by ClpXP¹⁶⁵.

Cleaving of the polar factor PodJ is a ClpXP independent example for complex proteolysis in *C. crescentus*. Two forms of PodJ are involved in the cell cycle, PodJ_L and PodJ_S. PodJ_L localizes PleC to the swarmer pole. Then the periplasmic protease PerP truncates PodJ to PodJ_S with a new function in chemotaxis and holdfast formation. Finally yet another protease MmpA releases PodJ_S into the cytoplasm where it can be degraded¹⁶².

1.7.4 The ShkA-TacA pathway is necessary for G1-to-S-phase transition and development

To initiate gene transcription, a class of proteins called sigma factors are needed. Two broad classes of sigma factors exist, the sigma 70 factor (σ^{70}) family and sigma 54 factor (σ^{54}) family¹⁶⁶.

Sigma factors guide the RNA polymerase specifically to the promoter and melt the DNA duplex to allow transcription. In this process, first the polymerase subunits assemble the core RNA polymerase complex. σ^{70} binds and targets the protein complex to two conserved sequences, generally located -10 and -35 nucleotides upstream of the transcriptional start site, and melts the DNA in the -10 region¹⁶⁷.

The alternative σ^{54} family is structurally and functionally distinct from the σ^{70} family. In contrast to σ^{70} , σ^{54} binds to a region -24 and -12 from the transcriptional start site with a highly conserved consensus¹⁶⁸. σ^{54} expression can be temporally controlled. This is the case in *C. crescentus*, where the σ^{54} gene *rpoN* is expressed during the swarmer to stalked cell transition¹⁶⁹. However, there is an additional level of control. The most significant difference to σ^{70} is given by the requirement of a bacterial enhancer binding protein (bEBP) to activate σ^{54} transcription¹⁷⁰. bEBPs bind 80 to 150 bp upstream of the transcriptional starting site. In order to initiate melting of the DNA, bEBPs need to interact with the RNA polymerase complex and require energy from ATP¹⁷¹. According to the function of bEBPs, they consist usually of three domains: An AAA⁺ domain responsible for ATP hydrolysis, a domain containing a helix-turn-helix (HTH) motif that binds to the DNA, and a regulatory domain to control the protein¹⁷². The regulatory domain can be very diverse or entirely missing. In many cases however, bEBPs are part of a two-component system and regulated by phosphorylation from a histidine kinase¹⁷³.

In *C. crescentus*, this is the case for the ShkA-TacA pathway. TacA is a transcription factor of the bEBP family¹⁷⁴. In this pathway, TacA is controlled by the hybrid histidine kinase ShkA that is as part of a His-Asp phosphorelay involved in cell morphogenesis and development. Interestingly, this histidine kinase is predicted to lack any transmembrane or sensor domains and therefore belongs to a small subgroup of cytoplasmic regulators of which little is known. Adding to the unusual protein architecture are two receiver domains that are attached to the kinase domain. The first one is a pseudo-receiver domain, lacking key residues that would allow it to be phosphorylated. The second receiver domain can be phosphorylated and transfers its phosphate to the phosphotransferase ShpA. ShpA then phosphorylates TacA (Figure 1.5).

The expression of *tacA* itself is dependent on CtrA and PleC¹⁵¹. The ShkA-TacA pathway is active early in the G1-to-S phase transition and quickly turned off by ClpXP degradation^{70,174}.

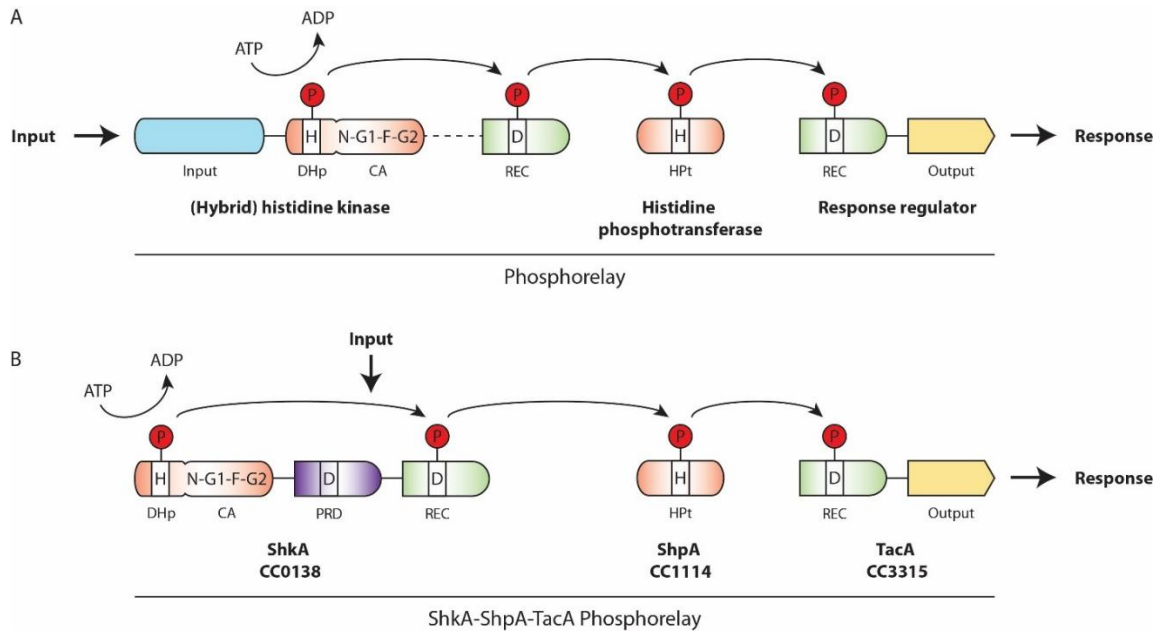


Figure 1.5: The ShkA-TacA pathway resembles a traditional phosphorelay. However, ShkA does not have a transmembrane domain or an input domain. The pseudoreceiver domain of ShkA cannot be phosphorylated, due to residues missing that are essential for M^{2+} binding.

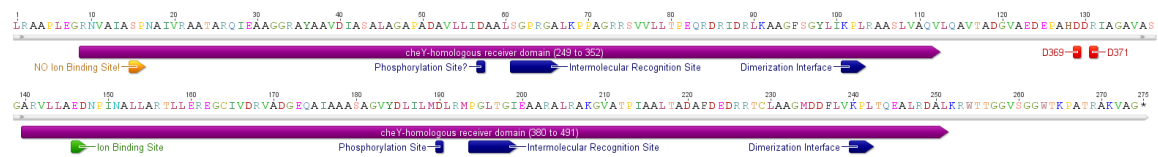


Figure 1.6: Sequence analysis of the pseudo-receiver domain and the receiver domain of ShkA, reveals that the pseudo receiver domain cannot be phosphorylated (missing ion-binding site indicated in orange).

One of the genes controlled by the ShkA-TacA phosphorelay is *staR*, which is a transcription factor involved in *C. crescentus* stalk biogenesis and responsible for controlling stalk length¹⁷⁴. StaR is also involved in holdfast regulation by inhibiting the promoter of the *hfiA* gene. The HfiA protein inhibits HfsJ, a glycosyltransferase required for holdfast production¹⁷⁵. Holdfast production is additionally controlled by c-di-GMP, in a StaR-independent fashion¹⁷⁶.

The other well-described target gene of TacA is *spmX*. SpmX is a lysozyme-like protein that localizes the DivJ kinase to the future stalked cell pole in the swarmer cell and activates DivJ to phosphorylate the cell fate determinant DivK¹⁵¹. The regulatory protein SpmY might influence *spmX* expression and ShkA-TacA pathway activity¹⁷⁷. SpmX itself is localized to the pole by another factor, PopZ, by direct binding. At the pole SpmX forms oligomers of trimers¹⁶⁰. PopZ tethers the centromere in the swarmer cell to the flagellated pole by interacting with the chromosome partitioning protein ParB^{178,179}. During G1-to-S phase transition, PopZ switches function to act as a localization factor. Multiple proteins apart from SpmX need PopZ for

robust polar localization, including DivK, CpdR, RcdA, ClpX and CckA. PopZ remains its function at the stalked pole, however during replication, new PopZ localizes to the opposite pole regaining its centromere tethering function¹⁸⁰ (Figure 1.7).

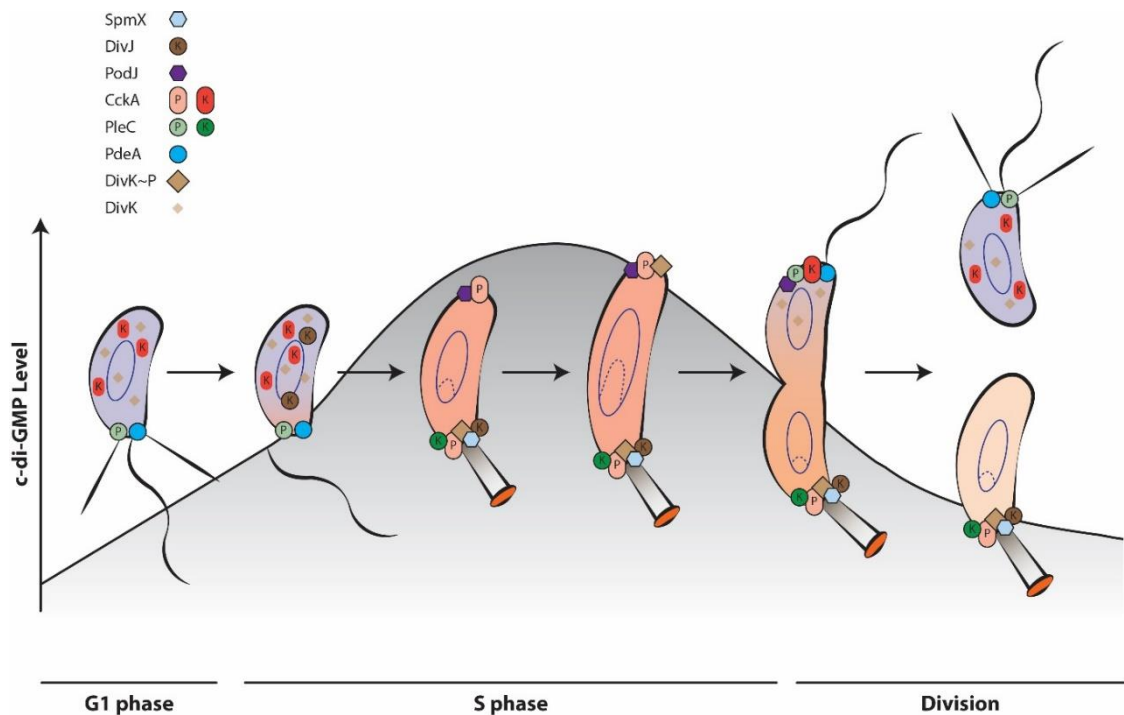


Figure 1.7: Polar localization of key drivers of cell cycle progression in *C. crescentus*. The letter K indicates kinase mode, the letter P phosphatase mode. The peak of c-di-GMP levels is qualitatively shown as a grey curve. Low cellular c-di-GMP levels are indicated in blue, high cellular c-di-GMP levels in orange.

2 AIM OF THE THESIS

The second messenger c-di-GMP controls *C. crescentus* development and coordinates this process with cell cycle progression. Recently Lori *et al.* have shown, that c-di-GMP triggers S-phase entry and replication initiation by controlling the histidine kinase CckA¹⁰. However, the role of c-di-GMP in gene expression during the G1-S transition has remained elusive.

In a Capture Compound Mass Spectrometry (CCMS) screen, Jutta Nesper identified ShkA to be a putative c-di-GMP binder. Levels of c-di-GMP rise early in the cell cycle⁸⁷ during the G1-S transition when also the ShkA-TacA pathway is highly active.

The aim of my thesis was to investigate how c-di-GMP regulates the ShkA-TacA pathway to control cell cycle timing, gene expression and morphology during the G1-to-S phase transition.

3 PROJECT ABSTRACT

The following chapters are based on the publication manuscript in preparation:

A c-di-GMP controlled phosphorelay drives a bacterial cell cycle by inducing a G1/S specific transcriptional network

Kaczmarczyk, A.*, Hempel, A.M.*, von Arx, C.*, Nesper, J., Jenal U.

* Equal contribution / order to be discussed

Bacteria can adapt their growth rates to the prevailing nutritional conditions. Proliferation rates are controlled by the cell cycle and are essentially determined by the step committing cells to initiate chromosome replication. The transcriptional network controlling this process is still largely unknown. Here we show that in the alpha-proteobacterium *C. crescentus*, a G1/S specific transcriptional network orchestrates entry into the replicative cycle. We demonstrate that fluctuating levels of the second messenger c-di-GMP control the ShkA-TacA phosphorylation cascade during the cell cycle, leading to the expression of a specific set of genes required to prepare cells for replication initiation and to coordinate this process with morphogenesis. C-di-GMP specifically binds to a pseudo-receiver domain of the ShkA kinase to alleviate its autoinhibitory function. This stimulates kinase activity, leads to the phosphorylation and activation of the TacA transcription factor and the activation of TacA-dependent gene expression during the G1/S transition. We further demonstrate that c-di-GMP mediated activation of ShkA together with delayed c-di-GMP dependent degradation of TacA, limiting gene expression to a narrow window during the G1/S transition. This is reminiscent of G1/S control in eukaryotes where cyclins and cyclin-dependent kinases define the timing of the G1/S specific transcriptional network by a combination of controlled phosphorylation and protein degradation.

4 PROJECT INTRODUCTION

Metazoan development and tissue homeostasis relies on self-renewal by quiescent stem cells that retain the capacity to re-enter the cell cycle. Conversely, misregulation of these cells results in uncontrolled proliferation and cancer¹⁸¹. A pivotal step of the cell cycle is the progression from G1 to S phase, which commits cells to chromosome replication and eventually to cytokinesis^{182,183}. The transcriptional network regulating cell cycle progression is ultimately controlled by members of the conserved cell cycle machinery including cyclin-dependent kinases and cyclins, their stage-specific regulatory subunits^{184,185}. Cell cycle control in bacteria is less well understood. Bacteria need to coordinate cell growth and differentiation with their metabolic status and nutrient availability. Their cell cycle is divided into three stages, the period between birth and the initiation of chromosome replication (B period or G1); the period required for chromosome replication (C period or S); and the time between the completion of replication and the end of cell division (D period or G2)¹⁸⁶. Since the C and D periods remain essentially constant over a wide range of growth rates¹⁸⁷, the step committing cells to initiate chromosome replication largely determines bacterial proliferation rates. Moreover, chromosome replication initiates at a constant cell volume irrespective of the cell's size at birth, indicating that this represents the initiating step of the bacterial cell cycle^{188,189}. Although recent work has improved our understanding of how cell growth and cell cycle progression are coupled (reviewed in^{190,191}), a molecular frame of the regulatory network driving G1/S transition is still largely missing.

To accomplish rapid growth, bacteria like *E. coli* or *B. subtilis* can initiate new rounds of replication before completing previous rounds of genome replication¹⁸⁷. In contrast, *C. crescentus* strictly separates its cell cycle stages in a eukaryote-like manner, initiating chromosome replication only once per division cycle¹⁹². This, and the fact that different stages of the cell cycle have distinct morphologies and can be separated from each other experimentally, makes *C. crescentus* particularly amenable to study bacterial cell cycle control¹⁹³. *Caulobacter* divides asymmetrically to generate a sessile stalked cell (ST), which enters S-phase immediately and a motile swarmer cell (SW) that enters G1 phase, in which replication is blocked. After a defined period of motility, SW cells initiate a program to exit G1 into S-phase. Concomitant with initiating genome replication cells change morphology and behavior by replacing the rotary motor with an extension of the cell body, the stalk, and an adhesive holdfast that anchors sessile ST cells to surfaces. Replication initiation requires the

accumulation of the essential and highly conserved initiator protein DnaA, which binds to the chromosomal origin of replication (*Cori*) to promote duplex unwinding and replisome assembly^{145,194–197}. DnaA activity is antagonized by the replication initiation inhibitor CtrA, an essential response regulator, which in its phosphorylated form binds to several sites in the *Cori* and blocks replication initiation¹⁵². Levels of DnaA are low in G1 and raise above a threshold level during G1/S to initiate chromosome replication¹⁴⁶. Conversely, CtrA is phosphorylated and active in G1 but is inactivated and rapidly degraded by the ClpXP protease prior to S phase entry¹⁰⁴.

CtrA activity is controlled by the central cell cycle kinase CckA, a bifunctional enzyme that can act both as kinase and as phosphatase to control CtrA phosphorylation via the phosphotransfer protein ChpT^{153,157,198}. CckA is a kinase in G1, but switches to phosphatase mode upon entry into S phase, resulting in the inactivation of CtrA and clearance of the replication block. This central cell cycle switch is ultimately controlled by the cell fate determinants DivJ and PleC, two histidine kinase/phosphatase antagonists, which localize to opposite cell poles and during division asymmetrically partition into the daughters to determine their respective programs¹⁴⁷. DivJ and PleC control the phosphorylation of a single domain response regulator, DivK, which in turn regulates CckA activity via its interaction with the pseudokinase DivL^{159,199}. Because the G1 swarmer program is dominated by the PleC phosphatase, DivK~P levels remain low and CckA adopts default kinase activity. During G1/S, PleC is replaced by DivJ, leading to DivK phosphorylation which in turn stimulates the CckA phosphatase activity. According to this regulatory scheme, the appearance and activation of the stalked cell specific DivJ kinase represents a key step during G1/S transition. Activation of DivJ is directed by the SpmX scaffolding protein, which accumulates during G1/S and recruits the DivJ kinase to the incipient stalked pole¹⁵¹. Thus, SpmX is not only a critical element of the temporal control of DivJ during G1/S, but also ensures that DivJ partitions with the stalked daughter cell at the next cytokinetic event¹⁵¹. While this makes SpmX accumulation the earliest known event to trigger S phase entry, it is unclear how the G1/S-specific transcriptional network orchestrates *spmX* expression during the cell cycle. Transcription of the *spmX* gene is regulated by the response regulator TacA, which in its phosphorylated form also induces the expression of genes required for the SW-to-ST cell morphogenesis^{151,174}. Although TacA was recently shown to be phosphorylated by the sensor histidine kinase ShkA and the phosphotransferase protein ShpA, the signals that activate this phosphorelay have remained unknown.

Recent findings suggested that *C. crescentus* cell cycle progression is controlled by the guanosine-based second messengers ppGpp and c-di-GMP^{78,200}. While ppGpp appears to delay G1/S transition by stabilizing CtrA^{120,201}, c-di-GMP directs the SW-to-ST cell transition and promotes the entry of differentiating cells into the replicative cycle^{10,87,104}. Levels of c-di-GMP are low in swarmer cells, increase during G1/S and peak in stalked cells concomitant with replication initiation^{27,86,87}. One of the main drivers of c-di-GMP fluctuations is the diguanylate cyclase PleD, which is active in stalked but turned off in swarmer cells⁹². PleD is a response regulator, the activity of which is controlled by PleC and DivJ, the cell fate determinants that also regulate DivK phosphorylation levels during the cell cycle. Thus, PleD activity perfectly parallels the activation profile of DivK during the cell cycle²⁷. In line with this, when peak levels of c-di-GMP are reached at the onset of S phase, the ligand directly binds to CckA to direct its kinase/phosphatase switch and to initiate chromosome replication¹⁰. In addition to CtrA dephosphorylation, c-di-GMP also triggers CtrA degradation by the ClpXP protease by binding to and activating the protease adaptor protein PopA^{104,156,202}. Thus c-di-GMP acts at two independent levels to promote S phase entry by removing CtrA.

Here we show that in addition to its key role in S-phase entry, c-di-GMP also orchestrates the G1/S specific gene expression program that leads to SpmX synthesis, DivJ activation and eventually DivK- and PleD-dependent CtrA inactivation. A combination of genetic and biochemical data revealed that c-di-GMP controls the ShkA-TacA pathway by directly binding to the ShkA sensor histidine kinase to strongly stimulate its kinase activity. Upon c-di-GMP mediated autophosphorylation, ShkA transfers phosphate to its C-terminal receiver domain from where it is passed on via the phosphotransfer protein ShpA to TacA, resulting in active TacA~P. We demonstrate that binding of c-di-GMP to a pseudo-receiver domain of ShkA, which is positioned between the kinase core and the receiver domain, alleviates ShkA auto-inhibition leading to the activation of the ShkA-TacA pathway. We show that c-di-GMP-mediated activation of ShkA and the subsequent c-di-GMP mediated proteolysis of ShkA together define a window of ShkA activity during the cell cycle. This window is sharpened to a narrow, G1/S specific period by TacA degradation, which precedes the degradation of ShkA. Thus, *C. crescentus* orchestrates G1/S specific gene expression in high temporal resolution through a combination of c-di-GMP mediated activation and degradation of ShkA-TacA phosphorylation components. Because ShkA binds c-di-GMP with higher affinity than CckA, the ShkA-mediated G1/S transcriptional network precedes the CckA switch leading to chromosome replication initiation as c-di-GMP levels are building up during the cell cycle. Together, these

results propose a model, where an upshift of c-di-GMP drives consecutive steps of the G1/S cell cycle progression in *C. crescentus* by sequentially activating hierarchized phosphorylation pathways.

5 RESULTS

Author contribution

Figure 5.1	von Arx, C.
Figure 5.2	von Arx, C.
Table 5.1	Nesper, J.
Figure 5.3	von Arx, C.
Figure 5.4	von Arx, C.
Figure 5.5	5.5A, B, C, D, F: Kaczmarczyk, A. 5.5E: von Arx, C.
Figure 5.6	Kaczmarczyk, A.
Figure 5.7	Kaczmarczyk, A.
Figure 5.8	Kaczmarczyk, A.
Figure 5.9	5.9A, B, C, D, G: von Arx, C. 5.9E, F: Kaczmarczyk, A.
Figure 5.10	Hempel, A.M.
Figure 5.11	Hempel, A.M.

5.1 C-DI-GMP CONTROLS THE SHKA-TACA PHOSPHORELAY

A *C. crescentus* strain lacking all known or predicted diguanylate cyclases (referred to as cdG^0 strain in the following) shows severe developmental and morphological abnormalities⁸⁷. Cells are elongated, irregularly shaped and lack all polar appendages including the stalk. Stalk biogenesis was recently shown to depend on an active ShkA-TacA phosphorelay. Moreover, *shkA* and *tacA* mutants show morphology and motility defects that partially phenocopy a cdG^0 strain. This opened the possibility that c-di-GMP controls *C. crescentus* growth and behavior by directly imposing control on the central ShkA-TacA regulatory pathway. To test this idea, we analyzed stalk biogenesis in the cdG^0 strain expressing TacA^{D54E}, a phospho-mimetic form of TacA¹⁷⁴. In this strain stalk biogenesis was restored¹⁷⁴. We analyzed ShkA-TacA activity in the cdG^0 strain using a transcriptional *lacZ* reporter fusion to *spmX*, a TacA target gene involved in *C. crescentus* development and cell cycle progression^{133,151}. While *spmX* transcription was greatly reduced in the cdG^0 , *shkA* and *tacA* strains, *spmX* promoter activity was restored in the presence of TacA^{D54E} (Figure 5.1B). *spmX* transcription was also restored when c-di-GMP was provided in the cdG^0 background or in a strain that lacks all DGC and PDEs (referred to as $rcdG^0$ strain) by IPTG-mediated expression of *dgcZ* from *E. coli* (Figure 5.2A). Thus, c-di-GMP itself and not a specific DGC of *C. crescentus*, drives *spmX* expression. In agreement with the transcription data we found that a SpmX-mCherry fusion fails to localize to the stalked pole in a $\Delta shkA$ mutant and in the cdG^0 strain. However, ectopic expression of TacA^{D54E} rescued polar localization of a SpmX-mCherry fusion in the $\Delta shkA$ and the cdG^0 strain (Figure 5.1C, Figure 5.2D, C) and restored stalk biogenesis (Figure 5.2B).

To corroborate the influence of c-di-GMP on ShkA-TacA activity, we sought to directly analyze phosphorylation of ShkA and TacA *in vivo*. Strains harboring chromosomally encoded TacA or ShkA with N-terminal 3xFLAG tags were examined using Phos-Tag PAGE and subsequent immunoblot analysis. In wild-type strains, FLAG-tagged ShkA or TacA migrated as two distinct bands, the upper one representing the phosphorylated species. In contrast, in strains lacking c-di-GMP, both proteins were unphosphorylated but phosphorylation was restored by expressing the constitutively active DGC PleD*²⁵ (Figure 5.1E). When c-di-GMP was gradually degraded in wild-type strains by overexpression of the heterologous PDE PA5295 from *P. aeruginosa*⁸⁷, the phosphorylated forms of both TacA and ShkA disappeared over time (Figure 5.1F).

Altogether, these results provided strong evidence that c-di-GMP acts upstream of the ShkA-TacA phosphorelay and that it is required for the activity of this pathway.

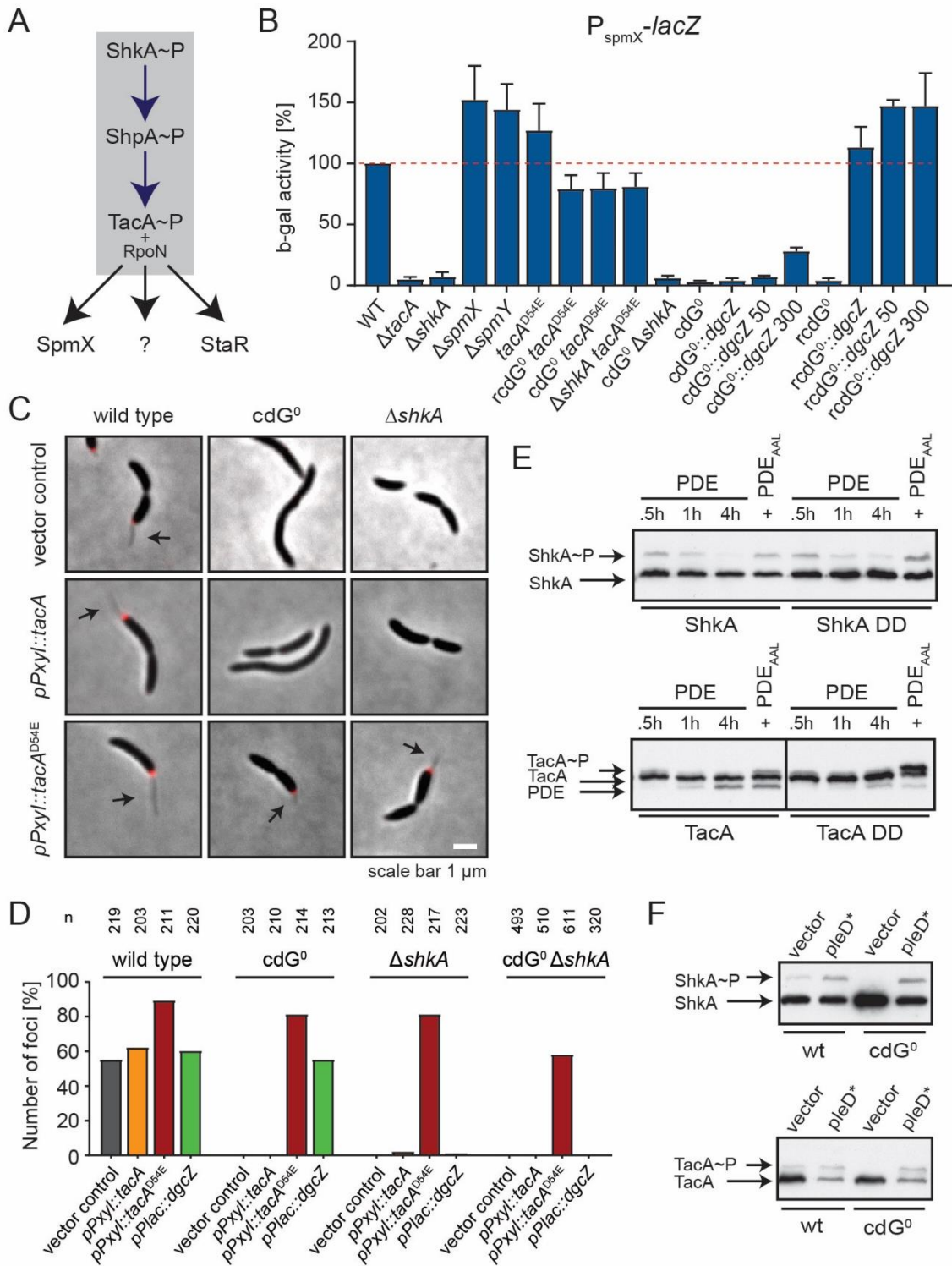


Figure 5.1: C-di-GMP controls the ShkA-TacA phosphorelay

(A) The histidine kinase ShkA phosphorylates the phosphotransfer protein ShpA which in turn phosphorylates the response regulator and transcription factor TacA. TacA controls RpoN-dependent expression of downstream targets, including the lysozyme-like localization factor SpmX and the transcription factor StaR.

(B) The expression of *spmX* is dependent on the ShkA-TacA pathway as well as on c-di-GMP levels. β -galactosidase assays were performed with the pP_{spmX} -*lacZ* reporter plasmid. Promoter activity of *spmX* was measured in wild-type and mutant strains. Data represent mean \pm SD.

(C) The phospho-mimetic form of TacA, TacA^{D54E}, restores stalk biogenesis and *spmX*-mCherry localization in the cdG⁰ strain. Microscopy of wild-type, cdG⁰ and Δ *shkA* strains that express a chromosomal *spmX*-mCherry fusion was performed. Both the cdG⁰ and the Δ *shkA* strains lacked stalk biogenesis and *spmX*-mCherry localization. Expressing *tacA* from the pP_{*xyl*}::*tacA* plasmid did not affect these phenotypes. However, by expressing the phospho-mimetic mutant *tacA*^{D54E} from the pP_{*xyl*}::*tacA*^{D54E} plasmid, both stalk biogenesis and *spmX*-localization were restored.

(D) Evaluation of *spmX*-mCherry localization in the cdG⁰, Δ *shkA* and cdG⁰ Δ *shkA* strains. Only the wild-type background localizes *spmX*-mCherry and the expression plasmid pP_{*xyl*}::*tacA* cannot restore localization. However, by expressing the plasmid containing the phospho-mimetic form pP_{*xyl*}::*tacA*^{D54E}, *spmX*-mCherry localized in all backgrounds. Increasing c-di-GMP levels by expressing the *E. coli* DGC *dgcZ* from the pPlac::*dgcZ* plasmid could only restore localization in the cdG⁰ strain.

(E) Degrading c-di-GMP in wild-type strains by overexpression of the heterologous *P. aeruginosa* PDE PA5295, phosphorylated forms of both FLAG-tagged ShkA and TacA disappeared over time. At indicated time points the expression plasmid pP_{Q5}-PA5295 was induced with cumate. As a negative control, inactive PA5295_{AAL} was expressed from the pP_{Q5}-PA5295_{AAL} plasmid. Lysates of exponentially growing cultures of wild-type strains with either N-terminal FLAG-tagged TacA or N-terminal FLAG-tagged ShkA were run on Phos-Tag PAGE gels. Western blots were performed with α -FLAG antibodies.

(F) Expressing a constitutively active *pleD* mutant (*pleD*^{*}) in the cdG⁰ strain restored phosphorylation of FLAG-tagged ShkA and TacA. Wild-type and cdG⁰ strains with either N-terminal FLAG-tagged ShkA or N-terminal FLAG-tagged TacA were investigated for their phosphorylation levels. In each strain, c-di-GMP levels were complemented with the pP_{*pleD*}-*pleD*^{*} expression plasmid. Lysates of exponentially growing cultures were run on Phos-Tag PAGE gels. Western blots were performed with α -FLAG antibodies.

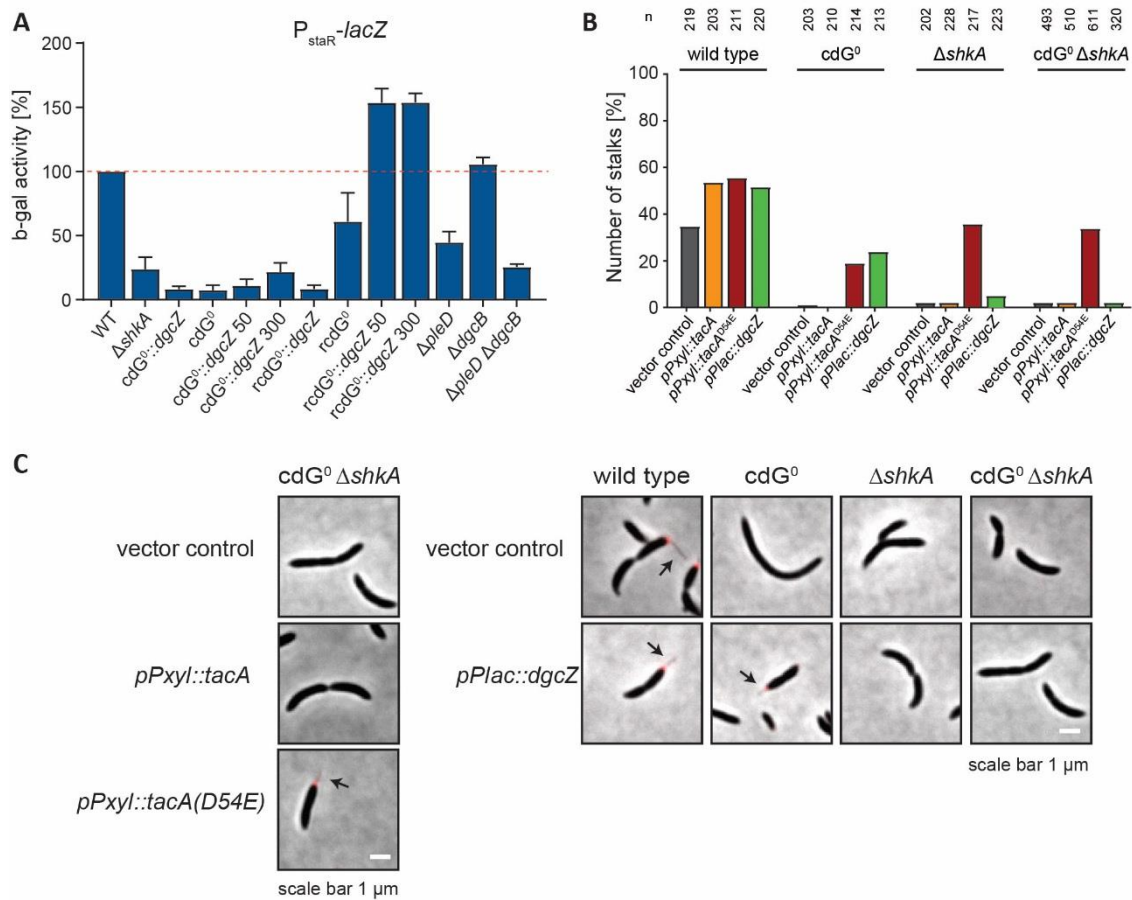


Figure 5.2 C-di-GMP controls the ShkA-TacA phosphorelay

(A) The expression of *staR* is dependent on the ShkA-TacA pathway as well as on c-di-GMP levels. β -galactosidase assays were performed with the pP_{staR} -*lacZ* reporter plasmid. Promoter activity of *staR* was measured in wild-type and mutant strains. Data represent mean \pm SD.

(B) Evaluation of stalk biogenesis in the cdG^0 , $\Delta shkA$ and $cdG^0 \Delta shkA$ strains. Only in the wild-type background stalks are formed and the plasmid pPxyI::*tacA* cannot restore biogenesis. However, by expressing the plasmid containing the phospho-mimetic form pPxyI::*tacA*^{D54E}, stalks were formed in all backgrounds. Increasing c-di-GMP levels by expressing the *E. coli* DGC *dgcZ* from the pPlac::*dgcZ* plasmid could only restore stalk formation in the cdG^0 strain.

(C) The phospho-mimetic form of TacA, TacA^{D54E}, restores stalk biogenesis and *spmX*-mCherry localization in the cdG^0 strain $\Delta shkA$. The *E. coli* DGC *dgcZ* restores stalk biogenesis and *spmX* localization only in the cdG^0 strain. Microscopy of wild-type, cdG^0 , $\Delta shkA$ and $cdG^0 \Delta shkA$ strains that express a chromosomal *spmX*-mCherry fusion was performed. The cdG^0 , $\Delta shkA$ and $cdG^0 \Delta shkA$ strains lacked stalk biogenesis and *spmX*-mCherry localization. Expressing *tacA* from the pPxyI::*tacA* plasmid did not affect these phenotypes. However, by expressing the phospho-mimetic mutant *tacA*^{D54E} from the pPxyI::*tacA*^{D54E} plasmid, both stalk biogenesis and *spmX*-localization were restored. Expressing the *E. coli* DGC *dgcZ* from the pPlac::*dgcZ* plasmid could only restore stalk biogenesis and *spmX* localization in the cdG^0 strain.

5.2 C-DI-GMP STIMULATES SHKA KINASE ACTIVITY

The above *in vivo* observations hinted at ShkA as the target of c-di-GMP. This was supported by a parallel unbiased approach that made use of Capture Mass Spectrometry (CCMS) to identify c-di-GMP effector proteins²⁰³. These experiments repeatedly identified ShkA as one of the top hits (Table 5.1).

Table 5.1: ShkA identified by c-di-GMP capture compound mass spectrometry (CCMS)

Protein Name	ID	CCMS experiment/CCMS competition ¹⁾			
		No of spectral counts of identified peptides			
Experiment No ²⁾		1	2	3	4
ShkA	CC0138	2/0	3/1	3/0	6/0
TipF	CC0710	4/0	11/1	12/1	12/1
PopA	CC1842	20/4	32/9	20/6	36/10
DGC ³⁾	CC0857	4/0	6/1	8/0	5/0

¹⁾All competition experiments were performed in the presence of 1 mM c-di-GMP.

²⁾Experiment 1 and 2 were performed with 8 μ M c-di-GMP-CC, experiment 3 and 4 with 4 μ M c-di-GMP-CC.

³⁾Unnamed *C. crescentus* diguanylate cyclase

Isothermal titration calorimetry (ITC) revealed that ShkA indeed binds c-di-GMP with nanomolar affinity (K_D 745 nM) (Figure 5.3, Figure 5.4). These results were reproduced qualitatively using UV-crosslinks with ShkA and P32-labelled c-di-GMP (Figure 5.7). *In vitro* phosphorylation experiments then demonstrated that c-di-GMP strongly stimulates the ShkA autokinase activity. This effect was highly specific, as none of the other nucleotides tested could stimulate ShkA (Figure 5.3).

Earlier attempts using full-length ShkA protein had failed to show autophosphorylation activity. Autokinase activity was only observed, when the catalytic core of ShkA (including DHp, CA and REC1 domain) was separated from the C-terminal REC2 domain¹⁷⁴. When recapitulating these experiments, ShkA autophosphorylation and phosphotransfer to TacA via ShkA-REC2 and ShpA was obtained irrespective of the presence of c-di-GMP (Figure 5.3). In contrast, when these experiments were carried out with full-length kinase, ShkA autophosphorylation and phosphotransfer to ShpA and TacA was readily observed, but only when c-di-GMP was added to the reactions (Figure 5.3).

In sum, we conclude that c-di-GMP directly binds to the ShkA kinase with high affinity and specificity to stimulate its autokinase activity and to promote phosphotransfer via ShpA to activate the response regulator TacA.

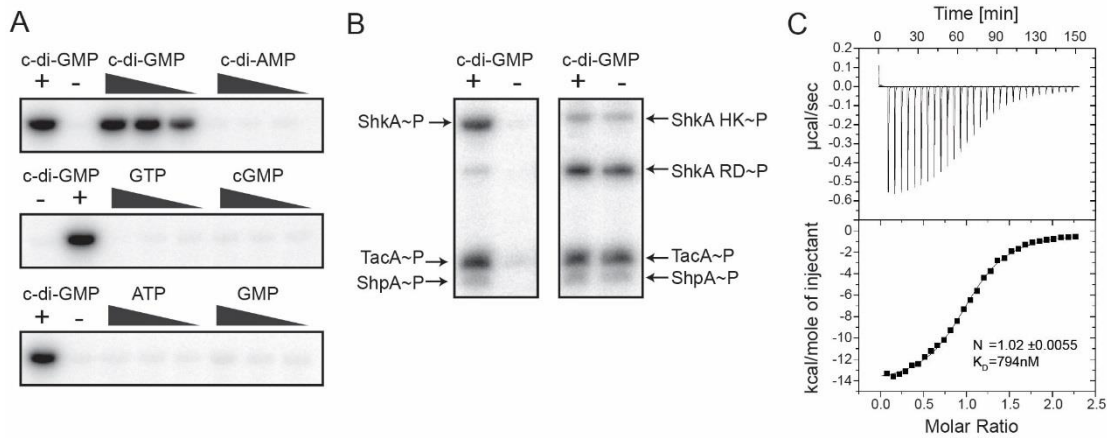


Figure 5.3: C-di-GMP stimulates ShkA kinase activity

(A) C-di-GMP specifically and exclusively stimulates ShkA phosphorylation. Multiple nucleotides were added to purified ShkA protein in different concentrations, 1000 μ M, 100 μ M and 10 μ M. Then [32 P]ATP was added to determine ShkA activity. For positive controls 100 μ M c-di-GMP was added, for negative controls H₂O.

(B) C-di-GMP is needed to activate full length ShkA, while ShkA activity can be uncoupled from c-di-GMP by expressing its REC2 domain separately. C-di-GMP or H₂O was added to purified full length ShkA, ShpA and the receiver domain of TacA. Phosphorylation was then analyzed by adding [32 P]ATP (left). The experiment was repeated by purifying the histidine kinase domain and the REC1 domain separately from the REC2 domain (right).

(C) Isothermal titration calorimetry performed with ShkA and c-di-GMP yielded an average K_D of 745 nM. Adding to 12 μ M ShkA in the cell, 130 μ M c-di-GMP was injected in one 3 μ L step and 29 10 μ L steps. One measurement out of five is shown.

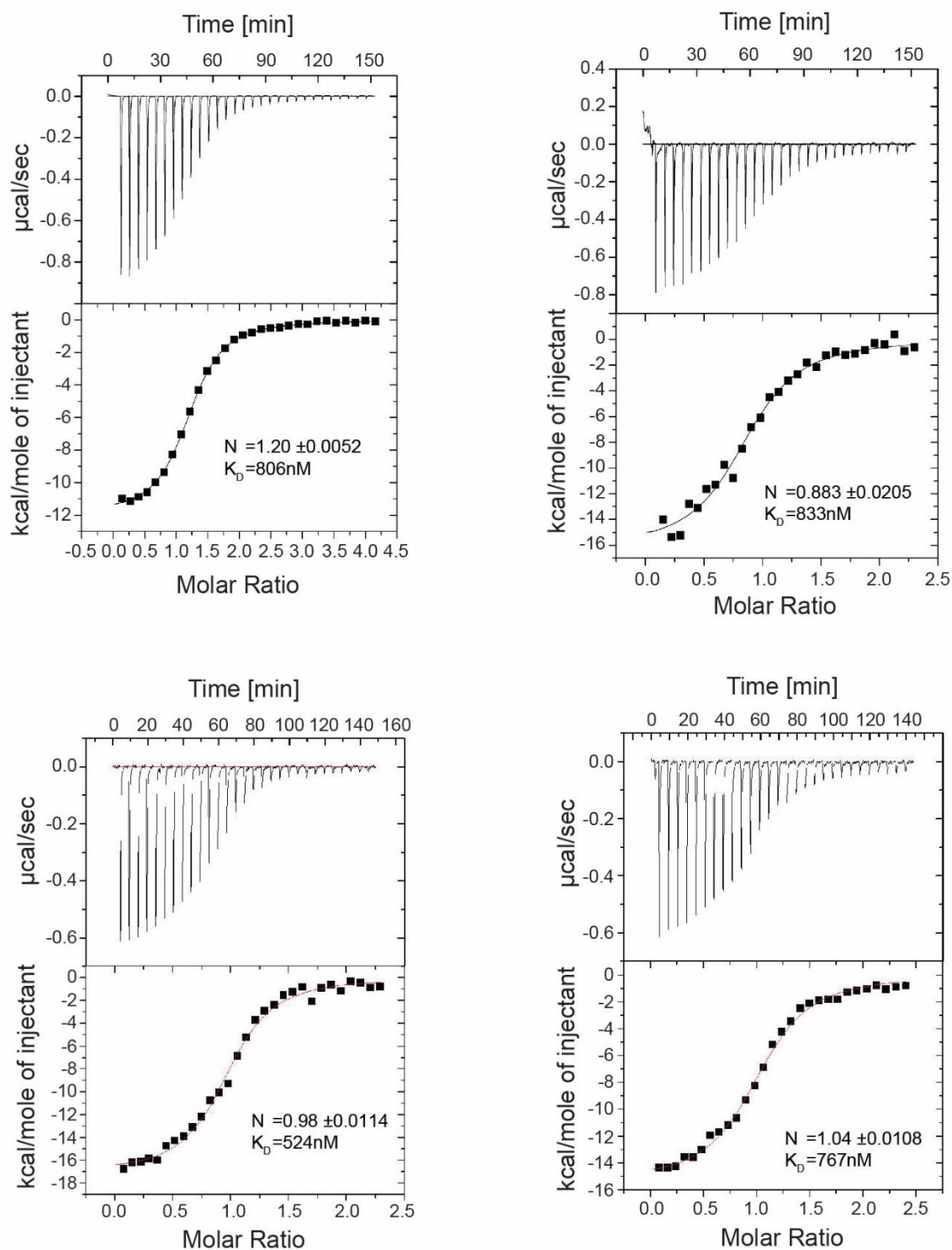


Figure 5.4: Isothermal titration calorimetry performed with ShkA and c-di-GMP yielded an average K_D of 745 nM

Adding to 12 μM ShkA in the cell, 130 μM c-di-GMP was injected in one $3\mu\text{L}$ step and 29 $10\mu\text{L}$ steps. Four independent measurements are shown.

5.3 C-DI-GMP BINDING ALLEVIATES SHKA AUTO-INHIBITION

Having identified ShkA as a target of c-di-GMP, we next sought to disclose the mechanism by which the ShkA kinase is activated. We reasoned that isolating c-di-GMP-independent ShkA mutants, i.e. ShkA variants that display kinase activity in the absence of c-di-GMP, would not only help to uncover the mechanism by which c-di-GMP activates ShkA, but would also provide an entry point into studying the role of this control during the *C. crescentus* cell cycle. We devised a genetic selection (see Materials and Methods) to isolate mutations in *shkA* that restored *spmX* expression in a *rcdG*⁰ strain. Four independent mutations (D369N, D369G, R371S and R371P) were identified in two nearby residues, D369 and R371, located in a short stretch of amino acids (referred to as “DDR” motif) in the linker region between REC1 and REC2 (Figure 5.5A). The DDR motif is conserved in ShkA orthologs from closely related Caulobacterales, including the orders *Caulobacter*, *Asticcacaulis*, *Phenylobacterium* and *Brevundimonas*, but is absent in ShkA orthologs of more distantly related Alphaproteobacteria (Figure 5.6).

In the following studies, we focused on the D369N mutation, since this is the chemically most conservative among the substitutions found. Transduction into clean wild-type and *rcdG*⁰ backgrounds followed by reporter assays confirmed that the *shkA*^{D369N} allele restored *spmX* expression to wild-type levels in a *rcdG*⁰ strain (Figure 5.5D). Likewise, the *shkA*^{D369N} allele restored *in vivo* phosphorylation of TacA or a stabilized version of TacA (TacA^{DD}, see below) in the *cdG*⁰ strain (Figure 5.5E). Together, this indicated that ShkA^{D369N} kinase activity is uncoupled from its strict requirement for c-di-GMP. This was confirmed using purified ShkA^{D369N} protein. ShkA^{D369N} showed strong autophosphorylation activity even in the absence of c-di-GMP, although the mutant retained some c-di-GMP-mediated stimulation (Figure 5.5B,C). This indicated that although kinase activity of the ShkA^{D369N} variant was independent of c-di-GMP, this mutant was still able to bind c-di-GMP. This was confirmed by UV-crosslink experiments with ³²P-labelled c-di-GMP demonstrating that the mutant protein binds c-di-GMP with wild-type-like affinity (Figure 5.5E). These results are also in line with *in vivo* data, demonstrating that the *shkA*^{D369N} allele generates higher levels of *spmX* transcription in a strain producing c-di-GMP compared to the *cdG*⁰ background (Figure 5.5D).

The above results identified the REC1-REC2 linker region as critical determinants of c-di-GMP-mediated ShkA activation. In contrast, no such mutations were found in the neighboring REC2 domain. This was surprising, since a previous study had found that ShkA lacking the REC2 domain is competent for autophosphorylation *in vitro*¹⁷⁴, irrespective of c-di-GMP, implying

that REC2 can inhibit autokinase function of the catalytic core. Based on this we reasoned that REC2 residues important for c-di-GMP mediated control may exist, but that they were impossible to be recovered in our genetic selection because of their essential nature for the phosphor-transfer function of REC2. To test this notion, we mutated the most strictly conserved acidic amino acids known to contribute to REC domain function in general⁴⁴. In the case of ShkA REC2 these included E386 (mutated to Q) and D387 (mutated to N) being part of the magnesium binding pocket, the phosphoryl-acceptor D430 (mutated to N), and K480 (mutated to R), involved in the stabilization of the D430-aspartyl moiety. All mutants showed autokinase activity irrespective of c-di-GMP (Figure 5.5F).

Together, these data demonstrate that specific mutations in the REC1-REC2 linker region and in REC2 uncouple ShkA kinase activity from its strict requirement for c-di-GMP. These results outline a mechanistic model, in which the REC1-REC2 linker region together with conserved residues in the REC2 domain that are also critical for receiver domain function itself inhibit autokinase activity of ShkA.

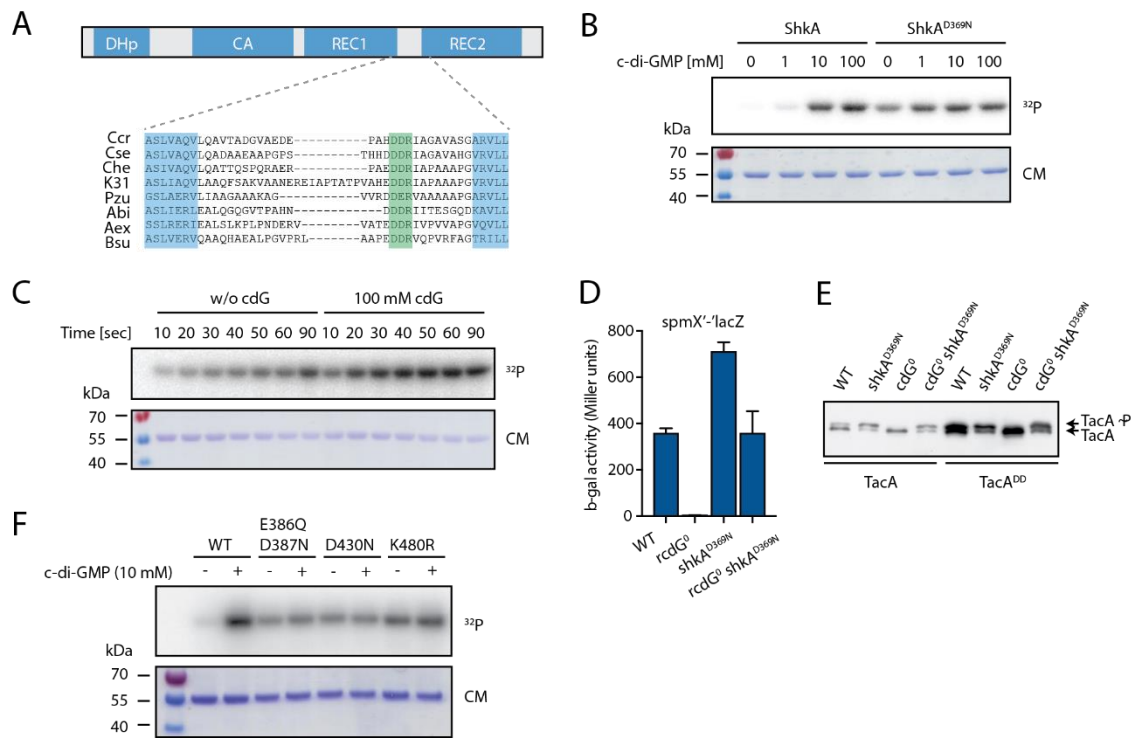


Figure 5.5 Bypassing the dependence of ShkA autophosphorylation on c-di-GMP through mutations in the DDR motif and REC2

(A) Schematic of ShkA domain architecture drawn to scale (top) and alignment of the REC1-REC2 linker harboring the DDR motif (highlighted in green) of ShkA orthologs from several *Alphaproteobacteria* (bottom). Ccr, *C. crescentus*; Cse, *Caulobacter segnis*; Che, *Caulobacter henricii*; K31, *Caulobacter sp.* K31; Pzu, *Phenylobacterium zucineum*; Abi, *Asticcacaulis biprosthecium*; Aex, *Asticcacaulis excentricus*; Bsu, *Brevundimonas subvibrioides*.

(B) *In vitro* autophosphorylation assays of ShkA and ShkA^{D369N}. Reactions contained different concentrations of c-di-GMP as indicated and autophosphorylation could proceed for 3.5 min at room temperature. Top: Autoradiograph; bottom: Coomassie stain of the same gel.

(C) Time course of ShkA^{D369N} autophosphorylation at 4°C with or without c-di-GMP. Top: Autoradiograph; bottom: Coomassie stain of the same gel.

(D) β-Gal activities of indicated strains harboring the *spmX'*-*lacZ* fusion (plasmid pAK502-*spmX*). Shown are means and standard deviations of three biological replicates.

(E) PhosTag PAGE western blots of strains harboring a 3xFLAG-*tacA* or 3xFLAG-*tacA*^{DD} fusion as indicated.

(F) *In vitro* autophosphorylation assays of wild-type ShkA and indicated mutant variants with or without c-di-GMP. Autophosphorylation could proceed for 5 min at room temperature. Top: Autoradiograph; bottom: Coomassie stain of the same gel.

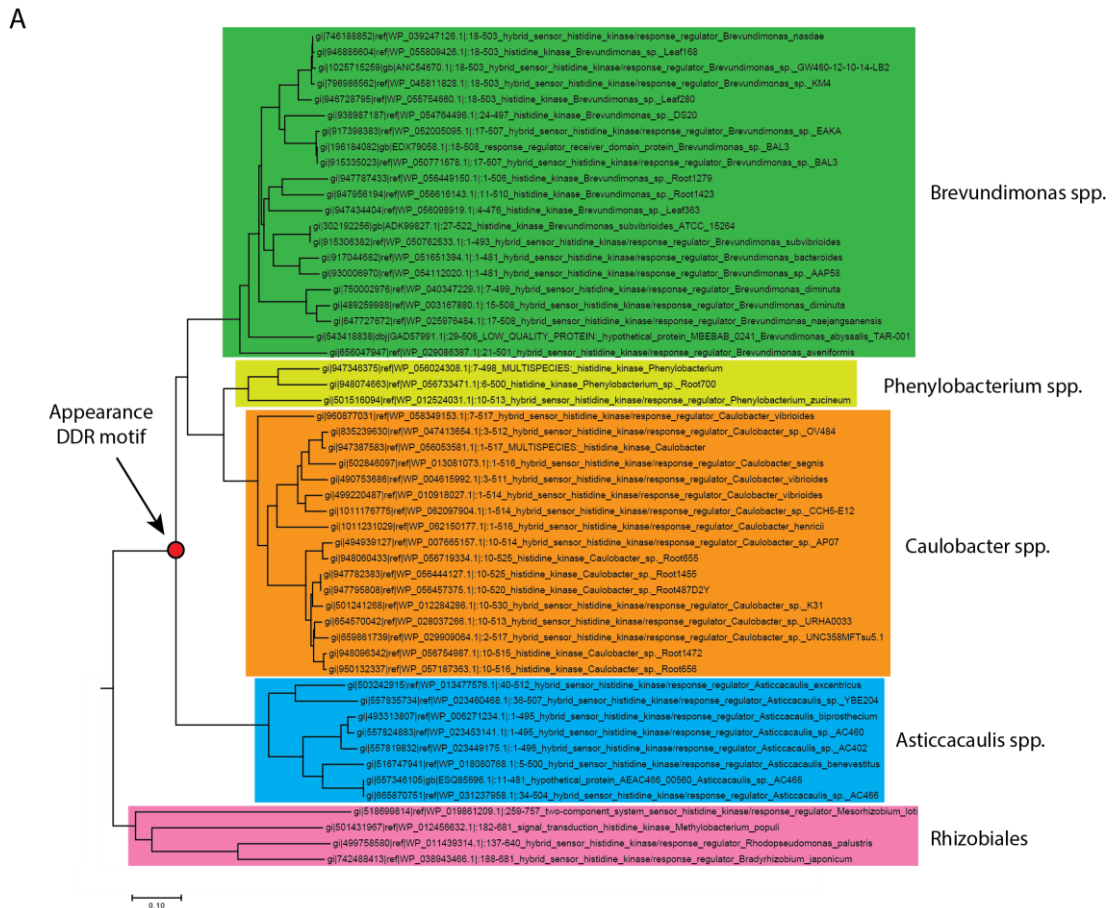


Figure 5.6 Phylogenetic analysis of ShkA orthologs and conservation of the DDR motif

(A) Phylogenetic tree of ShkA orthologs.

(B) Weblogo based on an alignment of ShkA orthologs within the *Caulobacteraceae* shown in (A). Circles below amino acid residues indicate residues that were mutated and tested for an effect on ShkA activity *in vivo* (red), were isolated as mutations that render ShkA activity c-di-GMP-independent (green), or were tested *in vitro* for their role in ShkA autoinhibition (orange).

5.4 C-DI-GMP BINDS TO THE SHKA REC1 PSEUDO-RECEIVER DOMAIN

The isolation of a c-di-GMP-independent *shkA* allele offered a convenient way to screen for residues that were involved in c-di-GMP binding or c-di-GMP-mediated intramolecular signal transduction. The rationale was that any mutation in *shkA* that impaired kinase activity due to a specific defect in c-di-GMP binding or cdG-dependent activation should be rescued when combined with the D369N mutation, while other, more general kinase defects would not be recuperated. For this analysis we mainly focused on Arg residues and on aromatic and acidic amino acids as they represent key determinants of c-di-GMP binding sites²⁰⁴. An alignment of ShkA orthologs from *C. crescentus* and related organisms revealed several candidate residues for c-di-GMP binding (Figure 5.7A). Single or double point mutations of candidate residues were engineered in *shkA* on a low-copy number plasmid and introduced into a $\Delta shkA$ strain harboring a *spmX-lacZ* reporter to assay ShkA activity. Residues that are generally conserved in histidine kinase activity (H-, N-, G1-, G2- and F-boxes) or in receiver domain function (REC2) were not considered. However, because the REC1 domain is a pseudo-receiver domain lacking the acidic magnesium-binding pocket, we tested some of the REC1 residues that are normally important for receiver domain function. A D430N substitution that eliminates the Asp phosphoryl-acceptor of REC2 was included as a negative control.

Mutations that affected ShkA kinase activity *in vivo* were found in the kinase catalytic core (DHp and CA domains) and the REC1 domain, but not in REC2 (Figure 5.7A). The most severe effects were observed for the F230A/F234A double substitutions in the CA domain and the R324A and Y338A single substitutions in the REC1 domain (Figure 5.7B). Next we focused on mutations that resulted in less than 50% of wild-type activity and combined them with the D369N mutation conferring c-di-GMP independence. Except for the F230/F234A substitutions, introduction of D369N restored *spmX-lacZ* activity to wild-type levels in all cases, indicating a functional role of these residues in c-di-GMP-mediated ShkA activation (Figure 5.7C). Binding assays with purified ShkA variants and radiolabeled c-di-GMP identified several mutants with reduced binding (Figure 5.7E). The strongest reduction in binding affinity was observed for ShkA with the Y338A mutation, implying a direct role of this residue in c-di-GMP binding (Figure 5.7E). Congruent with these binding studies and with *in vivo* results (above), both R324A and Y338A variants were inactive both in the presence and absence of c-di-GMP, but were competent for autophosphorylation when combined with the D369N mutation (Figure 5.7D). In agreement with their binding affinities (Figure 5.7E), the R324A mutation largely retained stimulation by c-di-GMP when combined with D369N, while the Y338A variant

displayed only marginal stimulation by c-di-GMP (Figure 5.7D). We next asked whether REC1 alone was sufficient to bind c-di-GMP. To this end, the purified REC1 domain was subjected to UV crosslinking experiments with radiolabeled c-di-GMP and was indeed found to strongly bind c-di-GMP (Figure 5.7F). Altogether, these experiments exposed the REC1 pseudo-receiver domain of ShkA as the primary docking site for c-di-GMP and identified candidate residues for c-di-GMP binding.

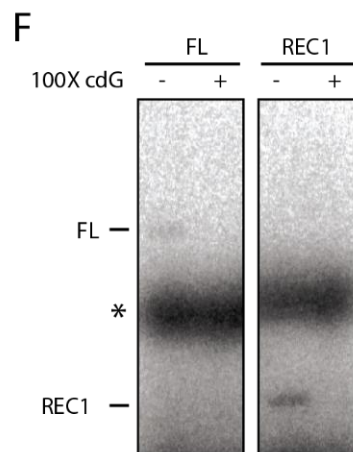
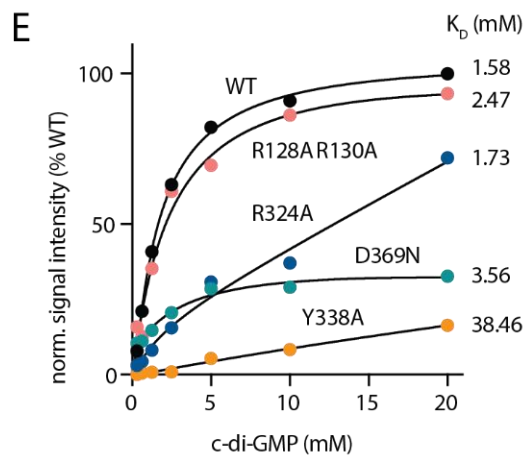
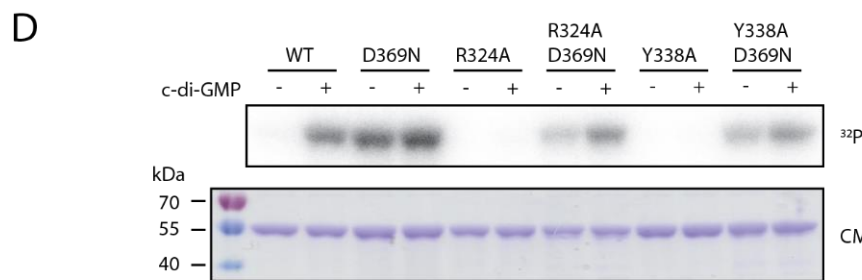
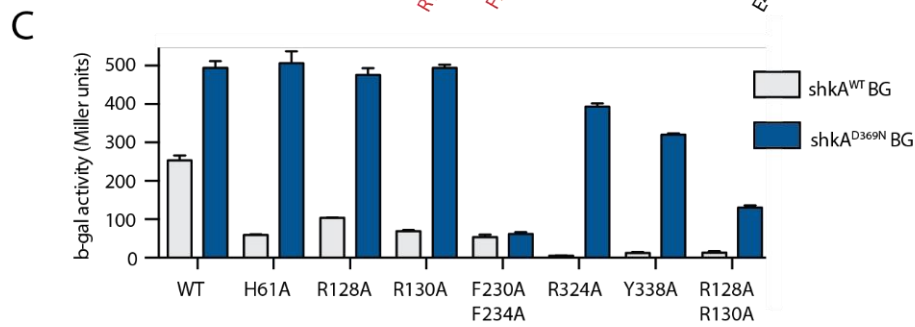
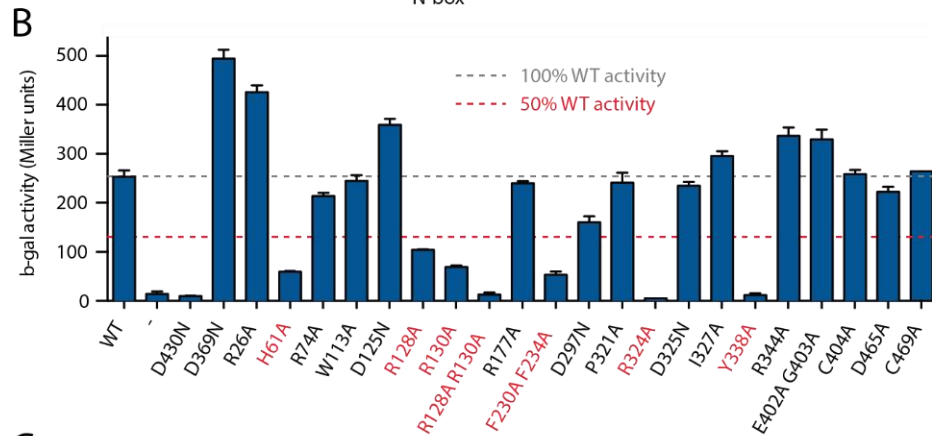
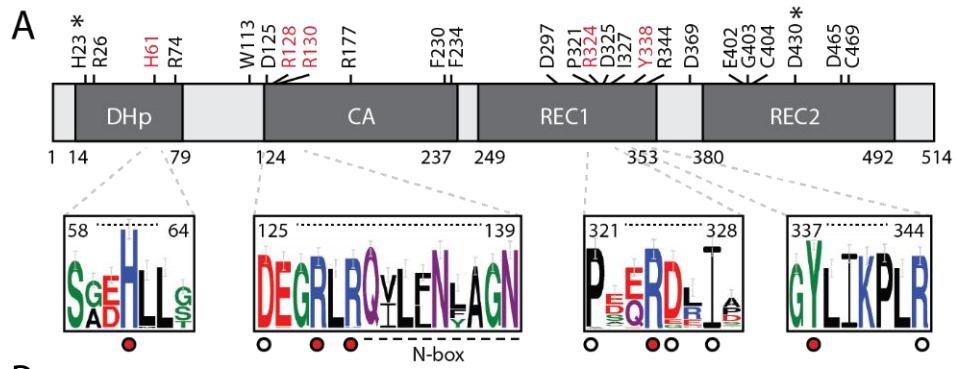


Figure 5.7 A degenerate REC domain is the primary c-di-GMP docking site in ShkA

(A) Schematic of ShkA domain architecture drawn to scale (top). Number below the schematic indicate domain boundaries. Residues that were mutagenized and tested *in vivo* are indicated above the schematic. Residues that when mutated impair c-di-GMP-dependent ShkA autophosphorylation are highlighted in red. The phosphorylatable His and Asp residues in the DHp and REC2 domain, respectively, are indicated by an asterisk. Weblogs (based on alignments shown in Figure 5.6) of selected regions that harbor amino acids implicated in c-di-GMP-dependent activation (indicated by a red dot) are shown at the bottom. Residues that were mutagenized and tested, but showed no adverse effects ShkA activity *in vivo* are indicated by a white circle.

(B) β -Gal activities a strain ($\Delta shkA \Delta lacA::\Omega$ / pAK502-*spmX*; UJ9691) expressing indicated *shkA* alleles in trans from plasmid pQF (no inducer added). Shown are means and standard deviations of three biological replicates.

(C) β -Gal activities a strain ($\Delta shkA \Delta lacA::\Omega$ / pAK502-*spmX*; UJ9691) expressing *shkA* alleles with indicated amino acid substitutions in isolation (*shkA*^{WT} BG) or in combination with the D369N substitution (*shkA*^{D369N} BG). Note that the values shown for the *shkA*^{WT} BG are the same as in (B). Shown are means and standard deviations of three biological replicates.

(D) *In vitro* autophosphorylation assays of wild-type ShkA and indicated mutant variants with (10 μ M) or without c-di-GMP. Autophosphorylation was allowed to proceed for 5 min at room temperature. Top: Autoradiograph; bottom: Coomassie stain of the same gel.

(E) Quantification of *in vitro* UV crosslinking experiments with ³²P-labelled c-di-GMP and indicated ShkA variants.

(F) *In vitro* UV crosslinking experiments with ³²P-labelled c-di-GMP (10 μ M) and full-length ShkA or the isolated REC1 domain of ShkA. For competition, a 100-fold molar excess of unlabeled c-di-GMP was added to the reaction mix before UV crosslinking. The asterisk indicates a radiolabeled background smear.

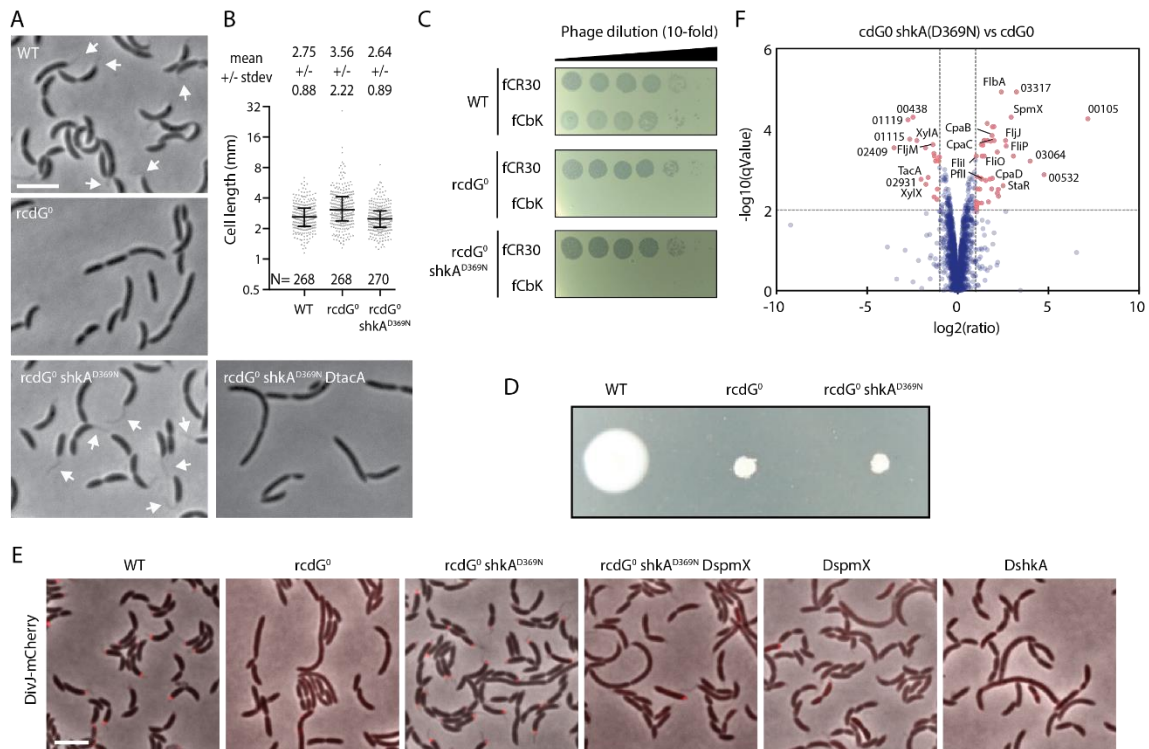


Figure 5.8 c-di-GMP-independent activation of ShkA restores morphological and cell cycle defects of a strain lacking c-di-GMP.

(A) Phase contrast micrographs of indicated strains. Arrows point to stalks. The scale bar represents 4 μ m.

(B) Quantification of cell length of strains shown in (A). The median with interquartile range is shown and the means +/- standard deviations are indicated above the graph (in μ m). Cell detection was performed with Outfit.

(C) Sensitivity of indicated strains towards phage ϕ CbK or ϕ CR30 infection. Plates were incubated 24h at 30°C.

(D) Motility of indicated strains on semi-solid agar. Plates were incubated 3 days at 30°C.

(E) DivJ-mCherry localization in indicated strains. Shown are merges between the phase contrast channel and the mCherry channel. The scale bar represents 4 μ m.

(F) Volcano plot comparing the proteomes of the *rcdG*⁰ strain and its derivative carrying the *shkA*^{D369N} allele. Selected proteins that are differentially abundant in the two strains with high confidence and fold-change are labelled by the NA1000 CCNA_ number.

5.5 C-DI-GMP-MEDIATED ACTIVATION AND PROTEOLYSIS DEFINES THE SHKA-TACA ACTIVITY WINDOW DURING THE CELL CYCLE

C-di-GMP regulates several processes during the *C. crescentus* cell cycle including cell polarity or the initiation of chromosome replication during G1/S transition^{10,87,165}. However, how individual pathways contribute to the pleiotropic phenotype of the cdG⁰ strain remained unclear. Introduction of the c-di-GMP independent *shkA*^{D369N} allele into the rcdG⁰ strain failed to re-establish motility or functional type IV pili, but restored stalk biogenesis and normal cell morphology (Figure 5.8). The latter observation suggested that ShkA-TacA is an integral part of the machinery regulating *C. crescentus* cell cycle progression. Recent studies had implicated the ShkA-TacA pathway in the SpmX-mediated polar localization and activation of the cell cycle kinase DivJ during G1/S transition¹⁵¹. In line with the above results, a DivJ-mCherry fusion, while completely delocalized in the cdG⁰ strain, localized normally in the presence of the *shkA*^{D369N} allele, a process that was fully dependent on the TacA target *spmX* (Figure 5.8). Moreover, rescue of normal cell morphology by the *shkA*^{D369N} allele also depended on *spmX* (Figure 5.8). Proteome analysis indicated that *shkA*^{D369N} indeed restored the expression of known TacA targets in the rcdG⁰ background, including SpmX and StaR (Figure 5.8). Thus, aberrant cell division of the cdG⁰ strain is caused largely by an inactive ShkA-TacA pathway and by the failure to induce the expression of the SpmX morphogen during G1/S.

Levels of c-di-GMP oscillate during the cell cycle^{27,86}. While being low in newborn SW cells (G1), c-di-GMP rapidly increases during the G1/S transition to reach peak levels upon entry into S-phase⁸⁷ (Figure 5.9A). The finding that c-di-GMP activates ShkA, together with the recent observation that TacA is rapidly degraded upon entry of cells into S-phase^{70,156}, argued that the ShkA-TacA pathway is tightly controlled during the cell cycle with a sharp peak of activity during G1/S. The analysis of TacA phosphorylation during the cell cycle revealed that active TacA~P was limited to a narrow window during G1/S (Figure 5.9B). As expected, TacA was rapidly degraded prior to S-phase entry and re-synthesized, but not phosphorylated, in G2 (Figure 5.9B). Degradation of TacA by the ClpXP protease required the adaptor proteins RcdA and CpdR (Figure 5.9C). When TacA was stabilized by replacing the C-terminal Ala-Gly degradation motif with Asp residues (TacA^{DD}) both TacA and TacA~P prevailed during the entire cell cycle (Figure 5.9B). This argued that degradation of TacA limits the cell cycle window during which TacA is active.

Akin to TacA~P, phosphorylated ShkA, ShkA~P, was only detected in G1 (Figure 5.9B). Both TacA~P and ShkA~P levels were detected immediately after harvesting a pure population of G1

swarmer cells by density gradient centrifugation (see Materials and Methods). Because the synchronization technique harvests all high-density swarmer cells irrespective of their exact age after division, ShkA~P and TacA~P levels represent population averages rather than exact values corresponding to a distinct cell cycle stage⁸⁷. Moreover, because sample preparation includes a short period of temperature equilibration, phosphorylation levels at the first sampling point are likely overestimated as a subset of the population has already increased c-di-GMP levels. Surprisingly, ShkA was also degraded during the cell cycle, although with a delay of about 20 minutes as compared to TacA (Figure 5.9B). This delay was explained by the finding that, in contrast to TacA degradation, which depends on CpdR and RcdA, degradation of ShkA also requires PopA, the third member of the adaptor hierarchy regulating ClpXP-dependent degradation during the *C. crescentus* cell cycle (Figure 5.9D)¹⁵⁶. ShkA also harbors a C-terminal Ala-Gly degradation motif, which when replaced by Asp residues (ShkA^{DD}) lead to stable ShkA protein and to an extended ShkA activity window during the cell cycle, as ShkA~P levels also prevailed (Figure 5.9D).

Based on these observations, we proposed that the ShkA-TacA activity is confined to the G1/S transition by sequential c-di-GMP mediated activation of the ShkA kinase and ClpXP-dependent degradation of both TacA and ShkA. While activation of TacA target genes during G1/S facilitates “just-in-time” expression of genes required for the next stage of the cell cycle or development, it is less clear why the ShkA-TacA pathway is confined to such a narrow window by specific proteolysis of its key components. To simulate a ShkA-TacA pathway that remains constitutively active throughout the cell cycle and to investigate the consequences of such dysregulation, alleles leading to constitutive activity and/or stability of ShkA and TacA were assembled in different combinations. As shown in Figure 5.9E and F, cell division and morphology remained wild-type-like in all strains that retained either TacA degradation or ShkA control. Combining TacA^{DD} either with ShkA^{DD} or with ShkA^{D369N} in the same strain led to a significant increase of cell length, which was aggravated in a strain that contained all three mutations. Importantly, the severe morphology defect in cells with a dysregulated ShkA-TacA pathway was entirely dependent on an intact copy of *spmX*, arguing that the observed defect is due to misregulation of the SpmX morphogen. Thus, these experiments confirmed that not only the timing of ShkA-TacA activation is important but also its exact window of activity. This provides the rationale for the highly sophisticated regulatory mechanisms that are in place to limiting TacA-dependent transcription to a short phase of the cell cycle.

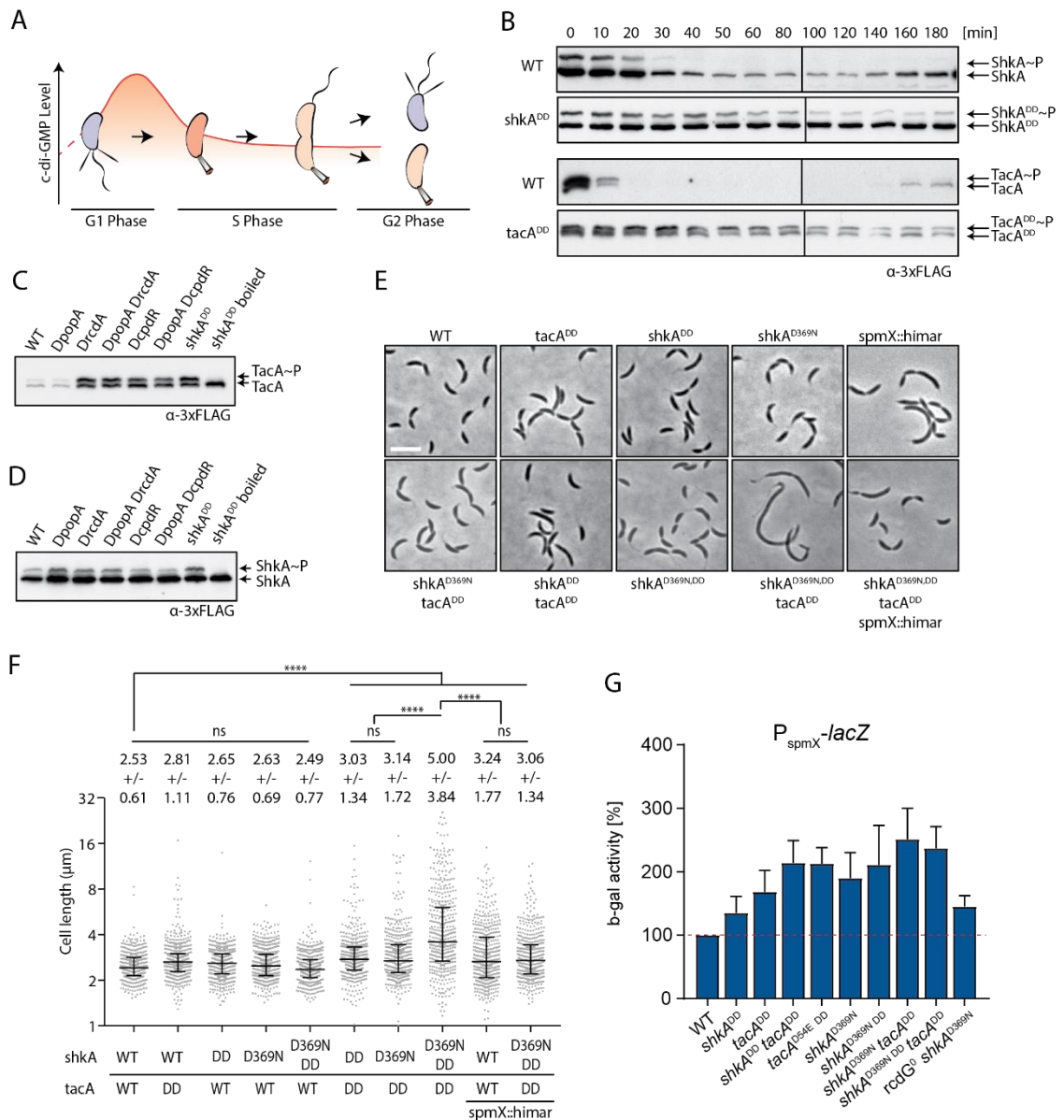


Figure 5.9 Precise ShkA-TacA activation by phosphorylation and shut-down by degradation ensure proper cell cycle progression and morphogenesis.

(A) Scheme of c-di-GMP oscillations during the cell cycle.

(B) PhosTag PAGE western blots of synchronized cultures of strains carrying 3xFLAG-tagged *tacA* or *shkA* or their stabilized derivatives, *tacA^{DD}* or *shkA^{DD}*.

(C) PhosTag PAGE western blots of mixed cultures of various mutant strains carrying 3xFLAG-tagged *tacA*. A boiled sample was included to specifically deplete the phosphorylated protein band.

(D) PhosTag PAGE western blots of mixed cultures of various mutant strains carrying 3xFLAG-tagged *shkA*. A boiled sample was included to specifically deplete the phosphorylated protein band.

(E) Phase contrast micrographs of strains that carry combinations of alleles encoding TacA or ShkA variants blocked for degradation (DD) and/or ShkA carrying the constitutively active, c-di-GMP independent D369N mutation (DN). The scale bar represents 4μM.

The scale bar represents 4μM.

(F) Quantification of cell length of strains shown in (E). The median with interquartile range is shown and the means +/- standard deviations are indicated above the graph (in μm). Cell detection was performed with Oufiti and statistical analysis with GraphPad Prism 7 on 480-489 random cells for each strain using the Kruskal-Wallis test. *, **, *** and **** indicate P values of < 0.1, <0.01, <0.001 and <0.0001, respectively; ns, not significant.

(G) The expression of *spmX* can be increased by stabilizing proteins in the ShkA-TacA pathway as well as expressing constitutively active ShkA^{D369N}. β -galactosidase assays performed with the p_{*spmX-lacZ*} reporter plasmid. Promoter activity of *spmX* was measured in wild-type and mutant strains. Data represent mean \pm SD.

5.6 THE SHKA-TACA PATHWAY LIMITS GENE EXPRESSION TO G1/S

To visualize TacA activity in individual cells progressing through the cell cycle and to validate the G1/S specific expression profile of TacA target genes, we developed a fluorescent reporter system, in which we fused the *spmX* promoter to the photoconvertible fluorescent protein *dendra2*. This reporter is capable of photoconversion from green to red fluorescence in response to UV light²⁰⁵ and thus allows to distinguish old red reporter from newly synthesized green reporter. Photoconversion at different time points during a specific time window provides information regarding both ON and OFF kinetics of transcription. When predivisional cells expressing a *spmX::dendra2* promoter fusion were followed through the division process after photoconversion, increase of green fluorescence and thus *spmX* promoter activity was only observed in the SW but not in the ST progenies (Figure 5.10A). Quantification of SW offspring over time indicated transcription of *spmX* is activated 15-30 min after photoconversion (Figure 5.10B). Next, we performed a similar experiment but applied photoconversion at different time points during the G1/S transition to determine the OFF kinetics of the *spmX* promoter (Figure 5.10B). Matching the data from both experiments revealed that transcription of *spmX* peaks about 15-30 minutes after cells had reached the predivisional stage (Figure 5.10B). For several reasons, the actual response time of *spmX* transcription after birth is likely shorter. First, because exact monitoring of cell division is difficult, photoconversion was generally applied prior to division. Second, for microscopy cells were cultivated on agar pads reducing their growth rate as compared to cells grown in liquid (Figure 5.10A,E). Finally, folding of the reporter sets off fluorescence appearance from the time of gene expression.

To verify that the *spmX* promoter is transcribed exclusively during G1/S and to probe the role of c-di-GMP and the ShkA-TacA pathway in *spmX* gene expression control, the *spmX-dendra2* reporter output was monitored in individual cells and during three consecutive cell divisions. The analysis of individual lineages revealed that in a *C. crescentus* wild type strain reporter activity was only detected in cells progressing through G1/S, while it was absent in ST progeny

(Figure 5.10D, Figure 5.11). This stage-specific pattern is in part due to c-di-GMP oscillations during the cell cycle as expression of the *E. coli* DGC *dgcZ* from the constitutive *Plac* promoter induced *spmX* transcription in ST progeny lineages (Figure 5.10D, Figure 5.11). Similarly, in lineages of cells expressing a stable version of TacA (TacA^{DD}), the strong preference for G1/S expression was abolished. Finally, expression patterns lost stage-specificity completely in all lineages co-expressing TacA^{DD} and *dgcZ* or expressing TacA^{DD} together with the constitutive ShkA variant, ShkA^{D369N} (Figure 5.10C,D, Figure 5.11).

Altogether, these experiments provide direct evidence that the activity of the ShkA-TacA pathway is strictly limited to swarmer progeny going through the G1/S cell cycle transition. Moreover, these experiments on a single cell level confirm data obtained with synchronized populations of cells indicating that the strict temporal control of ShkA-TacA activity during the cell cycle results from a combination of c-di-GMP-mediated kinase activation and protein degradation.

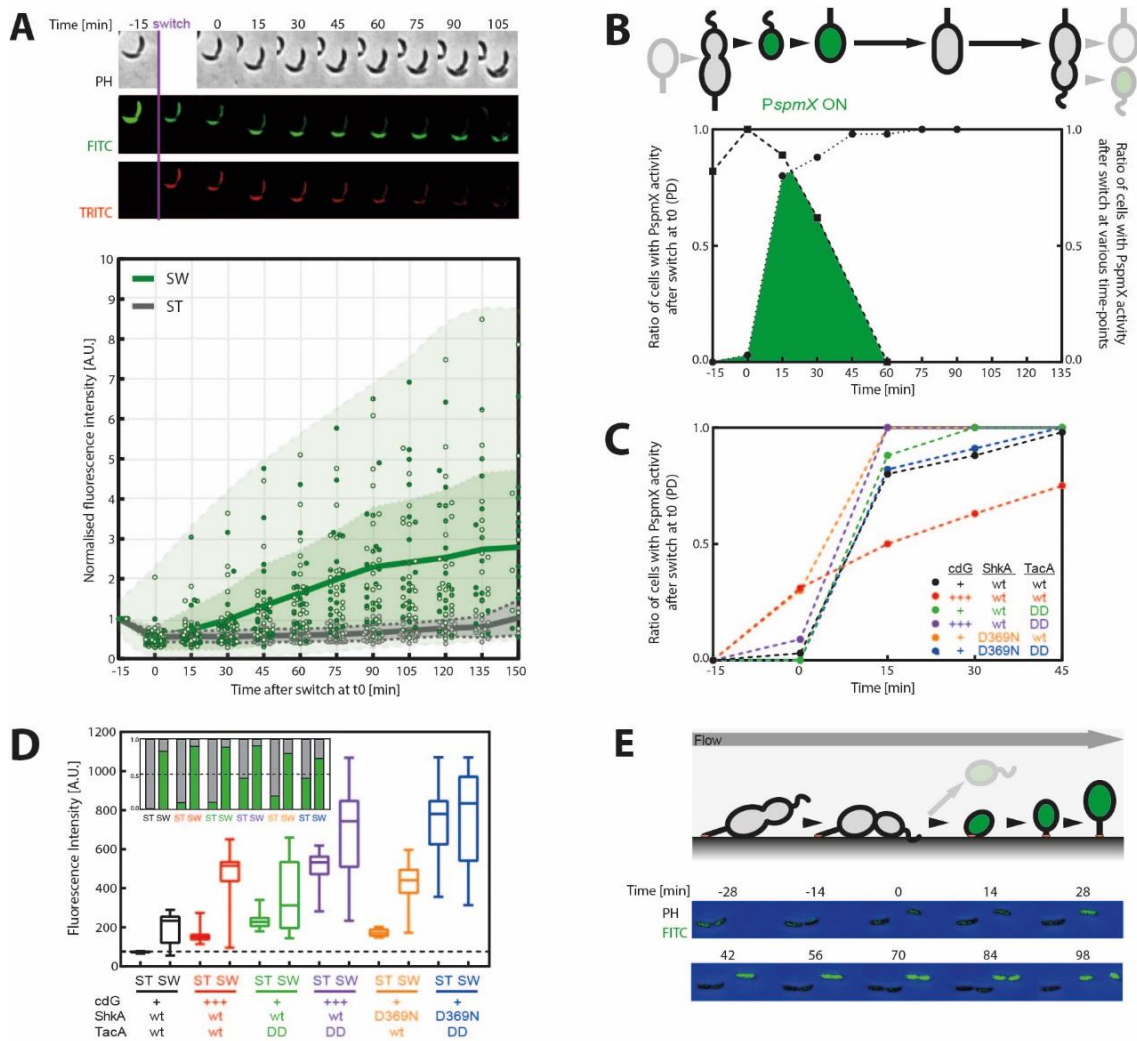


Figure 5.10 TacA activity is limited to the G1-S transition and strictly dependent on c-di-GMP oscillations, ShkA activation and TacA degradation

TacA activity is deduced by the timing of *spmX* promoter activity visualized using a promoter fusion to the fluorescent reporter dendra2. In contrast to the wild type, strains with increased c-di-GMP levels, producing degradation-independent TacA as well as c-di-GMP-independent hyper-active ShkA shift this activity window.

Lineages of cells were analyzed originating from the same parental PD, this late PD was used as a reference time-point to determine cell septation before motile and swarmer cells were analyzed over the course of the cell cycle. The last time-point marks the last frame before the cell septation. During time-lapse imaging frames were taken every 15 minutes. Time-point zero refers to the first frame after septation of the two cells. Unless stated otherwise the green fluorescence of PD cells was switched to red 15 minutes before division using UV light (DAPI) and the increase of newly synthesised dendra2 (green fluorescence) was determined over time in various genetic backgrounds. *PspmX* activity is shown in green, absence in gray. Abbreviations: ST = stalked cells, SW = swarmer cells, PD = predivisional cell.

(A) *PspmX* activity rises sharply in wild-type swarmer cells but remains absent in stalked cells. Fluorescence of the offspring of 39 PDs was plotted over one cell cycle.

(B) The window of TacA activity follows the G1-S transition between 15 to 30 minutes after septation as inferred from the ON and OFF kinetics in wild-type swarmer cells. For up-kinetics, 39 PD cells were switched 15 minutes

before division using UV light and the time of the increase of fluorescence in the swarmer population. For down kinetics, 80 cells at different stages during the cell cycle were switched using UV light and the increase of fluorescence was determined using the time-point after septation as reference time-point zero. Ratio of cells with *PspmX* activity was plotted over time.

(C) Increased c-di-GMP levels and c-di-GMP-independent hyper-active ShkA^{D369N} increase the probability that swarmer cells activate the *spmX* promoter just after septation and thereby *spmX* activity is preponed. Inferred ON kinetics of wild-type compared to different mutant strains, between 10-39 PD cells just before division were switched using UV light and the increase of fluorescence was determined over time. Ratio of cells with *spmX* activity was plotted over time.

(D) As soon as c-di-GMP levels are not oscillating, TacA degradation is perturbed and ShkA is hyper-active, *spmX* activity is switched on in stalked cells and increases dramatically. Cell fluorescence of 10-40 cells was measured over the cell cycle of swarmer and stalked cells of wild-type and various mutant strains. The inlay graph shows the fraction of swarmer/stalked cells scored with *PspmX* active (green) or inactive (gray).

(E) Preliminary microfluidic experiments reinstate the delay of rising *spmX* promoter activity after division towards G1-S phase transition. Cells were allowed to grow and attach in microfluidic chambers subjected to constant flow of 0.002 μ l/s.

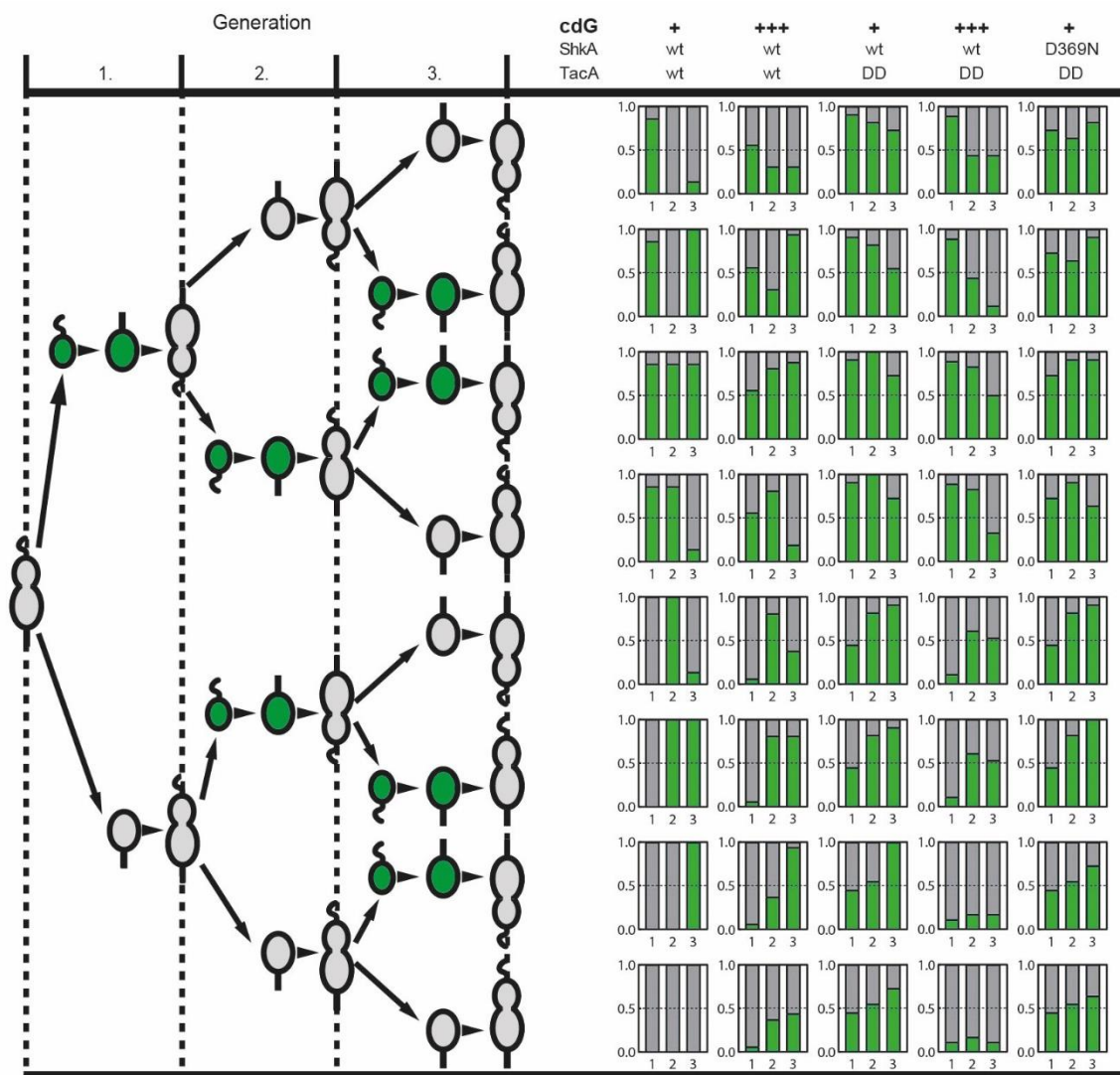


Figure 5.11 The oscillation of *spmX* activity is dependent on a functional ShkA-TacA pathway and oscillating c-di-GMP levels.

During three consecutive generations starting of at least 10 PD only G1-S-cells in wild-type show oscillating *spmX* activity. As soon as c-di-GMP levels are not oscillating, TacA degradation is perturbed and ShkA is hyper-active, the *spmX* promoter is constitutively more active in all cell types. Plotted is the fraction of cells with *PspmX* active (green) or inactive (gray).

6 DISCUSSION & OUTLOOK

In recent years, we have gained a deep understanding of how the bacterial model organism *C. crescentus* coordinates cell division with morphological and behavioral changes. *C. crescentus* divides asymmetrically to produce a replication competent ST and a replication-inert SW cell. After a defined period (called G1) the motile SW cell regains its replicative potential and enters S-phase, a process during which it also differentiates into a sessile ST cell. Three regulatory mechanisms orchestrate the unidirectional G1-S transition in parallel: A complex phosphorylation network of two-component systems promotes cell cycle progression; controlled proteolysis removes key G1 components to advance the cell cycle irreversibly; and rising levels of c-di-GMP coordinate morphogenesis with the underlying cell cycle. However, the details of how these mechanisms are interlinked have remained incomplete.

A *C. crescentus* strain that lacks all diguanylate cyclases (cdG^0) and therefore cannot produce c-di-GMP has severe division defects and expresses no polar appendages⁸⁷. Adding to these phenotypes, we could show that neither ShkA nor TacA are phosphorylated in this background. Intriguingly, when we expressed a constitutively active *tacA*^{D54E} mutant in the cdG^0 background to simulate and activate the ShkA-TacA pathway, not only *spmX* expression was rescued, but also stalk biogenesis. In addition, c-di-GMP was sufficient to induce phosphorylation of both ShkA and TacA *in vivo*. This evidence suggested that this pathway is part of the transcriptional network orchestrating cell cycle progression and that its activity is controlled by the c-di-GMP upshift during this transition.

By showing *in vitro* that c-di-GMP not only binds to ShkA strongly but also stimulates its phosphorylation activity, we could establish a direct link between the ShkA-TacA pathway and c-di-GMP phenotypes. Counterintuitively, ShkA does neither have a classical c-di-GMP binding motif nor an input domain. However, the protein contains two receiver domains, one of them, REC1, lacking residues important for phosphorylation. In a genetic screen, we found a highly conserved, short stretch of amino acids (DDR motif). When we mutated residues in this motif, for example D369N, ShkA phosphorylation was released from its c-di-GMP control.

By expressing this c-di-GMP independent *shkA*^{D369N} allele in the cdG^0 background, we could restore cell morphology and stalk biogenesis. However, phenotypes linked to motile SW cells including pili biogenesis and motility stayed impaired. The fact that ShkA^{D369N} only restored phenotypes directly linked to G1-to-S phase transition, suggested that the ShkA-TacA pathway is linked to this phase in dependence of c-di-GMP.

In a ShkA^{D369N} mutation that is active independently of c-di-GMP, binding itself was not obliterated. This allowed us to track residues that are likely involved in binding c-di-GMP. Mutating the still conserved tyrosine switch residue in the nonfunctional REC1 domain, Y338A, reduced binding to c-di-GMP strongly. In addition, autokinase activity of ShkA was turned off even in the presence of c-di-GMP. However, by introducing the D369N mutation, autokinase activity was restored. This strongly suggests, that Y338 is involved in c-di-GMP binding to control kinase activity. Upon the phosphorylation of a functional receiver domain, the switch residue generally initiates a conformational change⁴⁵. As the REC1 of ShkA cannot be phosphorylated, it is possible that c-di-GMP binding induces a conformational change instead (Figure 6.1).

ShkA is active *in vitro* when the REC2 domain is expressed separately even in the absence of c-di-GMP. This loss of inhibition indicates, that the REC1 usually prevents phosphorylation to take place by coordinating the other domains of ShkA into an inhibitory conformation. Mutating the phosphorylation site or residues in the magnesium binding pocket of the REC2 domain impaired phosphotransfer but restored autokinase activity. This indicates that the REC2 domain itself is also involved in kinase regulation. A conformational change initiated by c-di-GMP might therefore free the domains to initiate autophosphorylation and phosphotransfer. Solving the protein structure of ShkA will help us describe the mechanistic details of this novel regulatory kinase mechanism at a later stage.

Our data suggests, that the c-di-GMP regulation of ShkA must work differently to another *C. crescentus* histidine kinase also under the control of c-di-GMP. It was recently shown, that c-di-GMP forces the histidine kinase CckA from a kinase into a phosphatase. C-di-GMP thereby binds to the DHp domain and forces CckA into an open conformation that allows its receiver domain access for dephosphorylation²⁹. While this means that c-di-GMP directly binds to the CckA DHp domain to switch it from a kinase to a phosphatase, ShkA binds c-di-GMP in its pseudo receiver domain which activates kinase activity.

As the DDR motif that couples c-di-GMP regulation to kinase activity is conserved in ShkA orthologs of *Caulobacteraceae*, it would be exciting to test whether these are also under control of c-di-GMP or if they are regulated differently. ShkA is a determining factor in regulating the lifestyle of *C. crescentus* and might have similar functions in other bacteria. However, adapting to different ecological niches might also require another regulation of ShkA.

Intriguingly, many kinases exist with two receiver domains. In these kinases, one of the receiver domains may also perform regulatory functions. This means that similar mechanisms to control kinase activity may be widespread in bacteria.

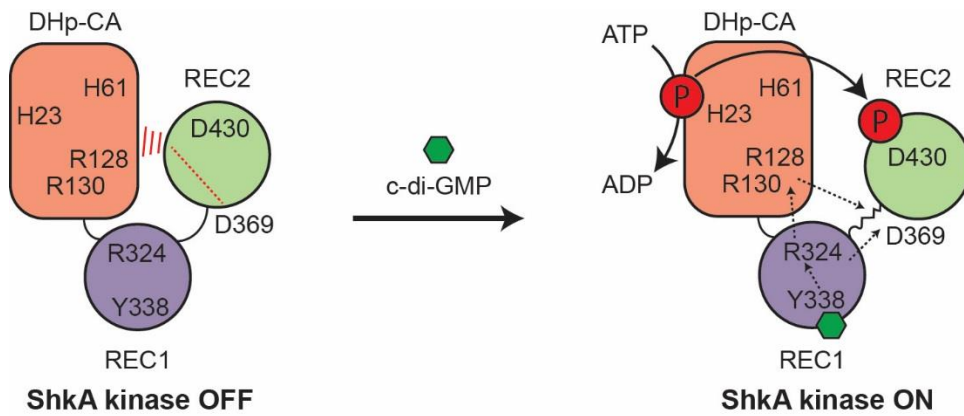


Figure 6.1: Without c-di-GMP, the histidine kinase ShkA cannot autophosphorylate (H23) or phosphotransfer (D430) to REC2. After c-di-GMP binds to the switch residue Y338, autophosphorylation and phosphotransfer is activated. Residues that are involved in ShkA activity are indicated. Based on data from Figure 5.7.

In the *C. crescentus* cell cycle, both TacA and ShkA are specifically degraded by ClpXP adaptors. It was shown before, that TacA degradation is dependent on the adaptors RcdA and CpdR¹⁵⁶. Adding to that, we showed that ShkA is degraded in a 20-minute delay by the third adaptor PopA in a c-di-GMP dependent manner. Both proteins are phosphorylated early in the cell cycle what coincides with a rise of c-di-GMP levels early in G1-to-S phase transition⁸⁷. As ShkA phosphorylation is activated by c-di-GMP, we reasoned that its activity is dependent on a certain threshold of emerging c-di-GMP levels, while the pathway later is turned off by protein degradation.

To assess how c-di-GMP levels and protein degradation influence pathway activity, we performed experiments on a single cell level with fluorescence reporters. This allowed us to measure and compare up- and down-kinetics of a *spmX::dendra2* promoter fusion. With this assay, we could demonstrate, that *spmX* expression is indeed limited to G1-to-S phase transition with no expression in S-phase. However, this specific expression window was lost when the *E. coli* diguanylate cyclase *dgcZ* was expressed, or when the pathway was uncoupled from c-di-GMP control by expressing *shkA*^{D369N}. The clear pattern of *spmX* expression could also be abolished on an output level. When we impaired degradation of the pathway components TacA or ShkA by stabilizing them, *spmX* expression was active in all cell stages.

Taken together, these data demonstrate that *spmX* expression is limited to G1-S phase by activation of ShkA by rising c-di-GMP levels and deactivation by degrading of TacA. By

regulating the ShkA-TacA pathway on an input level as well as on an output level, it can be delicately controlled. Early in G1-to-S phase transition, ShkA phosphorylation is activated in dependence of c-di-GMP. Then, proteolysis sharply turns off the pathway by degrading TacA and later ShkA. This pathway regulation is necessary, as impairing proteolysis of ShkA and TacA and uncoupling ShkA activity from c-di-GMP leads to severe division defects, most likely due to a misregulation of SpmX (Figure 6.2).

Based on our findings, we can answer the outstanding question of how G1-to-S phase transition is regulated in *C. crescentus*. Kinase activity and proteolysis drive the *C. crescentus* G1-to-S phase transition. However, this process is under the control of c-di-GMP in a highly regulated and tightly timed fashion. Rising levels of c-di-GMP in the SW cell successively activate cell cycle checkpoints: First emerging levels of c-di-GMP likely activate ShkA phosphorylation to express *spmX*. SpmX localizes and stimulates DivJ kinase activity. DivJ then phosphorylates the diguanylate cyclase PleD which initiates a feedback loop to quickly rise c-di-GMP levels in the cell. In addition, DivJ together with DivK~P and c-di-GMP turns off the CckA-Chpt-CtrA pathway by switching CckA into phosphatase mode and allowing the cell to start replication. Switching CckA into a phosphatase also activates the first ClpXP adaptor CpdR to activate proteolysis of the phosphodiesterase PdeA, allowing c-di-GMP levels to rise even higher. During this time, TacA is also acting as a transcription factor for *staR* and thereby has initiated stalk biogenesis and holdfast production. The protease adaptor RcdA then binds to the ClpXP-CpdR complex to degrade TacA. This turns off the ShkA-TacA switch, defining a close window in which this pathway is active and provides the SW cell with what it needs to turn into a ST cell. Finally, c-di-GMP reaches peak levels to activate the last ClpXP adapter PopA to degrade CtrA and ShkA. This largely completes G1-to-S phase transition.

Taken together, we show that the second messenger c-di-GMP defines and controls the entire G1-to-S phase transition in *C. crescentus*. Rising levels of c-di-GMP progressively trigger cell cycle checkpoints by activating kinase pathways. Additionally, c-di-GMP helps to enforce unidirectional cell cycle progression by controlling proteolysis. C-di-GMP therefore elegantly orchestrates and integrates the complex networks of G1-to-S phase transition.

Due to the immense complexity of the *C. crescentus* G1-to-S phase transition, open questions remain. While TacA is degraded early by RcdA, ShkA is degraded later by PopA. This could mean that the ShkA-ShpA pathway branches off and controls more than only TacA activity. More importantly, it is not clear what initially triggers the G1-to-S phase transition. DivJ and PleC are important to start the cell cycle by phosphorylating DivK. However, a $\Delta divJ \Delta pleC$

double mutant is viable, while a $\Delta divK$ mutant is lethal. As DivK does not have domains that allow autophosphorylation, there could be additional kinases activating DivK.

Very early in G1-to-S phase transition, ShkA activity needs to be upregulated by emerging levels of c-di-GMP to initiate the c-di-GMP feedback loop. It would seem natural that one of the many diguanylate cyclases in *C. crescentus* with unknown function and regulation could be responsible for this initial push. PleC most likely plays an important role in regulating this process, as no *spmX* expression remains in a $\Delta pleC$ strain, however it is still unclear how the initial push into cell division is regulated. Solving the open questions of how *C. crescentus* cell division is initiated will most likely expand our knowledge on this complex regulatory network even further.

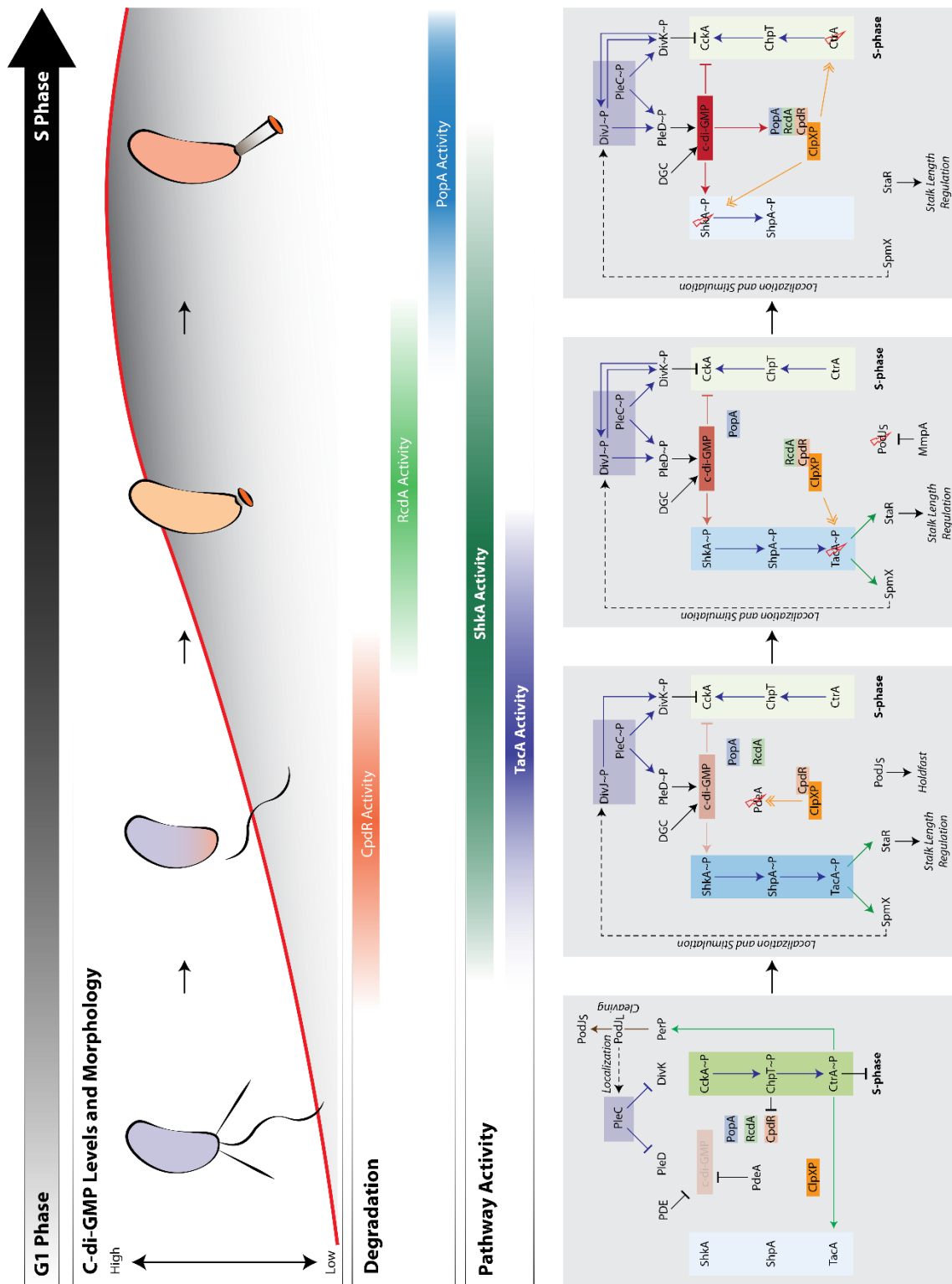


Figure 6.2: G1-to-S phase transition. Pathway activity of ShkA and TacA is defined by rising c-di-GMP levels that induce ShkA kinase, and protein degradation by ClpXP adaptors. TacA is degraded early by RcdA. This leads to a short activity window of the ShkA-TacA pathway. ShkA is degraded by PopA at a later stage to possibly phosphorylate other targets.

7 MATERIAL & METHODS

7.1 STRAINS USED IN THIS STUDY

For *E. coli*, recombinant DNA techniques and procedures for DNA purification, restriction, ligation and transformation were performed as described before²⁰⁶. For *C. crescentus*, bi-parental conjugation with *E. coli* S17-S, tri-parental conjugation with *E. coli* DH10b and an *E. coli* donor strain with the RP4 plasmid, or transduction with ϕ CR30 phage was carried out as described before²⁰⁷. Restriction enzymes were obtained from New England Biolabs (NEB) and PCR reactions were performed with Phusion polymerase (NEB). Oligonucleotides were purchased from Sigma-Aldrich. All constructs were sequence verified.

Strain	Genotype	Reference
<i>E. coli</i>		
	BL21 Rosetta	Novagen
	DH10B	Life Technologies
	DH5a	Woodcock et al. 1989
	S17	Simon et al. 1983
	MT607	Vargas et al. 1999
<i>C. crescentus</i>		
UJ4475	NA1000 (wild-type strain, synchronizable, CB15N)	Evinger & Agabian, 1977
AKS1	CB15 rcdG0 Δ lacA::W ampG::pNPTStet-ampG	Kaczmarczyk, A.
AKS4	CB15 rcdG0 Δ lacA::W	Kaczmarczyk, A.
AKS17	CB15 rcdG0 Δ lacA::W/pAK502-spmX	Kaczmarczyk, A.
AKS30	CB15 rcdG0 Δ lacA::W shkA(D369N)/pAK502-spmX	Kaczmarczyk, A.
AKS102	NA1000 Δ spmX::pNPTSDspmX	Kaczmarczyk, A.
AKS118	NA1000 Δ spmX	Kaczmarczyk, A.
AKS121	NA1000 rcdG0 shkA(D369N) DspmX	Kaczmarczyk, A.
AKS152	NA1000 divJ::mCherry	Kaczmarczyk, A.
AKS153	NA1000 rcdG0 divJ::mCherry	Kaczmarczyk, A.
AKS154	NA1000 rcdG0 shkA(D369N) divJ::mCherry	Kaczmarczyk, A.
AKS155	NA1000 Δ spmX divJ::mCherry	Kaczmarczyk, A.
AKS156	NA1000 rcdG0 shkA(D369N) DspmX divJ::mCherry	Kaczmarczyk, A.
AKS181	NA1000 Δ shkA divJ::mCherry	Kaczmarczyk, A.
AKS182	NA1000 tacA(A491D,G492D)::pNPTS-tacADD	Kaczmarczyk, A.
AKS216	NA1000 rcdG ⁰ Δ shkA	Kaczmarczyk, A.
AKS217	NA1000 shkA(D369N,A513D,G514D) tacA(A491D,G492D)	Kaczmarczyk, A.
AKS236	NA1000 shkA(D369N,A513D,G514D) tacA(A491D,G492D) Δ spmX	Kaczmarczyk, A.
AKS237	NA1000 Δ pleC shkA(D369N)	Kaczmarczyk, A.

AKS255	NA1000 $\Delta pleC shkA(D369N) divJ::mCherry$	Kaczmarczyk, A.
AKS256	NA1000 $\Delta pleC divJ::mCherry$	Kaczmarczyk, A.
AKS257	NA1000 $shkA(D369N) divJ::mCherry$	Kaczmarczyk, A.
UJ6168	CB15 $\Delta lacA::W$	Arellano et al., 2010
UJ9652	NA1000 $\Delta shkA \Delta lacA::W$	Kaczmarczyk, A.
AKS147	NA1000 $\Delta shkA::pNPTSDshkA \Delta lacA::W$	Kaczmarczyk, A.
UJ5065	NA1000 cdG^0	Abel et al., 2013
UJ9056	NA1000 $\Delta shkA$	von Arx, C.
CvA32	NA1000 $cdG^0 \Delta shkA$	von Arx, C.
CvA03	NA1000 $spmX$ -mCherry	von Arx, C.
CvA04	NA1000 $cdG^0 spmX$ -mCherry	von Arx, C.
CvA06	NA1000 $\Delta shkA spmX$ -mCherry	von Arx, C.
CvA50	NA1000 $cdG^0 \Delta shkA spmX$ -mCherry	von Arx, C.
UJ8535	NA1000 3xFlag- $shkA$	von Arx, C.
UJ8536	NA1000 3xFlag- $shkA cdG^0$	von Arx, C.
UJ8959	NA1000 3xFlag- $shkA r$ - cdG^0	Hempel, A.M.
UJ8533	NA1000 3xFlag- $tacA$	von Arx, C.
UJ8961	NA1000 3xFlag- $tacA r$ - cdG^0	Hempel, A.M.
UJ8888	NA1000 3xFlag- $shkA$ DD (A513D, G514D)	von Arx, C.
UJ8926	NA1000 3xFlag- $tacA$ DD (A491D, A492D)	Hempel, A.M.
UJ2827	NA1000 $\Delta popA$	Duerig et al., 2009
UJ3628	NA1000 $\Delta rcdA$	McGrath et al., 2006
UJ3656	NA1000 $\Delta popA \Delta rcdA$	Duerig et al., 2009
UJ4373	NA1000 $\Delta cpdR$	Skerker et al., 2005
UJ4401	NA1000 $\Delta popA \Delta cpdR$	Duerig et al., 2009
UJ9455	NA1000 3xFlag- $tacA \Delta popA$	von Arx, C.
UJ9456	NA1000 3xFlag- $tacA \Delta rcdA$	von Arx, C.
UJ9457	NA1000 3xFlag- $tacA \Delta rcdA \Delta popA$	von Arx, C.
UJ9458	NA1000 3xFlag- $tacA \Delta cpdR$	von Arx, C.
UJ9459	NA1000 3xFlag- $tacA \Delta cpdR \Delta popA$	von Arx, C.
UJ9554	NA1000 3xFlag- $shkA \Delta pdeA$	von Arx, C.
UJ9460	NA1000 3xFlag- $shkA \Delta popA$	von Arx, C.
UJ9555	NA1000 3xFlag- $shkA \Delta popA \Delta pdeA$	von Arx, C.
UJ9461	NA1000 3xFlag- $shkA \Delta rcdA$	von Arx, C.
UJ9556	NA1000 3xFlag- $shkA \Delta rcdA \Delta pdeA$	von Arx, C.
UJ9462	NA1000 3xFlag- $shkA \Delta rcdA \Delta popA$	von Arx, C.
UJ9557	NA1000 3xFlag- $shkA \Delta rcdA \Delta popA \Delta pdeA$	von Arx, C.
UJ9463	NA1000 3xFlag- $shkA \Delta cpdR$	von Arx, C.
UJ9558	NA1000 3xFlag- $shkA \Delta cpdR \Delta pdeA$	von Arx, C.
UJ9464	NA1000 3xFlag- $shkA \Delta cpdR \Delta popA$	von Arx, C.
UJ9559	NA1000 3xFlag- $shkA \Delta cpdR \Delta popA \Delta pdeA$	von Arx, C.
SoA0764	NA1000 r - cdG^0	Abel et al., 2013

SoA1587	NA1000 r-cdG ⁰ :: <i>dgcZ</i>	Abel et al., 2013
UJ9619	NA1000 r-cdG ⁰ <i>shkA</i> D369N	Kaczmarczyk, A.
UJ9170	NA1000 <i>tacA</i> DD (A491D, A492D)	von Arx, C.
UJ8987	NA1000 <i>tacA</i> D54E	von Arx, C.
UJ9621	NA1000 <i>tacA</i> DD (A491D, A492D) <i>shkA</i> D369N	Kaczmarczyk, A.
UJ9701	NA1000 <i>shkA</i> DD (A513D, G514D)	von Arx, C.
UJ9168	NA1000 <i>shkA</i> DD (A513D, G514D) <i>TacA</i> DD (A491D, A492D)	von Arx, C.
UJ9703	NA1000 <i>shkA</i> D369N DD (A513D, G514D)	von Arx, C.
UJ9620	NA1000 r-cdG ⁰ :: <i>dgcZ</i> <i>shkA</i> D369N	Kaczmarczyk, A.
UJ5059	NA1000 cdG ⁰ :: <i>pleD</i>	Abel et al., 2013
UJ4450	NA1000 Δ <i>pleD</i>	Abel et al., 2013
UJ4449	NA1000 Δ <i>dgcB</i>	Abel et al., 2013
UJ5790	NA1000 Δ <i>pleD</i> Δ <i>dgcB</i>	Abel et al., 2013
UJ4454	NA1000 Δ <i>pdeA</i>	Abel et al., 2013
UJ9412	NA1000 <i>tacA</i> D54E DD (A491D, A492D)	von Arx, C.
UJ9618	NA1000 <i>shkA</i> D369N	Kaczmarczyk, A.
UJ6712	NA1000 Δ <i>spmY</i>	Nesper, J.
UJ8568	NA1000 Δ <i>tacA</i>	von Arx, C.
UJ4687	NA1000 Δ <i>spmX</i>	Radhakrishnan et al., 2008
UJ998	NA1000 Δ <i>divJ</i>	Aldridge et al., 2003
UJ506	NA1000 Δ <i>pleC</i>	Aldridge et al., 2003
UJ508	NA1000 Δ <i>pleC</i> Δ <i>pleD</i>	Aldridge et al., 2003
UJ999	NA1000 Δ <i>divJ</i> Δ <i>pleD</i>	Aldridge et al., 2003
UJ1001	NA1000 Δ <i>divJ</i> Δ <i>pleC</i> Δ <i>pleD</i>	Aldridge et al., 2003
UJ1000	NA1000 Δ <i>divJ</i> Δ <i>pleC</i>	Aldridge et al., 2003
SoA1293	NA1000 cdG ⁰ :: <i>dgcZ</i>	Abel et al., 2013
AKS217	NA1000 <i>shkA</i> D369N DD (A513D, G514D) <i>tacA</i> DD (A491D, A492D)	Kaczmarczyk, A.
UJ9685	NA1000 3xFlag- <i>tacA</i> <i>shkA</i> D369N	Kaczmarczyk, A.
UJ9686	NA1000 cdG ⁰ 3xFlag- <i>tacA</i> <i>shkA</i> D369N	Kaczmarczyk, A.
UJ9687	NA1000 3xFlag- <i>tacA</i> DD (A491D, A492D) <i>shkA</i> D369N	Kaczmarczyk, A.
UJ9688	NA1000 cdG ⁰ 3xFlag- <i>tacA</i> DD (A491D, A492D) <i>shkA</i> D369N	Kaczmarczyk, A.
UJ8964	NA1000 Δ <i>shkA</i> <i>tacA</i> D54E	Hempel, A.M.
UJ8971	NA1000 r-cdG ⁰ <i>tacA</i> D54E	von Arx, C.
UJ8976	NA1000 cdG ⁰ <i>tacA</i> D54E 1	von Arx, C.
UJ8977	NA1000 cdG ⁰ <i>tacA</i> D54E 2	von Arx, C.

7.2 PLASMIDS

pAK502: Part of *lacZ* was PCR-amplified from pAK501 using primers 9060/9061, the product was digested with KpnI/DraIII and cloned into pAK501 digested with the same enzymes.

pAK503: *nptII* without RBS and start codon was PCR-amplified from pAK405 using primers 8959/9495, the product was digested with BsrGI/XbaI and cloned into pAK501 cut with Acc65I/XbaI.

pAK502-*spmX*: The *spmX* promoter and part of the codon sequence were PCR-amplified from *C. crescentus* gDNA using primers 8966/9064, the product was digested with XbaI/KpnI and cloned into pAK502 digested with the same enzymes.

pAK503-*spmX*: The *spmX* promoter and part of the codon sequence were PCR-amplified from *C. crescentus* gDNA using primers 8966/9064, the product was digested with XbaI/KpnI and cloned into pAK503 digested with the same enzymes.

pNPTStet: *tetA* and *tetR* were PCR-amplified from pQF using primers 9552/9553, the product was digested with SpeI/NdeI and cloned into pNPTS138 digested with AseI/XbaI.

pNPTStet-*ampG*: Part of *ampG* located downstream of *shkA* was PCR-amplified from *C. crescentus* gDNA with primers 9554/9555, the product was digested with SpeI/KpnI and cloned into pNPTStet digested with the same enzymes.

pET28a-*shkA*: *shkA* was PCR-amplified from *C. crescentus* gDNA with primers 9745/9746, the product was digested with NdeI/EcoRI and cloned into pET28a digested with the same enzymes.

pET28a-*shkA*(D369N): *shkA*(D369N) was amplified from *C. crescentus* strain UJ9618 by colony-PCR using primers 9745/9746, the product was digested with NdeI/EcoRI and cloned into pET28a digested with the same enzymes.

pQF-*shkA*: *shkA* was PCR-amplified from *C. crescentus* gDNA with primers 9745/9746, the product was digested with NdeI/EcoRI and cloned into pQF digested with AseI/EcoRI.

pQF-*shkA*(D369N): *shkA*(D369N) was amplified from *C. crescentus* strain UJ9618 by colony-PCR using primers 9745/9746, the product was digested with NdeI/EcoRI and cloned into pQF digested with AseI/EcoRI.

pQF-*shkA*(R26A): The mutant allele was generated by SOE-PCR using pET28a-*shkA* as template and flanking primers 669/670 and mutagenic primers 9904/9905. The product was digested with NdeI/EcoRI and cloned into pQF digested with AseI/EcoRI.

pQF-*shkA*(H61A): The mutant allele was generated by SOE-PCR using pET28a-*shkA* as template and flanking primers 669/670 and mutagenic primers 9968/9969. The product was digested with NdeI/EcoRI and cloned into pQF digested with AseI/EcoRI.

pQF-*shkA*(R74A): The mutant allele was generated by SOE-PCR using pET28a-*shkA* as template and flanking primers 669/670 and mutagenic primers 9970/9971. The product was digested with NdeI/EcoRI and cloned into pQF digested with AseI/EcoRI. This *shkA* allele contains a second mutation, A451V.

pQF-*shkA*(W113A): The mutant allele was generated by SOE-PCR using pET28a-*shkA* as template and flanking primers 669/670 and mutagenic primers 9906/9907. The product was digested with NdeI/EcoRI and cloned into pQF digested with AseI/EcoRI. This *shkA* allele contains a second mutation, A451V.

pQF-*shkA*(D125N): The mutant allele was generated by SOE-PCR using pET28a-*shkA* as template and flanking primers 669/670 and mutagenic primers 10009/10010. The product was digested with NdeI/EcoRI and cloned into pQF digested with AseI/EcoRI.

pQF-*shkA*(R128A): The mutant allele was generated by SOE-PCR using pET28a-*shkA* as template and flanking primers 669/670 and mutagenic primers 10005/10006. The product was digested with NdeI/EcoRI and cloned into pQF digested with AseI/EcoRI.

pQF-*shkA*(R130A): The mutant allele was generated by SOE-PCR using pET28a-*shkA* as template and flanking primers 669/670 and mutagenic primers 10007/10008. The product was digested with NdeI/EcoRI and cloned into pQF digested with AseI/EcoRI.

pQF-*shkA*(R128A,R130A): The mutant allele was generated by SOE-PCR using pET28a-*shkA* as template and flanking primers 669/670 and mutagenic primers 9908/9909. The product was digested with NdeI/EcoRI and cloned into pQF digested with AseI/EcoRI.

pQF-*shkA*(R177A): The mutant allele was generated by SOE-PCR using pET28a-*shkA* as template and flanking primers 669/670 and mutagenic primers 9910/9911. The product was digested with NdeI/EcoRI and cloned into pQF digested with AseI/EcoRI. This *shkA* allele contains a second mutation, P233L.

pQF-*shkA*(F230A,F234A): The mutant allele was generated by SOE-PCR using pET28a-*shkA* as template and flanking primers 669/670 and mutagenic primers 9972/9973. The product was digested with NdeI/EcoRI and cloned into pQF digested with AseI/EcoRI.

pQF-*shkA*(D297N): The mutant allele was generated by SOE-PCR using pET28a-*shkA* as template and flanking primers 669/670 and mutagenic primers 9974/9975. The product was digested with NdeI/EcoRI and cloned into pQF digested with AseI/EcoRI.

pQF-*shkA*(P321A): The mutant allele was generated by SOE-PCR using pET28a-*shkA* as template and flanking primers 669/670 and mutagenic primers 10013/10014. The product was digested with NdeI/EcoRI and cloned into pQF digested with AseI/EcoRI.

pQF-*shkA*(R324A): The mutant allele was generated by SOE-PCR using pET28a-*shkA* as template and flanking primers 669/670 and mutagenic primers 9912/9913. The product was digested with NdeI/EcoRI and cloned into pQF digested with AseI/EcoRI.

pQF-*shkA*(D325N): The mutant allele was generated by SOE-PCR using pET28a-*shkA* as template and flanking primers 669/670 and mutagenic primers 10011/10012. The product was digested with NdeI/EcoRI and cloned into pQF digested with AseI/EcoRI.

pQF-*shkA*(I327A): The mutant allele was generated by SOE-PCR using pET28a-*shkA* as template and flanking primers 669/670 and mutagenic primers 9976/9977. The product was digested with NdeI/EcoRI and cloned into pQF digested with AseI/EcoRI. This *shkA* allele contains a second mutation, A451V.

pQF-*shkA*(Y338A): The mutant allele was generated by SOE-PCR using pET28a-*shkA* as template and flanking primers 669/670 and mutagenic primers 9978/9979. The product was digested with NdeI/EcoRI and cloned into pQF digested with AseI/EcoRI.

pQF-*shkA*(R344A): The mutant allele was generated by SOE-PCR using pET28a-*shkA* as template and flanking primers 669/670 and mutagenic primers 9914/9915. The product was digested with NdeI/EcoRI and cloned into pQF digested with AseI/EcoRI. This *shkA* allele contains a second mutation, A451V.

pQF-*shkA*(E402A,G403A): The mutant allele was generated by SOE-PCR using pET28a-*shkA* as template and flanking primers 669/670 and mutagenic primers 9980/9981. The product was digested with NdeI/EcoRI and cloned into pQF digested with AseI/EcoRI.

pQF-*shkA*(C404A): The mutant allele was generated by SOE-PCR using pET28a-*shkA* as template and flanking primers 669/670 and mutagenic primers 9986/9987. The product was digested with NdeI/EcoRI and cloned into pQF digested with AseI/EcoRI.

pQF-*shkA*(D430N): The mutant allele was generated by SOE-PCR using pET28a-*shkA* as template and flanking primers 669/670 and mutagenic primers 10028/10029. The product was digested with NdeI/EcoRI and cloned into pQF digested with AseI/EcoRI.

pQF-*shkA*(D465A): The mutant allele was generated by SOE-PCR using pET28a-*shkA* as template and flanking primers 669/670 and mutagenic primers 9982/9983. The product was digested with NdeI/EcoRI and cloned into pQF digested with AseI/EcoRI. This *shkA* allele contains a second mutation, A451V.

pQF-*shkA*(C469A): The mutant allele was generated by SOE-PCR using pET28a-*shkA* as template and flanking primers 669/670 and mutagenic primers 9984/9985. The product was digested with NdeI/EcoRI and cloned into pQF digested with AseI/EcoRI. This *shkA* allele contains a second mutation, A451V.

pQF-*shkA*(D369N,H61A): A fragment harboring part of *shkA* was released from pQF-*shkA*(H61A) by digestion with SpeI/PstI and cloned into pQF-*shkA*(D369N) digested with the same enzymes.

pQF-*shkA*(D369N,R128A): A fragment harboring part of *shkA* was released from pQF-*shkA*(R128A) by digestion with SpeI/PstI and cloned into pQF-*shkA*(D369N) digested with the same enzymes.

pQF-*shkA*(D369N,R130): A fragment harboring part of *shkA* was released from pQF-*shkA*(R130A) by digestion with SpeI/PstI and cloned into pQF-*shkA*(D369N) digested with the same enzymes.

pQF-*shkA*(D369N,R128A,R130A): A fragment harboring part of *shkA* was released from pQF-*shkA*(R128A,R130A) by digestion with SpeI/PstI and cloned into pQF-*shkA*(D369N) digested with the same enzymes.

pQF-*shkA*(D369N,F230A,F234A): A fragment harboring part of *shkA* was released from pQF-*shkA*(F230A,F234A) by digestion with SpeI/PstI and cloned into pQF-*shkA*(D369N) digested with the same enzymes.

pQF-*shkA*(D369N,R128A): A fragment harboring part of *shkA* was released from pQF-*shkA*(R128A) by digestion with SpeI/PstI and cloned into pQF-*shkA*(D369N) digested with the same enzymes.

pQF-*shkA*(D369N,R324A): A fragment harboring part of *shkA* was released from pQF-*shkA*(R324A) by digestion with SpeI/PstI and cloned into pQF-*shkA*(D369N) digested with the same enzymes.

pQF-*shkA*(D369N,Y338A): A fragment harboring part of *shkA* was released from pQF-*shkA*(Y338A) by digestion with SpeI/PstI and cloned into pQF-*shkA*(D369N) digested with the same enzymes.

pET28a-*shkA*(D430N): The mutant allele was generated by SOE-PCR using pET28a-*shkA* as template and flanking primers 669/670 and mutagenic primers 10028/10029. The product was digested with NdeI/EcoRI and cloned into pET28a digested with NdeI/EcoRI.

pET28a-*shkA*(E386Q,D387N): The mutant allele was generated by SOE-PCR using pET28a-*shkA* as template and flanking primers 669/670 and mutagenic primers 10026/10027. The product was digested with NdeI/EcoRI and cloned into pET28a digested with NdeI/EcoRI.

pET28a-*shkA*(K480R): The mutant allele was generated by SOE-PCR using pET28a-*shkA* as template and flanking primers 669/670 and mutagenic primers 10024/10025. The product was digested with NdeI/EcoRI and cloned into pET28a digested with NdeI/EcoRI.

pET28a-*shkA*(R324A): A fragment harboring part of *shkA* was released from pQF-*shkA*(R324A) by digestion with AscI/PstI and cloned into pET28a-*shkA* digested with the same enzymes.

pET28a-*shkA*(D369N,R324A): A fragment harboring part of *shkA* was released from pQF-*shkA*(R324A) by digestion with AscI/PstI and cloned into pET28a-*shkA*(D369N) digested with the same enzymes.

pET28a-*shkA*(Y338A): A fragment harboring part of *shkA* was released from pQF-*shkA*(Y338A) by digestion with AscI/PstI and cloned into pET28a-*shkA* digested with the same enzymes.

pET28a-*shkA*(D369N,Y338A): A fragment harboring part of *shkA* was released from pQF-*shkA*(Y338A) by digestion with AscI/PstI and cloned into pET28a-*shkA*(D369N) digested with the same enzymes.

pET28a-*shkA*(R128A,R130A): The mutant allele was generated by SOE-PCR using pET28a-*shkA* as template and flanking primers 669/670 and mutagenic primers 9908/9909. The product was digested with NdeI/EcoRI and cloned into pET28a digested with the same enzymes.

pDivJ-mCherry: The 3' part of *divJ* was PCR-amplified from *C. crescentus* gDNA with primers 10205/10206, the product was digested with KpnI/AgeI and cloned into pCHYC-4 digested with the same enzymes.

pNPTS138- Δ tacA: Two DNA fragments flanking the *tacA* ORF were PCR-amplified from *C. crescentus* gDNA. Fragment 1 was amplified with primers 6535/6098, then digested with PstI/KpnI. Fragment 2 was amplified with primers 6098/6536, then digested with KpnI/EcoRI. The two fragments were ligated to pNPTS138 digested with PstI/EcoRI.

pNPTS138- Δ shkA: Two DNA fragments flanking the *shkA* ORF were PCR-amplified from *C. crescentus* gDNA. Fragment 1 was amplified with primers 6085/6086, then digested with PstI/KpnI. Fragment 2 was amplified with primers 6087/6088, then digested with KpnI/EcoRI. The two fragments were ligated to pNPTS138 digested with PstI/EcoRI.

pNPTS138-3xFlag-Tag-tacA: The upstream region of the *tacA* ORF was PCR-amplified from *C. crescentus* gDNA with primers 6438/6439 (fragment 1). A 3' part of *tacA* was PCR-amplified from *C. crescentus* gDNA with primers 6440/7604 (fragment 2), and then used as a template with primers 6441/7604 to insert the coding sequence of the 3xFlag-Tag (fragment 3). SOE-PCR was performed with fragment 1 and 3 as template and primers 6438/7604. The resulting product was then digested with PstI/EcoRI and ligated into pNPTS138 digested with the same enzymes.

pNPTS138-3xFlag-Tag-shkA: The upstream region of the *shkA* ORF was PCR-amplified from *C. crescentus* gDNA with primers 6442/6443 (fragment 1). A 3' part of *shkA* was PCR-amplified from *C. crescentus* gDNA with primers 6444/7605 (fragment 2), and then used as a template with primers 6444/7605 to insert the coding sequence of the 3xFlag-Tag (fragment 3). SOE-PCR was performed with fragment 1 and 3 as template and primers 6442/7605. The resulting product was then digested with PstI/EcoRI and ligated into pNPTS138 digested with the same enzymes.

pNPTS138-shkA-DD: The 5' region of *shkA* was PCR-amplified from *C. crescentus* gDNA with primers 8169/8170 (fragment 1). The downstream region of the *shkA* ORF was PCR-amplified from *C. crescentus* gDNA with primers 8171/8172 (fragment 2). SOE-PCR was performed with the two fragments as template and primers 8169/8172. The resulting product was then digested with BamHI/EcoRI and ligated into pNPTS138 digested with the same enzymes.

pNPTS138-tacA-DD: The 5' region of *tacA* was PCR-amplified from *C. crescentus* gDNA with primers 7925/7716 (fragment 1). The downstream region of the *tacA* ORF was PCR-amplified

from *C. crescentus* gDNA with primers 7717/7718 (fragment 2). SOE-PCR was performed with the two fragments as template and primers 7925/7718. The resulting product was then digested with HindIII/EcoRI and ligated into pNPTS138 digested with the same enzymes.

pNPTS138-*tacA*-D54E: The mutant allele was generated by SOE-PCR using *C. crescentus* gDNA as template and flanking primers 7958/7961 and mutagenic primers 7959/7960. The product was digested with PstI/EcoRI and cloned into pNPTS138 digested with the same enzymes.

pNPTS138-3xFlag-*tacA*-D54E: The mutant allele was generated by SOE-PCR using *C. crescentus* gDNA of strain UJ8533 as template and flanking primers 7958/7961 and mutagenic primers 7959/7960. The product was digested with PstI/EcoRI and cloned into pNPTS138 digested with the same enzymes.

For *in vitro* experiments, proteins were expressed from pet28a and pet32b plasmids.

pET28a-His-*shkA*: *shkA* was PCR-amplified from *C. crescentus* gDNA with primers 5988/5486, the product was digested with NdeI/HindIII and cloned into pET28a digested with the same enzymes.

pET28a-His-*shpA*: *shpA* was PCR-amplified from *C. crescentus* gDNA with primers 6015/6016, the product was digested with HindIII/EcoRI and cloned into pET28a digested with the same enzymes.

pET28a-His-*tacA*-RD: The sequence of *tacA* encoding the receiver domain was PCR-amplified from *C. crescentus* gDNA with primers 7925/6013, the product was digested with HindIII/EcoRI and cloned into pET28a digested with the same enzymes.

pET32b-Trx-His-*shkA*-HK: The sequence of *shkA* encoding the kinase catalytic core including the REC1 domain was PCR-amplified from *C. crescentus* gDNA with primers 6110/6011, the product was digested with HindIII/EcoRI and cloned into pET32b digested with the same enzymes.

pET32b-Trx-His-*shkA*-RD2: The sequence of *shkA* encoding the REC2 domain was PCR-amplified from *C. crescentus* gDNA with primers 6109/6009, the product was digested with HindIII/EcoRI and cloned into pET32b digested with the same enzymes.

pMT687-*tacA*: *tacA* was PCR-amplified from *C. crescentus* gDNA with primers 5487/5490, the product was digested with NdeI/KpnI and cloned into pMT687 digested with the same enzymes.

pMT687-tacA-DE: The mutant allele was generated by SOE-PCR using *C. crescentus* gDNA as template and flanking primers 5487/5490 and mutagenic primers 5488/5489. The product was digested with NdeI/KpnI and cloned into pNPTS138 digested with the same enzymes.

pQF-PA5295: PA5295 was PCR-amplified from pRV-PA5295 with primers 8974/8975, the product was digested with HindIII/KpnI and cloned into pMT687 digested with the same enzymes.

pQF-PA5295-AAL: PA5295_{AAL} was PCR-amplified from pRV-PA5295_{AAL} with primers 8974/8975, the product was digested with HindIII/KpnI and cloned into pMT687 digested with the same enzymes.

pRKlac290-spmX: The promoter region of *spmX* was PCR-amplified from *C. crescentus* gDNA with primers 6864/6865. The resulting product was digested with EcoRI/PstI and ligated into pRKlac290 digested with the same enzymes.

pRKlac290-staR: The promoter region of *staR* was PCR-amplified from *C. crescentus* gDNA with primers 6621/6622. The resulting product was digested with EcoRI/PstI and ligated into pRKlac290 digested with the same enzymes.

pAH10 is a pUC19-derivative containing a NsiI-PacI-flanked cassette consisting of the *rrnBT1* terminators and a multiple cloning site.

pAH87 is a low-copy replicative plasmid derivative of pMT375, in which the XbaI insert was replaced with the NsiI-PacI cassette of pAH10.

pAH99 is a derivative of pAH87. The *dendra2* gene was PCR-amplified from pDHL851 using primers 7503 and 7507, which also introduced a stop codon and the RBS of pQE70 upstream of *dendra2*. The product was digested with HindIII and PacI and ligated into pAH87 digested with the same restriction enzymes.

pAH111: The promoter region and parts of the gene of *spmX* was PCR-amplified from *C. crescentus* genomic DNA with primers 6864 and 7512. The resulting product was digested with EcoRI and HindIII and ligated into pAH99 digested with the same enzymes to generate a transcriptional fusion of *dendra2* to the *spmX* promoter.

7.3 GROWTH CONDITIONS

Either Peptone Yeast extract medium (PYE) or minimal medium supplemented with glucose (M2G)^{207,208} was used to grow *C. crescentus* at 30°C. The appropriate antibiotics

(Chloramphenicol in PYE 1µg/ml, Kanamycin in PYE 5µg/ml, Oxytetracycline in PYE 2.5 µg/ml) were added under growth conditions with plasmids. Plasmids were induced with either Cumate or IPTG as indicated in the figures. Synchronization assays¹⁹³ were performed with LUDOX²⁰⁹ or Percoll™ (GE Healthcare) density gradients²¹⁰ in M2G medium.

7.4 PHOS-TAG IMMUNOBLOTTING

C. crescentus overnight cultures were diluted 1:20 in PYE medium (containing 100µM cumate and 2.5µg/ml Oxytetracycline for strains harboring pQF plasmids). The bacteria were grown to an OD₆₆₀ of 0.4 to 0.5 at 30°C. An equivalent of 0.5mL OD₆₆₀ 0.5 was spun down and lysed in 100µL Lysis Buffer (10mM Tris-HCL pH7.5, 4% SDS, 1 PhosSTOP™ tablet (Roche) in 5mL volume, DNase I (NEB)) for 5min at RT. After spinning down the samples for 5min at max speed and RT, 80µL of full-cell lysate was taken up in 120µL 1.6X SDS sample buffer (0.1M Tris pH 6.8, 5% Glycerol, 0.2% SDS, 1% β-Mercaptoethanol, 0.025% Bromophenol blue) and kept on ice. 20µL was loaded on a gel and separated by 12% SDS-PAGE gels containing 100µM MnCl₂ and 50µM Phos-tag™ compound (Wako)²¹¹ and run for 4 to 5 hours at 100V at 4°C. Transfer was performed for 2h at 80V using a BioRad® wet blot system at 4°C. The protein was transferred to PVDF-membranes (Immobilon-P, Millipore).

An α-Flag antibody (F1804 Sigma, 1:10 000) was used as primary antibody, detected by HPR-conjugated rabbit anti-mouse (DakoCytomation, DK) secondary antibody. ECL detection reagent (Perkin Elmer Life Sciences) was used for development on a photo film (Fuji).

7.5 IMMUNOBLOTTING

Cells were harvested and the OD₆₆₀ normalized in 1x SDS sample buffer. All samples were boiled for 5min at 95°C and separated on 12% SDS-PAGE gels. Protein was transferred to PVDF-membranes (Immobilon-P, Millipore 0.45µm). α-MreB (1:20 000), α-SpmX (1:10 000), or α-Flag (F1804 Sigma, 1:10 000) antibodies were used as primary antibodies. HPR-conjugated rabbit anti-mouse or swine anti-rabbit secondary antibodies (Dako) were used for detection. ECL detection reagent (Perkin Elmer Life Sciences) was used for development on a photo film (Fuji).

7.6 CAPTURE COMPOUND MASS SPECTROMETRY (CCMS)

Capture Compound Mass Spectrometry (CCMS) was performed for the discovery of new c-di-GMP targets. Thereby an engineered trivalent chemical compound was used to isolate and analyze c-di-GMP binders. This compound consists of a c-di-GMP residue to specifically bind c-

di-GMP-binders, an UV-photoactivatable reactive group, allowing crosslinking of captured proteins, and a biotin to purify the captured protein. The isolated proteins then were digested and analyzed by mass spectrometry^{203,212}.

7.7 PROTEIN EXPRESSION AND PURIFICATION

E. coli BL21 Rosetta cells were used to express proteins from the pET28a and pET32b expression plasmids. The cells were grown to an OD₆₀₀ of 0.4 to 0.6 and then induced with 0.5mM IPTG for 4 hours at 30°C. Cells were harvested and frozen as pellets at -20°C. Purification was performed using an ÄKTApurifier 10 system (GE Healthcare) with 1ml HisTrap HP columns (GE Healthcare). To increase protein purity, the samples were run on a size exclusion column (HiLoad 16/60 Superdex 200). Buffers used for purification: Lysis buffer (Wash Buffer supplemented with protease inhibitor, DNase I (NEB)), Wash buffer (20mM HEPES-KOH pH 8.0, 0.5M NaCl, 10 % glycerol, 20mM imidazole, 1mM DTT), Elution buffer (20mM HEPES-KOH pH 8.0, 0.5M NaCl, 10% glycerol, 500mM imidazole, 1mM DTT), Storage buffer (10mM HEPES-KOH pH 8.0, 50mM KCl (or 100mM KCl), 10% glycerol, 0.1mM EDTA, 1mM DTT).

7.8 KINASE *IN VITRO* ASSAYS

Kinase assays were adapted from^{10,213,214}. Reactions were performed in Storage buffer supplemented with 500µM ATP and 5µCi [γ 32P]-ATP (3000Ci/mmol, Hartmann Analytic) at RT. Additional nucleotides were added as indicated in figures. Kinase reactions were stopped with SDS sample buffer and stored on ice, then run on 12.5% SDS PAGE gels. Gels were exposed to phosphor screen for 0.5h to 3h and then scanned by a Typhoon FLA 7000 imaging system (GE Healthcare).

7.9 ISOTHERMAL TITRATION CALORIMETRY (ITC) MEASUREMENTS

ITC binding assays were performed with a VP-ITC isothermal titration calorimeter (MicroCal). Concentrations were 12µM ShkA in the cell and 130µM c-di-GMP in the syringe. ITC Buffer: 10mM HEPES-KOH pH 8.0, 100mM NaCl, 10% glycerol, 1mM DTT. After a first injection of 3µl, 10µl was injected at 29 time points. Data analysis was performed with MicroCal (ORIGIN) and fitted with the *One binding site model* of ORIGIN.

7.10 B-GALACTOSIDASE MEASUREMENTS

C. crescentus overnight cultures grown in PYE supplemented with 2.5µg/ml Oxytetracycline were resuspended in the same, fresh medium. The bacteria were grown to an OD₆₆₀ of 0.3 to 0.5 and 1ml was pelleted and resuspended with 1ml Z-buffer (75mM Na₂HPO₄, 40mM NaH₂PO₄, 1mM KCl, 1mM MgSO₄; pH 7.0), supplemented with 50mM β-mercaptoethanol. Then 100µL 0.1% SDS and 20µL chloroform was added. Samples were vortexed for 10sec and lysed at RT for 0.5h to 1h. For every sample, 200µl was transferred to a 96-well plate with three biological replicates. 25µL of a 4mg/ml σ-nitrophenyl-β-D-galactopyranoside (σNPG) solution, dissolved in Z-buffer, was added as a substrate. Activity of the β-galactosidase was measured with a BioTek Instruments EL800 plate reader at 405nm (20 reads at the fastest interval). Activity was calculated as the initial slope at linear range.

7.11 MICROSCOPY

Phase-contrast and fluorescent microscopy analyses were performed using a DeltaVision system, Olympus IX71 microscope, and Photometrix CoolSnap HQ2 camera. Cells were mounted on 1% PYE medium agar pads containing appropriate supplements sealed with a double layer of gene frames (ABgene; 1.7 x 2.8 cm). For time-lapse, imaging pictures were taken every 15 minutes. Appropriate cells expressing dendra2 were subjected to UV light for 2 seconds to switch dendra2 from the green to the red-emitting state. For statistical analysis, fluorescent intensities, cell and stalk length were analyzed using the Fiji software package²¹⁵ and Oufiti²¹⁶.

7.12 SELECTION/SCREEN FOR C-DI-GMP INDEPENDENT MUTATIONS IN *SHKA*

Six independent colonies of strain AKS1 (CB15 *rcdG*⁰ *ΔlacA::Ω ampG::pNPTStet-ampG*) harboring in addition plasmid pAK503-*spmX* were inoculated into 5ml PYE containing Chloramphenicol (Cm) (1mg/l) and Tetracycline (Tc) (10mg/l) and grown overnight. For UV mutagenesis, 2ml of each culture was distributed in 6-well plates and irradiated with 10'000mj UV light using a Stratalinker, after which 5ml PYE containing Cm (1mg/l) and Tc (10mg/l) were added and cultures grown for 7h at 30°C with shaking. 500µl of each culture were plated on PYE plates containing Cm (1mg/l), Tc (10mg/l) and Kanamycin (Km) (6.25mg/l) and plates incubated at 30°C for 4 days. All colonies from one plate were pooled, diluted to an OD₆₆₀ of 0.1 and grown for 7h at 30°C, and phage lysates were prepared for each independent pool. Following transduction of strain AKS17 (CB15 *rcdG*⁰ *ΔlacA::Ω /pAK502-*spmX**) with individual

pool lysates, cells were plated on PYE containing Cm (1mg/l), Tc (10mg/l) and X-Gal (40mg/l) and incubated at 30°C for 3 days. Blue colonies were once re-streaked to confirm their blue colony phenotype, followed by colony PCR using primers 9765 and 9766 and sequencing (Microsynth, Balgach, Switzerland) of the PCR product using primers 9765, 9766, 6011 and 6498.

8 REFERENCES

1. Raddadi, N., Cherif, A., Daffonchio, D., Neifar, M. & Fava, F. Biotechnological applications of extremophiles, extremozymes and extremolytes. *Appl. Microbiol. Biotechnol.* **99**, 7907–13 (2015).
2. Wohlgemuth, R. Biocatalysis-key to sustainable industrial chemistry. *Curr. Opin. Biotechnol.* **21**, 713–24 (2010).
3. Qureshi, N., Annous, B. A., Ezeji, T. C., Karcher, P. & Maddox, I. S. Biofilm reactors for industrial bioconversion processes: employing potential of enhanced reaction rates. *Microb. Cell Fact.* **4**, 24 (2005).
4. Wendisch, V. F., Jorge, J. M. P., Pérez-García, F. & Sgobba, E. Updates on industrial production of amino acids using *Corynebacterium glutamicum*. *World J. Microbiol. Biotechnol.* **32**, 105 (2016).
5. Sánchez-Cañizares, C., Jorrín, B., Poole, P. S. & Tkacz, A. Understanding the holobiont: the interdependence of plants and their microbiome. *Curr. Opin. Microbiol.* **38**, 188–196 (2017).
6. Fang, Y. & Ramasamy, R. P. Current and Prospective Methods for Plant Disease Detection. *Biosensors* **5**, 537–61 (2015).
7. Kurilshikov, A., Wijmenga, C., Fu, J. & Zhernakova, A. Host Genetics and Gut Microbiome: Challenges and Perspectives. *Trends Immunol.* **xx**, 1–15 (2017).
8. Blanpain, C. & Simons, B. D. Unravelling stem cell dynamics by lineage tracing. *Nat. Rev. Mol. Cell Biol.* **14**, 489–502 (2013).
9. Poon, R. Y. C. Cell Cycle Control: A System of Interlinking Oscillators. *Methods Mol. Biol.* **1342**, 3–19 (2016).
10. Lori, C. *et al.* Cyclic di-GMP acts as a cell cycle oscillator to drive chromosome replication. *Nature* **523**, 236–239 (2015).
11. Midgett, C. R. *et al.* Bile salts and alkaline pH reciprocally modulate the interaction between the periplasmic domains of *Vibrio cholerae* ToxR and ToxS. *Mol. Microbiol.* **105**, 258–272 (2017).
12. Rauschmeier, M., Schüppel, V., Tetsch, L. & Jung, K. New insights into the interplay between the lysine transporter LysP and the pH sensor CadC in *Escherichia coli*. *J. Mol. Biol.* **426**, 215–29 (2014).
13. Ulrich, L. E., Koonin, E. V. & Zhulin, I. B. One-component systems dominate signal transduction in prokaryotes. *Trends Microbiol.* **13**, 52–56 (2005).
14. Lassak, K., Peeters, E., Wróbel, S. & Albers, S. V. The one-component system ArnR: A membrane-bound activator of the crenarchaeal archaellum. *Mol. Microbiol.* **88**, 125–139 (2013).
15. Fulcrand, G., Chapagain, P., Dunlap, D. & Leng, F. Direct observation of a 91 bp LacI-mediated, negatively supercoiled DNA loop by atomic force microscope. *FEBS Lett.* **590**, 613–618 (2016).

16. Lewis, M. *et al.* Crystal structure of the lactose operon repressor and its complexes with DNA and inducer. *Science (80-.)*. **271**, 1247–1254 (1996).
17. Wuichet, K., Cantwell, B. J. & Zhulin, I. B. Evolution and phyletic distribution of two-component signal transduction systems. *Curr. Opin. Microbiol.* **13**, 219–225 (2010).
18. Krell, T. *et al.* Bacterial Sensor Kinases: Diversity in the Recognition of Environmental Signals. *Annu. Rev. Microbiol.* **64**, 539–559 (2010).
19. Stock, A. M., Robinson, V. L. & Goudreau, P. N. Two-Component Signal Transduction. *Reactions* **69**, 183–215 (2000).
20. West, A. H. & Stock, A. M. Histidine kinases and response regulator proteins in two-component signaling systems. *Trends Biochem. Sci.* **26**, 369–376 (2001).
21. Laub, M. T. & Goulian, M. Specificity in two-component signal transduction pathways. *Annu. Rev. Genet.* **41**, 121–45 (2007).
22. Blair, J. A. *et al.* Branched signal wiring of an essential bacterial cell-cycle phosphotransfer protein. *Structure* **21**, 1590–1601 (2013).
23. Gao, R. & Stock, A. M. Biological Insights from Structures of Two-Component Proteins. *Annu. Rev. Microbiol.* **63**, 133–154 (2009).
24. Perry, J., Koteva, K. & Wright, G. Receptor domains of two-component signal transduction systems. *Mol. Biosyst.* **7**, 1388 (2011).
25. Aldridge, P., Paul, R., Goymer, P., Rainey, P. & Jenal, U. Role of the GGDEF regulator PleD in polar development of *Caulobacter crescentus*. *Mol. Microbiol.* **47**, 1695–1708 (2003).
26. Jenal, U. & Galperin, M. Y. Single domain response regulators: molecular switches with emerging roles in cell organization and dynamics. *Curr. Opin. Microbiol.* **12**, 152–160 (2009).
27. Paul, R. *et al.* Allosteric regulation of histidine kinases by their cognate response regulator determines cell fate. *Cell* **133**, 452–61 (2008).
28. Casino, P., Rubio, V. & Marina, A. The mechanism of signal transduction by two-component systems. *Curr. Opin. Struct. Biol.* **20**, 763–71 (2010).
29. Dubey, B. N. *et al.* Cyclic di-GMP mediates a histidine kinase/phosphatase switch by noncovalent domain cross-linking. *Sci. Adv.* **2**, e1600823 (2016).
30. Gao, R. & Stock, A. M. Quantitative Kinetic Analyses of Shutting Off a Two-Component System. *MBio* **8**, 1–15 (2017).
31. Song, Y., Peisach, D., Pioszak, A. A., Xu, Z. & Ninfa, A. J. Crystal structure of the C-terminal domain of the two-component system transmitter protein nitrogen regulator II (NRII; NtrB), regulator of nitrogen assimilation in *Escherichia coli*. *Biochemistry* **43**, 6670–6678 (2004).
32. Parkinson, J. S. & Kofoid, E. C. Communication modules in bacterial signaling proteins. *Annu. Rev. Genet.* **26**, 71–112 (1992).
33. Inouye, M. *et al.* Solution structure of the homodimeric core domain of *Escherichia coli* histidine kinase EnvZ. *Nat. Struct. Biol.* **6**, 729–734 (1999).

34. Bhate, M. A. P., Molnar, K. A. S., Goulian, M. & Degrado, W. F. Signal Transduction in Histidine Kinases: Insights from New Structures. *Structure* **23**, 981–996 (2015).
35. Yamada, S. *et al.* Structure of PAS-Linked Histidine Kinase and the Response Regulator Complex. *Structure* **17**, 1333–1344 (2009).
36. Ashenberg, O., Keating, A. E. & Laub, M. T. Helix bundle loops determine whether histidine kinases autophosphorylate in cis or in trans. *J. Mol. Biol.* **425**, 1198–1209 (2013).
37. Casino, P., Miguel-Romero, L. & Marina, A. Visualizing autophosphorylation in histidine kinases. *Nat. Commun.* **5**, 1–11 (2014).
38. Mechaly, A. E. *et al.* Structural Coupling between Autokinase and Phosphotransferase Reactions in a Bacterial Histidine Kinase. *Structure* **25**, 939–944.e3 (2017).
39. Huynh, T. N. & Stewart, V. Negative control in two-component signal transduction by transmitter phosphatase activity. *Mol. Microbiol.* **82**, 275–286 (2011).
40. Huynh, T. N., Noriega, C. E. & Stewart, V. Conserved mechanism for sensor phosphatase control of two-component signaling revealed in the nitrate sensor NarX. *Proc. Natl. Acad. Sci. U. S. A.* **107**, 21140–5 (2010).
41. Skerker, J. M. *et al.* Rewiring the Specificity of Two-Component Signal Transduction Systems. *Cell* **133**, 1043–1054 (2008).
42. Podgornaia, A. I., Casino, P., Marina, A. & Laub, M. T. Structural basis of a rationally rewired protein-protein interface critical to bacterial signaling. *Structure* **21**, 1636–1647 (2013).
43. Volz, K. Structural conservation in the CheY superfamily. *Biochemistry* **32**, 11741–53 (1993).
44. Bourret, R. B. Receiver domain structure and function in response regulator proteins. *Curr. Opin. Microbiol.* **13**, 142–9 (2010).
45. Gao, R. & Stock, A. M. Molecular strategies for phosphorylation-mediated regulation of response regulator activity. *Curr. Opin. Microbiol.* **13**, 160–167 (2010).
46. Fraser, J. S. *et al.* An atypical receiver domain controls the dynamic polar localization of the *Myxococcus xanthus* social motility protein FrzS. *Mol. Microbiol.* **65**, 319–332 (2007).
47. Hong, E. *et al.* Structure of an atypical orphan response regulator protein supports a new phosphorylation-independent regulatory mechanism. *J. Biol. Chem.* **282**, 20667–20675 (2007).
48. Ivleva, N. B., Gao, T., LiWang, A. C. & Golden, S. S. Quinone sensing by the circadian input kinase of the cyanobacterial circadian clock. *Proc. Natl. Acad. Sci. U. S. A.* **103**, 17468–17473 (2006).
49. Fioravanti, A. *et al.* Structural insights into ChpT, an essential dimeric histidine phosphotransferase regulating the cell cycle in *Caulobacter crescentus*. *Acta Crystallogr. Sect. F Struct. Biol. Cryst. Commun.* **68**, 1025–1029 (2012).
50. Xu, Q. *et al.* Crystal Structure of Histidine Phosphotransfer Protein ShpA, an Essential Regulator of Stalk Biogenesis in *Caulobacter crescentus*. *J. Mol. Biol.* **390**, 686–698

(2009).

51. Sourjik, V. & Wingreen, N. S. Responding to chemical gradients: Bacterial chemotaxis. *Curr. Opin. Cell Biol.* **24**, 262–268 (2012).
52. Lai, W. C., Beel, B. D. & Hazelbauer, G. L. Adaptational modification and ligand occupancy have opposite effects on positioning of the transmembrane signalling helix of a chemoreceptor. *Mol. Microbiol.* **61**, 1081–1090 (2006).
53. Djordjevic, S. & Stock, a M. Structural analysis of bacterial chemotaxis proteins: components of a dynamic signaling system. *J. Struct. Biol.* **124**, 189–200 (1998).
54. Wuichet, K. & Zhulin, I. B. Origins and Diversification of a Complex Signal Transduction System in Prokaryotes. *Sci. Signal.* **3**, ra50-ra50 (2010).
55. Khursigara, C. M., Wu, X. & Subramaniam, S. Chemoreceptors in *Caulobacter crescentus*: Trimers of receptor dimers in a partially ordered hexagonally packed array. *J. Bacteriol.* **190**, 6805–6810 (2008).
56. Alley, M. R. K., Maddock, J. R. & Shapiro, L. Polar localization of a bacterial chemoreceptor. *Genes Dev.* **6**, 825–836 (1992).
57. Parkinson, J. S., Hazelbauer, G. L. & Falke, J. J. Signaling and sensory adaptation in *Escherichia coli* chemoreceptors: 2015 update. *Trends Microbiol.* **23**, 257–266 (2015).
58. Hegde, M. *et al.* Chemotaxis to the quorum-sensing signal AI-2 requires the Tsr chemoreceptor and the periplasmic LsrB AI-2-binding protein. *J. Bacteriol.* **193**, 768–773 (2011).
59. Matilla, M. A. & Krell, T. Chemoreceptor-based signal sensing. *Curr. Opin. Biotechnol.* **45**, 8–14 (2017).
60. Hickman, J. W., Tifrea, D. F. & Harwood, C. S. A chemosensory system that regulates biofilm formation through modulation of cyclic diguanylate levels. *Proc. Natl. Acad. Sci.* **102**, 14422–14427 (2005).
61. O’Connor, J. R., Kuwada, N. J., Huangyutitham, V., Wiggins, P. A. & Harwood, C. S. Surface sensing and lateral subcellular localization of WspA, the receptor in a chemosensory-like system leading to c-di-GMP production. *Mol. Microbiol.* **86**, 720–729 (2012).
62. Fulcher, N. B., Holliday, P. M., Klem, E., Cann, M. J. & Wolfgang, M. C. The *Pseudomonas aeruginosa* Chp chemosensory system regulates intracellular cAMP levels by modulating adenylate cyclase activity. *Mol. Microbiol.* **76**, 889–904 (2010).
63. Olivares, A. O., Baker, T. A. & Sauer, R. T. Mechanistic insights into bacterial AAA+ proteases and protein-remodelling machines. *Nat. Rev. Microbiol.* **14**, 33–44 (2015).
64. Sauer, R. T. & Baker, T. A. AAA+ Proteases: ATP-Fueled Machines of Protein Destruction. *Annu. Rev. Biochem.* **80**, 587–612 (2011).
65. LaBreck, C. J., May, S., Viola, M. G., Conti, J. & Camberg, J. L. The protein chaperone ClpX targets native and non-native aggregated substrates for remodeling, disassembly and degradation with ClpP. *Front. Mol. Biosci.* **4**, 26 (2017).
66. Vass, R. H., Nascembeni, J. & Chien, P. The Essential Role of ClpXP in *Caulobacter crescentus* Requires Species Constrained Substrate Specificity. *Front. Mol. Biosci.* **4**, 1–9

- (2017).
67. Gottesman, S., Roche, E., Zhou, Y. & Sauer, R. T. The ClpXP and ClpAP proteases degrade proteins with carboxy-terminal peptide tails added by the SsrA-tagging system. *Genes Dev.* **12**, 1338–1347 (1998).
 68. Laachouch, J. E., Desmet, L., Geuskens, V., Grimaud, R. & Toussaint, A. Bacteriophage Mu repressor as a target for the Escherichia coli ATP-dependent Clp Protease. *EMBO J.* **15**, 437–44 (1996).
 69. Flynn, J. M., Neher, S. B., Kim, Y. I., Sauer, R. T. & Baker, T. A. Proteomic discovery of cellular substrates of the ClpXP protease reveals five classes of ClpX-recognition signals. *Mol. Cell* **11**, 671–83 (2003).
 70. Bhat, N. H., Vass, R. H., Stoddard, P. R., Shin, D. K. & Chien, P. Identification of ClpP substrates in Caulobacter crescentus reveals a role for regulated proteolysis in bacterial development. *Mol. Microbiol.* **88**, 1083–1092 (2013).
 71. Levchenko, I., Seidel, M., Sauer, R. T. & Baker, T. A. A specificity-enhancing factor for the ClpXP degradation machine. *Science* **289**, 2354–6 (2000).
 72. Kirstein, J., Molière, N., Dougan, D. A. & Turgay, K. Adapting the machine: adaptor proteins for Hsp100/Clp and AAA+ proteases. *Nat. Rev. Microbiol.* **7**, 589–99 (2009).
 73. Krüger, E., Zühlke, D., Witt, E., Ludwig, H. & Hecker, M. Clp-mediated proteolysis in Gram-positive bacteria is autoregulated by the stability of a repressor. *EMBO J.* **20**, 852–63 (2001).
 74. Dougan, D. A., Reid, B. G., Horwich, A. L. & Bukau, B. ClpS, a substrate modulator of the ClpAP machine. *Mol. Cell* **9**, 673–83 (2002).
 75. Kuhlmann, N. J. & Chien, P. Selective adaptor dependent protein degradation in bacteria. *Curr. Opin. Microbiol.* **36**, 118–127 (2017).
 76. Joshi, K. K., Sutherland, M. & Chien, P. Cargo engagement protects protease adaptors from degradation in a substrate-specific manner. *J. Biol. Chem.* jbc.M117.786392 (2017). doi:10.1074/jbc.M117.786392
 77. Ross, P. *et al.* Regulation of cellulose synthesis in Acetobacter xylinum by cyclic diguanylic acid. *Nature* **325**, 279–281 (1987).
 78. Jenal, U., Reinders, A. & Lori, C. Cyclic di-GMP: second messenger extraordinaire. *Nat. Rev. Microbiol.* **15**, 271–284 (2017).
 79. Jenal, U. & Malone, J. Mechanisms of Cyclic-di-GMP Signaling in Bacteria. *Annu. Rev. Genet.* **40**, 385–407 (2006).
 80. Egli, M. *et al.* Atomic-resolution structure of the cellulose synthase regulator cyclic diguanylic acid. *Proc. Natl. Acad. Sci.* **87**, 3235–3239 (1990).
 81. Zhang, L. & Meuwly, M. Stability and dynamics of cyclic diguanylic acid in solution. *ChemPhysChem* **12**, 295–302 (2011).
 82. Gentner, M., Allan, M. G., Zaehring, F., Schirmer, T. & Grzesiek, S. Oligomer formation of the bacterial second messenger c-di-GMP: Reaction rates and equilibrium constants indicate a monomeric state at physiological concentrations. *J. Am. Chem. Soc.* **134**, 1019–1029 (2012).

83. Tal, R. *et al.* Three *cdg* operons control cellular turnover of cyclic di-GMP in *Acetobacter xylinum*: genetic organization and occurrence of conserved domains in isoenzymes. *J. Bacteriol.* **180**, 4416–25 (1998).
84. Romling, U., Galperin, M. Y. & Gomelsky, M. Cyclic di-GMP: the first 25 years of a universal bacterial second messenger. *Microbiol. Mol. Biol. Rev.* **77**, 1–52 (2013).
85. Galperin, M. Y. Conserved ‘hypothetical’ proteins: New hints and new puzzles. *Comp. Funct. Genomics* **2**, 14–18 (2001).
86. Christen, M. *et al.* Asymmetrical Distribution of the Second Messenger c-di-GMP upon Bacterial Cell Division. *Science (80-)*. **328**, 1295–1297 (2010).
87. Abel, S. *et al.* Bi-modal Distribution of the Second Messenger c-di-GMP Controls Cell Fate and Asymmetry during the *Caulobacter* Cell Cycle. *PLoS Genet.* **9**, 5–11 (2013).
88. Römling, U., Gomelsky, M. & Galperin, M. Y. C-di-GMP: the dawning of a novel bacterial signalling system. *Mol. Microbiol.* **57**, 629–39 (2005).
89. Corrigan, R. M. & Gründling, A. Cyclic di-AMP: another second messenger enters the fray. *Nat. Rev. Microbiol.* **11**, 513–24 (2013).
90. Ausmees, N. *et al.* Genetic data indicate that proteins containing the GGDEF domain possess diguanylate cyclase activity. *FEMS Microbiol. Lett.* **204**, 163–167 (2001).
91. Ryjenkov, D. A., Tarutina, M., Moskvina, O. V. & Gomelsky, M. Cyclic diguanylate is a ubiquitous signaling molecule in bacteria: Insights into biochemistry of the GGDEF protein domain. *J. Bacteriol.* **187**, 1792–1798 (2005).
92. Chan, C. *et al.* Structural basis of activity and allosteric control of diguanylate cyclase. *Proc. Natl. Acad. Sci.* **101**, 17084–17089 (2004).
93. Zähringer, F., Lacanna, E., Jenal, U., Schirmer, T. & Boehm, A. Structure and signaling mechanism of a zinc-sensory diguanylate cyclase. *Structure* **21**, 1149–1157 (2013).
94. Schirmer, T. C-di-GMP Synthesis: Structural Aspects of Evolution, Catalysis and Regulation. *J. Mol. Biol.* **428**, 3683–3701 (2016).
95. Christen, B. *et al.* Allosteric control of cyclic di-GMP signaling. *J. Biol. Chem.* **281**, 32015–32024 (2006).
96. Schmidt, A. J., Ryjenkov, D. A. & Gomelsky, M. The ubiquitous protein domain EAL is a cyclic diguanylate-specific phosphodiesterase: enzymatically active and inactive EAL domains. *J. Bacteriol.* **187**, 4774–81 (2005).
97. Christen, M., Christen, B., Folcher, M., Schauerte, A. & Jenal, U. Identification and characterization of a cyclic di-GMP-specific phosphodiesterase and its allosteric control by GTP. *J. Biol. Chem.* **280**, 30829–30837 (2005).
98. Barends, T. R. M. *et al.* Structure and mechanism of a bacterial light-regulated cyclic nucleotide phosphodiesterase. *Nature* **459**, 1015–1018 (2009).
99. Orr, M. W. *et al.* Oligoribonuclease is the primary degradative enzyme for pGpG in *Pseudomonas aeruginosa* that is required for cyclic-di-GMP turnover. *Proc. Natl. Acad. Sci.* **112**, E5048–E5057 (2015).
100. Ryan, R. P. *et al.* Cell-cell signaling in *Xanthomonas campestris* involves an HD-GYP

- domain protein that functions in cyclic di-GMP turnover. *Proc. Natl. Acad. Sci.* **103**, 6712–6717 (2006).
101. Stelitano, V. *et al.* C-di-GMP Hydrolysis by *Pseudomonas aeruginosa* HD-GYP Phosphodiesterases: Analysis of the Reaction Mechanism and Novel Roles for pGpG. *PLoS One* **8**, 1–13 (2013).
 102. Bellini, D. *et al.* Crystal structure of an HD-GYP domain cyclic-di-GMP phosphodiesterase reveals an enzyme with a novel trinuclear catalytic iron centre. *Mol. Microbiol.* **91**, 26–38 (2014).
 103. Habazettl, J., Allan, M. G., Jenal, U. & Grzesiek, S. Solution structure of the PilZ domain protein PA4608 complex with cyclic di-GMP identifies charge clustering as molecular readout. *J. Biol. Chem.* **286**, 14304–14314 (2011).
 104. Duerig, A. *et al.* Second messenger-mediated spatiotemporal control of protein degradation regulates bacterial cell cycle progression. *Genes Dev.* **23**, 93–104 (2009).
 105. Navarro, M. V. A. S., De, N., Bae, N., Wang, Q. & Sondermann, H. Structural Analysis of the GGDEF-EAL Domain-Containing c-di-GMP Receptor FimX. *Structure* **17**, 1104–1116 (2009).
 106. Hickman, J. W. & Harwood, C. S. Identification of FleQ from *Pseudomonas aeruginosa* as a c-di-GMP-responsive transcription factor. *Mol. Microbiol.* **69**, 376–389 (2008).
 107. Kulshina, N., Baird, N. J. & Ferré-D’Amaré, A. R. Recognition of the bacterial second messenger cyclic diguanylate by its cognate riboswitch. *Nat. Struct. Mol. Biol.* **16**, 1212–1217 (2009).
 108. Hengge, R. Cyclic-di-GMP reaches out into the bacterial RNA world. *Sci. Signal.* **3**, pe44 (2010).
 109. Kariisa, A. T., Weeks, K. & Tamayo, R. The RNA Domain Vc1 Regulates Downstream Gene Expression in Response to Cyclic Diguanylate in *Vibrio cholerae*. *PLoS One* **11**, e0148478 (2016).
 110. Busby, S. & Ebright, R. H. Transcription activation by catabolite activator protein (CAP). *J. Mol. Biol.* **293**, 199–213 (1999).
 111. Bernlohr, R. W., Haddox, M. K. & Goldberg, N. D. Cyclic guanosine 3':5'-monophosphate in *Escherichia coli* and *Bacillus licheniformis*. *J. Biol. Chem.* **249**, 4329–31 (1974).
 112. Cashel, M. & Kalbacher, B. The control of ribonucleic acid synthesis in *Escherichia coli*. V. Characterization of a nucleotide associated with the stringent response. *J. Biol. Chem.* **245**, 2309–18 (1970).
 113. Witte, G., Hartung, S., Büttner, K. & Hopfner, K.-P. Structural biochemistry of a bacterial checkpoint protein reveals diadenylate cyclase activity regulated by DNA recombination intermediates. *Mol. Cell* **30**, 167–78 (2008).
 114. Hallberg, Z. F. *et al.* Hybrid promiscuous (Hypr) GGDEF enzymes produce cyclic AMP-GMP (3', 3'-cGAMP). *Proc. Natl. Acad. Sci. U. S. A.* **113**, 1790–5 (2016).
 115. Davies, B. W., Bogard, R. W., Young, T. S. & Mekalanos, J. J. Coordinated regulation of accessory genetic elements produces cyclic di-nucleotides for *V. cholerae* virulence. *Cell* **149**, 358–70 (2012).

116. Kolb, A., Busby, S., Buc, H., Garges, S. & Adhya, S. Transcriptional regulation by cAMP and its receptor protein. *Annu. Rev. Biochem.* **62**, 749–95 (1993).
117. Hufnagel, D. A. *et al.* The Catabolite Repressor Protein-Cyclic AMP Complex Regulates *csgD* and Biofilm Formation in Uropathogenic *Escherichia coli*. *J. Bacteriol.* **198**, 3329–3334 (2016).
118. McDonough, K. A. & Rodriguez, A. The myriad roles of cyclic AMP in microbial pathogens: from signal to sword. *Nat. Rev. Microbiol.* **10**, 27–38 (2011).
119. Potrykus, K. & Cashel, M. (p)ppGpp: still magical? *Annu. Rev. Microbiol.* **62**, 35–51 (2008).
120. Gonzalez, D. & Collier, J. Effects of (p)ppGpp on the progression of the cell cycle of *Caulobacter crescentus*. *J. Bacteriol.* **196**, 2514–25 (2014).
121. Gundlach, J. *et al.* Control of potassium homeostasis is an essential function of the second messenger cyclic di-AMP in *Bacillus subtilis*. *Sci. Signal.* **10**, eaal3011 (2017).
122. Seshasayee, A. S. N., Fraser, G. M. & Luscombe, N. M. Comparative genomics of cyclic-di-GMP signalling in bacteria: post-translational regulation and catalytic activity. *Nucleic Acids Res.* **38**, 5970–81 (2010).
123. Collier, J. Cell cycle control in Alphaproteobacteria. *Curr. Opin. Microbiol.* **30**, 107–13 (2016).
124. Angelakis, E., Bechah, Y. & Raoult, D. The History of Epidemic Typhus. *Microbiol. Spectr.* **4**, 81–92 (2016).
125. Andersson, S. G. E. *et al.* The genome sequence of *Rickettsia prowazekii* and the origin of mitochondria. *Nature* **396**, 133–140 (1998).
126. Andrews, M. & Andrews, M. E. Specificity in Legume-Rhizobia Symbioses. *Int. J. Mol. Sci.* **18**, 705 (2017).
127. Bourras, S., Rouxel, T. & Meyer, M. *Agrobacterium tumefaciens* Gene Transfer: How a Plant Pathogen Hacks the Nuclei of Plant and Nonplant Organisms. *Phytopathology* **105**, 1288–1301 (2015).
128. Fukuda, W. *et al.* *Polymorphobacter multimanifer* gen. nov., sp. nov., a polymorphic bacterium isolated from Antarctic white rock. *Int. J. Syst. Evol. Microbiol.* **64**, 2034–40 (2014).
129. Brill, M. *et al.* The diversity and evolution of cell cycle regulation in alpha-proteobacteria: a comparative genomic analysis. *BMC Syst. Biol.* **4**, 52 (2010).
130. Poindexter, J. S. BIOLOGICAL PROPERTIES AND CLASSIFICATION OF THE CAULOBACTER GROUP. *Bacteriol. Rev.* **28**, 231–95 (1964).
131. Iba, H., Fukuda, A. & Okada, Y. Synchronous cell differentiation in *Caulobacter crescentus*. *Jpn. J. Microbiol.* **19**, 441–6 (1975).
132. Henrici, A. T. & Johnson, D. E. Studies of Freshwater Bacteria: II. Stalked Bacteria, a New Order of Schizomycetes. *J. Bacteriol.* **30**, 61–93 (1935).
133. Jiang, C., Brown, P. J. B., Ducret, A. & Brun, Y. V. Sequential evolution of bacterial morphology by co-option of a developmental regulator. *Nature* **506**, 489–493 (2014).

134. Cserti, E. *et al.* Dynamics of the peptidoglycan biosynthetic machinery in the stalked budding bacterium *Hyphomonas neptunium*. *Mol. Microbiol.* **103**, 875–895 (2017).
135. Ireland, M. M. E., Karty, J. A., Quardokus, E. M., Reilly, J. P. & Brun, Y. V. Proteomic analysis of the *Caulobacter crescentus* stalk indicates competence for nutrient uptake. *Mol. Microbiol.* **45**, 1029–1041 (2002).
136. Wagner, J. K., Setayeshgar, S., Sharon, L. A., Reilly, J. P. & Brun, Y. V. A nutrient uptake role for bacterial cell envelope extensions. *Proc. Natl. Acad. Sci. U. S. A.* **103**, 11772–7 (2006).
137. Poindexter, J. S. The caulobacters: ubiquitous unusual bacteria. *Microbiol. Rev.* **45**, 123–79 (1981).
138. Tsang, P. H., Li, G., Brun, Y. V., Freund, L. Ben & Tang, J. X. Adhesion of single bacterial cells in the micronewton range. *Proc. Natl. Acad. Sci. U. S. A.* **103**, 5764–8 (2006).
139. Wortinger, M., Sackett, M. J. & Brun, Y. V. CtrA mediates a DNA replication checkpoint that prevents cell division in *Caulobacter crescentus*. *EMBO J.* **19**, 4503–12 (2000).
140. Li, G. *et al.* Surface contact stimulates the just-in-time deployment of bacterial adhesins. *Mol. Microbiol.* **83**, 41–51 (2012).
141. Persat, A., Stone, H. A. & Gitai, Z. The curved shape of *Caulobacter crescentus* enhances surface colonization in flow. *Nat. Commun.* **5**, 1–9 (2014).
142. Wolanski, M., Donczew, R., Zawilak-Pawlik, A. & Zakrzewska-Czerwinska, J. oriC-encoded instructions for the initiation of bacterial chromosome replication. *Front. Microbiol.* **6**, 1–14 (2015).
143. Ozaki, S. & Katayama, T. DnaA structure, function, and dynamics in the initiation at the chromosomal origin. *Plasmid* **62**, 71–82 (2009).
144. Viollier, P. H. *et al.* Rapid and sequential movement of individual chromosomal loci to specific subcellular locations during bacterial DNA replication. *Proc. Natl. Acad. Sci. U. S. A.* **101**, 9257–62 (2004).
145. Skarstad, K. & Katayama, T. Regulating DNA replication in bacteria. *Cold Spring Harb. Perspect. Biol.* **5**, a012922 (2013).
146. Jonas, K., Chen, Y. E. & Laub, M. T. Modularity of the bacterial cell cycle enables independent spatial and temporal control of DNA replication. *Curr. Biol.* **21**, 1092–101 (2011).
147. Wheeler, R. T. & Shapiro, L. Differential localization of two histidine kinases controlling bacterial cell differentiation. *Mol. Cell* **4**, 683–94 (1999).
148. Tsokos, C. G. & Laub, M. T. Polarity and cell fate asymmetry in *Caulobacter crescentus*. *Curr. Opin. Microbiol.* **15**, 744–750 (2012).
149. Quon, K. C., Marczyński, G. T. & Shapiro, L. Cell cycle control by an essential bacterial two-component signal transduction protein. *Cell* **84**, 83–93 (1996).
150. Laub, M. T., Chen, S. L., Shapiro, L. & McAdams, H. H. Genes directly controlled by CtrA, a master regulator of the *Caulobacter* cell cycle. *Proc. Natl. Acad. Sci. U. S. A.* **99**, 4632–7 (2002).

151. Radhakrishnan, S. K., Thanbichler, M. & Viollier, P. H. The dynamic interplay between a cell fate determinant and a lysozyme homolog drives the asymmetric division cycle of *Caulobacter crescentus*. *Genes Dev.* **22**, 212–225 (2008).
152. Quon, K. C., Yang, B., Domian, I. J., Shapiro, L. & Marczyński, G. T. Negative control of bacterial DNA replication by a cell cycle regulatory protein that binds at the chromosome origin. *Proc. Natl. Acad. Sci. U. S. A.* **95**, 120–5 (1998).
153. Biondi, E. G. *et al.* Regulation of the bacterial cell cycle by an integrated genetic circuit. *Nature* **444**, 899–904 (2006).
154. Iniesta, A. A., McGrath, P. T., Reisenauer, A., McAdams, H. H. & Shapiro, L. A phospho-signaling pathway controls the localization and activity of a protease complex critical for bacterial cell cycle progression. *Proc. Natl. Acad. Sci.* **103**, 10935–10940 (2006).
155. Iniesta, A. A. & Shapiro, L. A bacterial control circuit integrates polar localization and proteolysis of key regulatory proteins with a phospho-signaling cascade. *Proc. Natl. Acad. Sci.* **105**, 16602–16607 (2008).
156. Joshi, K. K., Bergé, M., Radhakrishnan, S. K., Viollier, P. H. & Chien, P. An Adaptor Hierarchy Regulates Proteolysis during a Bacterial Cell Cycle. *Cell* **163**, 419–431 (2015).
157. Chen, Y. E., Tsokos, C. G., Biondi, E. G., Perchuk, B. S. & Laub, M. T. Dynamics of two phosphorelays controlling cell cycle progression in *Caulobacter crescentus*. *J. Bacteriol.* **191**, 7417–7429 (2009).
158. Matroule, J.-Y., Lam, H., Burnette, D. T. & Jacobs-Wagner, C. Cytokinesis monitoring during development; rapid pole-to-pole shuttling of a signaling protein by localized kinase and phosphatase in *Caulobacter*. *Cell* **118**, 579–90 (2004).
159. Tsokos, C. G., Perchuk, B. S. & Laub, M. T. A dynamic complex of signaling proteins uses polar localization to regulate cell-fate asymmetry in *Caulobacter crescentus*. *Dev. Cell* **20**, 329–41 (2011).
160. Perez, A. M. *et al.* A Localized Complex of Two Protein Oligomers Controls the Orientation of Cell Polarity. *MBio* **8**, e02238-16 (2017).
161. Viollier, P. H., Sternheim, N. & Shapiro, L. Identification of a localization factor for the polar positioning of bacterial structural and regulatory proteins. *Proc. Natl. Acad. Sci.* **99**, 13831–13836 (2002).
162. Chen, J. C. *et al.* Cytokinesis signals truncation of the PodJ polarity factor by a cell cycle-regulated protease. *EMBO J.* **25**, 377–386 (2006).
163. Subramanian, K., Paul, M. R. & Tyson, J. J. Dynamical Localization of DivL and PleC in the Asymmetric Division Cycle of *Caulobacter crescentus*: A Theoretical Investigation of Alternative Models. *PLoS Comput. Biol.* **11**, e1004348 (2015).
164. Abel, S. *et al.* Regulatory cohesion of cell cycle and cell differentiation through interlinked phosphorylation and second messenger networks. *Mol. Cell* **43**, 550–60 (2011).
165. Davis, N. J. *et al.* De- and repolarization mechanism of flagellar morphogenesis during a bacterial cell cycle. *Genes Dev.* **27**, 2049–2062 (2013).
166. Lonetto, M., Gribskov, M. & Gross, C. A. The sigma 70 family: sequence conservation and evolutionary relationships. *J. Bacteriol.* **174**, 3843–9 (1992).

167. Davis, M. C., Kesthely, C. A., Franklin, E. A. & MacLellan, S. R. The essential activities of the bacterial sigma factor. *Can. J. Microbiol.* **63**, 89–99 (2017).
168. Merrick, M. J. In a class of its own - the RNA polymerase sigma factor sigma 54 (sigma N). *Mol. Microbiol.* **10**, 903–9 (1993).
169. Brun, Y. V & Shapiro, L. A temporally controlled sigma-factor is required for polar morphogenesis and normal cell division in *Caulobacter*. *Genes Dev.* **6**, 2395–408 (1992).
170. Popham, D. L., Szeto, D., Keener, J. & Kustu, S. Function of a bacterial activator protein that binds to transcriptional enhancers. *Science* **243**, 629–35 (1989).
171. Joly, N., Zhang, N., Buck, M. & Zhang, X. Coupling AAA protein function to regulated gene expression. *Biochim. Biophys. Acta* **1823**, 108–16 (2012).
172. Bush, M. & Dixon, R. The role of bacterial enhancer binding proteins as specialized activators of σ 54-dependent transcription. *Microbiol. Mol. Biol. Rev.* **76**, 497–529 (2012).
173. Studholme, D. J. & Dixon, R. Domain architectures of sigma54-dependent transcriptional activators. *J. Bacteriol.* **185**, 1757–67 (2003).
174. Biondi, E. G. *et al.* A phosphorelay system controls stalk biogenesis during cell cycle progression in *Caulobacter crescentus*. *Mol. Microbiol.* **59**, 386–401 (2006).
175. Fiebig, A. *et al.* A Cell Cycle and Nutritional Checkpoint Controlling Bacterial Surface Adhesion. *PLoS Genet.* **10**, (2014).
176. Sprecher, K. S. *et al.* Cohesive Properties of the *Caulobacter crescentus* Holdfast Adhesin Are Regulated by a Novel c-di-GMP Effector Protein. *MBio* **8**, e00294-17 (2017).
177. Janakiraman, B., Mignolet, J., Narayanan, S., Viollier, P. H. & Radhakrishnan, S. K. In-phase oscillation of global regulons is orchestrated by a pole-specific organizer. *Proc. Natl. Acad. Sci.* **113**, 12550–12555 (2016).
178. Easter, J. & Gober, J. W. ParB-Stimulated Nucleotide Exchange Regulates a Switch in Functionally Distinct ParA Activities. *Mol. Cell* **10**, 427–434 (2002).
179. Toro, E., Hong, S.-H., McAdams, H. H. & Shapiro, L. *Caulobacter* requires a dedicated mechanism to initiate chromosome segregation. *Proc. Natl. Acad. Sci.* **105**, 15435–15440 (2008).
180. Bowman, G. R. *et al.* *Caulobacter* PopZ forms a polar subdomain dictating sequential changes in pole composition and function. *Mol. Microbiol.* **76**, 173–189 (2010).
181. Xu, W. & McArthur, G. Cell Cycle Regulation and Melanoma. *Curr. Oncol. Rep.* **18**, 34 (2016).
182. Hendler, A., Medina, E. M., Buchler, N. E., de Bruin, R. A. M. & Aharoni, A. The evolution of a G1/S transcriptional network in yeasts. *Curr. Genet.* 1–6 (2017). doi:10.1007/s00294-017-0726-3
183. Miles, S. & Breeden, L. A common strategy for initiating the transition from proliferation to quiescence. *Curr. Genet.* **63**, 179–186 (2017).
184. Morgan, D. O. Cyclin-dependent kinases: engines, clocks, and microprocessors. *Annu. Rev. Cell Dev. Biol.* **13**, 261–91 (1997).

185. Möröy, T. & Geisen, C. Cyclin E. *Int. J. Biochem. Cell Biol.* **36**, 1424–39 (2004).
186. Wang, J. D. & Levin, P. A. Metabolism, cell growth and the bacterial cell cycle. *Nat. Rev. Microbiol.* **7**, 822–7 (2009).
187. Cooper, S. & Helmstetter, C. E. Chromosome replication and the division cycle of *Escherichia coli* B/r. *J. Mol. Biol.* **31**, 519–40 (1968).
188. Donachie, W. Relationship between cell size and time of initiation of DNA replication. *Nature* **219**, 1077–1079 (1968).
189. Wallden, M., Fange, D., Lundius, E. G., Baltekin, Ö. & Elf, J. The Synchronization of Replication and Division Cycles in Individual *E. coli* Cells. *Cell* **166**, 729–39 (2016).
190. Amir, A. Is cell size a spandrel? *Elife* **6**, 18261 (2017).
191. Willis, L. & Huang, K. C. Sizing up the bacterial cell cycle. *Nat. Rev. Microbiol.* (2017). doi:10.1038/nrmicro.2017.79
192. Laub, M. T., Shapiro, L. & McAdams, H. H. Systems biology of *Caulobacter*. *Annu. Rev. Genet.* **41**, 429–41 (2007).
193. Schrader, J. M. & Shapiro, L. Synchronization of *Caulobacter crescentus* for investigation of the bacterial cell cycle. *J. Vis. Exp.* **2**, e52633 (2015).
194. Gorbatyuk, B. & Marczyński, G. T. Physiological consequences of blocked *Caulobacter crescentus* *dnaA* expression, an essential DNA replication gene. *Mol. Microbiol.* **40**, 485–97 (2001).
195. Gorbatyuk, B. & Marczyński, G. T. Regulated degradation of chromosome replication proteins *DnaA* and *CtrA* in *Caulobacter crescentus*. *Mol. Microbiol.* **55**, 1233–45 (2005).
196. Flåtten, I., Fossum-Raunehaug, S., Taipale, R., Martinsen, S. & Skarstad, K. The *DnaA* Protein Is Not the Limiting Factor for Initiation of Replication in *Escherichia coli*. *PLoS Genet.* **11**, e1005276 (2015).
197. Collier, J., Murray, S. R. & Shapiro, L. *DnaA* couples DNA replication and the expression of two cell cycle master regulators. *EMBO J.* **25**, 346–56 (2006).
198. Jacobs, C., Domian, I. J., Maddock, J. R. & Shapiro, L. Cell cycle-dependent polar localization of an essential bacterial histidine kinase that controls DNA replication and cell division. *Cell* **97**, 111–20 (1999).
199. Childers, W. S. *et al.* Cell fate regulation governed by a repurposed bacterial histidine kinase. *PLoS Biol.* **12**, e1001979 (2014).
200. Hallez, R., Delaby, M., Sanselicio, S. & Viollier, P. H. Hit the right spots: cell cycle control by phosphorylated guanosines in alphaproteobacteria. *Nat. Rev. Microbiol.* **15**, 137–148 (2017).
201. Boutte, C. C., Henry, J. T. & Crosson, S. ppGpp and polyphosphate modulate cell cycle progression in *Caulobacter crescentus*. *J. Bacteriol.* **194**, 28–35 (2012).
202. Smith, S. C. *et al.* Cell cycle-dependent adaptor complex for ClpXP-mediated proteolysis directly integrates phosphorylation and second messenger signals. *Proc. Natl. Acad. Sci. U. S. A.* **111**, 14229–34 (2014).
203. Nesper, J., Reinders, A., Glatter, T., Schmidt, A. & Jenal, U. A novel capture compound

- for the identification and analysis of cyclic di-GMP binding proteins. *J. Proteomics* **75**, 4874–8 (2012).
204. Chou, S.-H. & Galperin, M. Y. Diversity of Cyclic Di-GMP-Binding Proteins and Mechanisms. *J. Bacteriol.* **198**, 32–46 (2016).
 205. Gurskaya, N. G. *et al.* Engineering of a monomeric green-to-red photoactivatable fluorescent protein induced by blue light. *Nat. Biotechnol.* **24**, 461–5 (2006).
 206. Maniatis, T., Fritsch, E. F. & Sambrook, J. *Molecular Cloning: A Laboratory Manual*. (Cold Spring Harbor, N.Y., 1982).
 207. Ely, B. Genetics of *Caulobacter crescentus*. *Methods Enzymol.* **204**, 372–84 (1991).
 208. Johnson, R. C. & Ely, B. Isolation of spontaneously derived mutants of *Caulobacter crescentus*. *Genetics* **86**, 25–32 (1977).
 209. Evinger, M. & Agabian, N. Envelope-associated nucleoid from *Caulobacter crescentus* stalked and swarmer cells. *J. Bacteriol.* **132**, 294–301 (1977).
 210. Huguenel, E. D. & Newton, A. Evidence that subcellular flagellin pools in *Caulobacter crescentus* are precursors in flagellum assembly. *J. Bacteriol.* **157**, 727–32 (1984).
 211. Kinoshita, E., Kinoshita-Kikuta, E., Takiyama, K. & Koike, T. Phosphate-binding tag, a new tool to visualize phosphorylated proteins. *Mol. Cell. Proteomics* **5**, 749–57 (2006).
 212. Laventie, B.-J. *et al.* Capture compound mass spectrometry—a powerful tool to identify novel c-di-GMP effector proteins. *J. Vis. Exp.* 1–11 (2015). doi:10.3791/51404
 213. Chen, Y. E., Tsokos, C. G., Biondi, E. G., Perchuk, B. S. & Laub, M. T. Dynamics of Two Phosphorelays Controlling Cell Cycle Progression in *Caulobacter crescentus*. *J. Bacteriol.* **191**, 7417–7429 (2009).
 214. Skerker, J. M., Prasol, M. S., Perchuk, B. S., Biondi, E. G. & Laub, M. T. Two-component signal transduction pathways regulating growth and cell cycle progression in a bacterium: a system-level analysis. *PLoS Biol.* **3**, e334 (2005).
 215. Schindelin, J. *et al.* Fiji: an open-source platform for biological-image analysis. *Nat. Methods* **9**, 676–82 (2012).
 216. Paintdakhi, A. *et al.* Oufiti: an integrated software package for high-accuracy, high-throughput quantitative microscopy analysis. *Mol. Microbiol.* **99**, 767–77 (2016).

9 ACKNOWLEDGMENTS

Professor Urs Jenal guided me through this research project and supported me along the way with input, discussions and good advice based on his incredible knowledge and wisdom. For that I am deeply grateful.

I thank the members of my PhD committee Professor Marek Basler and Professor Henning Stahlberg for their guidance.

Jutta Nesper laid the groundwork for this project and taught me everything I needed to start working on it. More importantly, she taught me the importance of facing challenges in a positive way, even under the worst circumstances. She is dearly missed.

Andreas Kaczmarczyk und Antje Hempel were my partners in crime working on this project. Without them, this story would nowhere be as great as it has become. I am thankful for their insights, their support, and their friendship.

I thank Christian Lori for the scientific discussions we've had, as well as the fun times. A brilliant mind that had always good advice to share.

Benoît Laventie has taught me everything about biochemical assays for what I am thankful.

It is very important to me to thank all the people that made working in our lab so enjoyable, Kathrin Sprecher, Isabelle Hug, Shogo Ozaki, and Kie Ozaki. They were always there for advice, help, and a lot of good conversations. Of course, this also includes all the other former and current lab members in the Jenal lab.

Special thanks go to Kerstin Lassak for her relentless positivity.

I am most thankful to my family. My mother Monika has the greatest of hearts and is always there for me in every situation. I can also always count on my brothers, Adrian and Thomas, even though their interest in my work has usually been fleeting. My dearest Nora has been supporting me and has been making my life beautiful.

Finally, I'd like to thank my father Adrian. Being my greatest role model, it is deeply saddening that he cannot be here. I know he would have supported me in every way, always.

10 CURRICULUM VITAE

Personal Details

Name Christoph von Arx
Hometown Olten
Date of Birth November 16th, 1984
Nationality Swiss

Scientific Education

09/2013 – 11/2017 **PhD studies in Molecular Microbiology**
Biozentrum, University of Basel, Switzerland; Prof. Dr. Urs Jenal
08/2012 – 09/2013 **Master of Science in Molecular Biology (M Sc)**
Biozentrum, University of Basel, Switzerland
09/2009 – 08/2012 **Bachelor of Science in Biology (B Sc), Major in Molecular Biology**
Biozentrum, University of Basel, Switzerland
08/2008 – 08/2009 **Complementary Exam to the Federal Vocational Baccalaureate**
Passerelle course for admission to universities, WKS Bern

Occupations and Previous Education

05/2012 – 09/2013 **X-Protect/VS AG**
Pomerngut F2, 4800 Zofingen; Function: Security guard
12/2009 – 04/2012 **BASE Sicherheitsdienst GmbH**
Sandackerweg 3, 4665 Oftringen; Function: Security guard
07/2007 – 02/2008 **EF Language Schools**
EF Dublin (Ireland), 6 months and EF Paris (France), 2 months
Exam: Certificate of Proficiency in English (CPE)
09/2004 – 05/2007 **Architekturbüro Della Giacoma & Krummenacher**
Mittelgäustrasse 33, 4616 Kappel; Function: Architectural draftsman
09/2004 – 05/2007 **Architectural studies: First Prediploma (Extra Occupational)**
Lucerne University of Applied Sciences and Arts
08/2000 – 07/2004 **Swiss Certificate of Qualification as an Architectural Draftsman, Federal Vocational Baccalaureate**
Architekturbüro Guldemann, 4618 Boningen

